Final report from 29 August 2024

Newcline

Advanced thermocline concepts for thermal energystorage for concentrated solar power

Source: © Deutsches Zentrum für Luft- und Raumfahrt (DLR)

Autors:
Ignacio Gurruchaga, SPF, ignacio.gurruchaga@ost.ch
Alex Hobé, SPF, alex.hobe@ost.ch
Daniel Carbonell, SPF, extern.carbonell@ost.ch

Collaborators:
Martin Neugebauer, SPF, martin.neugebauer@ost.ch

The authors bear the entire responsibility for the content of this report and for the conclusions drawn therefrom.

Summary

The Newcline project is focused on developing and analysing a novel storage concept for solar concentrating power (CSP) plants replacing the traditional two molten salt tanks with a single thermocline tank with a filler material. The aim was to reduce investment costs for thermal energy storage in CSP plants due to the lower amount of tanks and molten salt. The thermocline tank, which is designed to minimise the mixing of hot and cold temperatures, incorporates a novel structured ceramic filler, significantly reducing the volume of salts required for the same storage capacity. A diminished volume of salts lowers investment (CAPEX) and maintenance costs (OPEX). The anticipated savings in investment costs, in the project's proposal, for the storage subsystem were estimated to be up to 40%. This would result in overall CAPEX savings for the CSP plant of 5% - 10%, depending on the type of CSP plant used. Two types of solar concentrating power plants, Central Receiver (CR) and Parabolic Trough Collector (PTC), are considered within the project scope.

The overall project was implemented by five different international partners under the umbrella of the CSP-ERANET encompassing various tasks, e.g. the development of filler material, CFD characterisation of heat transfer processes, the experimental lab and large-scale thermocline analysis, structural analyses of the thermocline tank and transient system simulations of the complete CSP plant. The specific contributions from SPF-OST were on the development of the simulation framework for conducting dynamic simulations to integrate this novel storage concept into CSP plants. This simulation framework is based on the pytrnsys simulation environment, an open-source framework for setting up, simulating, and post-processing TRNSYS dynamic simulations developed at SPF (https://pytrnsys.readthedocs.io/en/latest/index.html).

SPF developed novel mathematical models representing the energy behaviour of the main components of solar power plants and complete system models for the whole CR and PTC CSP plants including both twotank (as reference case) and thermocline storage technologies. The development of this simulation framework had two primary objectives. Firstly, compare the energy performance of the thermocline CSP system with the reference case using two molten salt tank conventional storage. Secondly, conduct parametric studies to explore the thermocline system's capabilities and limitations for different schemes and sizes in order to optimise its operation. Economic analyses, specifically evaluating the CAPEX and OPEX to determine the levelized cost of energy (LCOE), were conducted to assess the techno-economic feasibility of the new thermocline technology compared with the state-of-the-art two-tank technology.

Energetic simulations with the new pytrnsys environment indicate a direct link between the energy performance of CSP plants and the control strategy to operate the thermocline tank. The control strategy of the termocline differs from the two-tank system because it not only depends on the mass and heat capacities of the materials and the maximum and minimum operational temperatures, but also on the temperature thresholds used to control the charging and discharging processes of the thermocline tank. By modifying these temperature threshold it is possible to store more or less thermal energy in the thermocline tank with a significant influence on the thermal energy that could be eventually converted into electricity.

A sensitivity analysis demonstrated that thermocline CSP systems generate between 70% to 100% of the electricity compared to conventional two-tank systems, depending on the previous charging and discharging temperature threshold when sized for the same nominal capacity, which can differ depending on how nominal conditions are defined. Specifically, for the temperature threshold selected in this study, the thermocline CR CSP plant generates 12.8% of the electricity less than a conventional two-tank CR plant, while a PTC system generates 3.1% less electricity compared to the conventional two-tank system. Translating in terms of the capacity factor of the CR CSP plant, this represents a capacity factor reduction from 71% for the conventional two-tank molten salt to 62% for the thermocline tank, and for the PT CSP from 45% to 43%. Thus, regardless of the case, thermocline systems sized with same energy capacity compared to two tank systems are expected to generate slightly less electricity compared to two tank systems. Thus, in order to obtain the same production of dispatchable electricity a thermocline storage should be designed to store more (from 5% to 25%) energy in nominal conditions

compared to two-tank systems due to the lower energetic efficiency for not having a perfectly stratified thermocline storage and considering the charging and discharging temperature thresholds.

The aforementioned anticipated investment cost savings from reducing the number of tanks by two were not fully achieved due to the increased complexity and cost of the tank's structural design needed to handle greater weights and thermal stresses. Moreover, the economic assessments of thermocline tank costs remain uncertain despite in-depth structural analysis, particularly concerning the final cost of the structured filler, its assembly inside the vessel, and the structural cost of the tank. These uncertainties in the structural design and filler material have an impact on the TES investment and in consequence in overall plant CAPEX savings. From the anticipated 5% to 10%, the actual estimated savings in the overall CSP plant are in the range of 3% to -10% for CR plants and of 7% to -9% for PTC plant. Negative values indicate that the Newcline systems result in higher CAPEX than conventional two-tank systems. The range is a result of several cost assumptions and uncertainties.

The decisive factor in reducing uncertainties is to minimise the uncertainty in both filler's brick manufacturing and assembly. Throughout the project, various brick models and chemical compositions have been assessed for their thermal performance and chemical stability and compatibility. However, the costs associated with brick mass production have not been fully investigated. Additionally, the current brick design has been developed for pilot plant production using a manual process. Scaling this up to a commercial plant would require a vast number of bricks, which could be improved with a new, likely larger, brick design tailored specifically for big commercial use. This would reduce assembly effort and lead to more cost-effective production. Consequently, developing a new brick design and evaluating its mass production costs would be the next steps to further reduce uncertainties.

Examining the differences between CR and PTC system's CAPEX, the advantage of salt reduction with the thermocline concept with filler materials depends on the proportion of molten salt cost in their total plant investment. The relative weight of salt cost depends largely on the thermal maximum and minimum operating temperature of the system. For the same nominal storage capacity, systems with lower temperature difference, such as PTC (95 K), require more salt mass compared to systems like CR with higher temperature difference (265 K). Consequently, systems with lower temperature difference such as PTC or industrial applications, are more likely to benefit from the Newcline thermocline concept. Thermocline systems also demonstrate consistent cost-effectiveness in operational expenses (OPEX), as reducing the number of tanks lowers maintenance costs.

In terms of the LCOE, PTC systems can be up to 6% more favourable compared to conventional two-tank systems considering the lowest cost value assumed for both technologies. However, the thermocline system can also have a 10% higher LCOE when using the upper cost assumptions of both technologies, which is influenced by the higher uncertainties associated, to a great extend, to the filler material. For CR plants and the costs assumed in this project, the implementation of thermocline storages does not offer any economic advantage in terms of LCOE. The main reasons are the lower amount of salts used in the two-tank system as well as the lower electricity produced by the thermocline concept. The latter could be compensated by increasing the size of the thermocline storage, but this case has not been assessed during the project.

Overall, the novel thermocline storage system developed within the Newcline project could be potentially beneficial for systems where the cost of molten salt constitutes a significant portion of the total investment such as the PTC CSP plants. Also, it is expected to be more cost economic for smaller volumes as analysed here. This extends the potential applications of thermocline concepts beyond CSP plants to industrial processes where high temperature storages could help in providing flexibility or in extending the use of operation when intermittent sources such as concentrating solar technologies are the main renewable source. Despite the cost benefit on smaller than CSP scale applications needs to be proven and quantified, several industrial processes have been identified as possible benefit from such a storage: Food Processing (baking or high-temperature short-time (HTST) pasteurization, and drying processes), Chemical Industry (Polymerization or distillation processes), Pharmaceutical Industry (sterilization and drying processes), Textile Industry (Dyeing and drying), Paper Industry and Automotive Industry among others.

Zusammenfassung

Das Newcline-Projekt konzentriert sich auf die Entwicklung und Analyse eines neuartigen Speicherkonzepts für solarthermische Kraftwerke (CSP), bei dem die herkömmlichen zwei Tanks mit geschmolzenem Salz durch einen einzigen Thermoklin-Tank mit Füllmaterial ersetzt werden. Ziel war es, die Investitionskosten für die Speicherung thermischer Energie in CSP-Anlagen aufgrund der geringeren Anzahl an Tanks und geschmolzenem Salz zu senken. Der Thermoklinetank, der so konzipiert ist, dass er die Vermischung von heissen und kalten Temperaturen minimiert, enthält einen neuartigen strukturierten Keramikfüllstoff, der das für die gleiche Speicherkapazität erforderliche Salzvolumen erheblich reduziert. Ein geringeres Salzvolumen senkt die Investitions- (CAPEX) und Wartungskosten (OPEX). Die erwarteten Einsparungen bei den Investitionskosten für das Speichersubsystem wurden im Projektvorschlag auf bis zu 40% geschätzt. Dies würde zu einer Gesamtersparnis bei den Investitionsausgaben für die CSP-Anlage von 5% bis 10% führen, je nach Art der verwendeten CSP-Anlage. Im Rahmen des Projekts werden zwei Arten von Solarkraftwerken mit konzentrierender Optik, Central Receiver (CR) und Parabolic Trough Collector (PTC), berücksichtigt.

Das Gesamtprojekt wurde von fünf verschiedenen internationalen Partnern unter dem Dach des CSP-ERANET durchgeführt und umfasste verschiedene Aufgaben, z. B. die Entwicklung von Füllmaterial, die CFD-Charakterisierung von Wärmeübertragungsprozessen, das Versuchslabor und die gross angelegte Thermoklinenanalyse, Strukturanalysen des Thermoklinentanks und transiente Systemsimulationen der gesamten CSP-Anlage. Die spezifischen Beiträge von SPF-OST betrafen die Entwicklung des Simulationsrahmens für die Durchführung dynamischer Simulationen zur Integration dieses neuartigen Speicherkonzepts in CSP-Anlagen. Dieser Simulationsrahmen basiert auf der Simulationsumgebung pytrnsys, einem Open-Source-Rahmen für die Einrichtung, Simulation und Nachbearbeitung dynamischer TRNSYS-Simulationen, der am SPF entwickelt wurde (https://pytrnsys.readthedocs.io/en/latest/index.html).

SPF entwickelte neuartige mathematische Modelle, die das Energieverhalten der Hauptkomponenten von Solarkraftwerken darstellen, sowie vollständige Systemmodelle für die gesamten CR- und PTC-CSP-Anlagen, einschliesslich der Speichertechnologien mit zwei Tanks (als Referenzfall) und Thermoklinenspeichern. Die Entwicklung dieses Simulationsrahmens hatte zwei Hauptziele. Erstens sollte die Energieleistung des Thermoklinen-CSP-Systems mit dem Referenzfall unter Verwendung von zwei konventionellen Salzschmelztankspeichern verglichen werden. Zweitens wurden parametrische Studien durchgeführt, um die Fähigkeiten und Grenzen des Thermoklinensystems für verschiedene Schemata und Grössen zu untersuchen und so seinen Betrieb zu optimieren. Es wurden wirtschaftliche Analysen durchgeführt, insbesondere zur Bewertung der Investitions- und Betriebskosten, um die technisch-wirtschaftliche Machbarkeit der neuen Thermoklinentechnologie im Vergleich zur modernen Zwei-Tank-Technologie zu ermitteln.

Energiesimulationen mit der neuen Pytrnsys-Umgebung zeigen einen direkten Zusammenhang zwischen der Energieeffizienz von CSP-Anlagen und der Steuerungsstrategie für den Betrieb des Thermoklinetanks. Die Steuerungsstrategie der Thermokline unterscheidet sich von der des Zwei-Tank-Systems, da sie nicht nur von der Masse und den Wärmekapazitäten der Materialien und den maximalen und minimalen Betriebstemperaturen abhängt, sondern auch von den Temperaturschwellen, die zur Steuerung der Lade- und Entladevorgänge des Thermoklinetanks verwendet werden. Durch die Änderung dieser Temperaturschwellen ist es möglich, mehr oder weniger Wärmeenergie im Thermoklinetank zu speichern, was einen erheblichen Einfluss auf die Wärmeenergie hat, die schliesslich in Elektrizität umgewandelt werden könnte.

Eine Sensitivitätsanalyse hat gezeigt, dass Thermokline-CSP-Systeme im Vergleich zu herkömmlichen Zwei-Tank-Systemen zwischen 70% und 100% des Stroms erzeugen, je nach vorheriger Lade- und Entladetemperaturschwelle bei gleicher Nennkapazität, die je nach Definition der Nennbedingungen unterschiedlich sein kann. Konkret erzeugt die Thermokline-CR-CSP-Anlage bei dem in dieser Studie gewählten Temperaturgrenzwert 12,8% weniger Strom als eine herkömmliche CR-Anlage mit zwei Tanks, während ein PTC-System im Vergleich zum herkömmlichen System mit zwei Tanks 3,1% weniger Strom erzeugt. In Bezug auf den Kapazitätsfaktor der CR-CSP-Anlage bedeutet dies eine

Reduzierung des Kapazitätsfaktors von 71% für die herkömmliche Zwei-Tank-Salzschmelze auf 62% für den Thermoklin-Tank und für die PT-CSP von 45% auf 43%. Daher wird erwartet, dass Thermoklin-Systeme, die im Vergleich zu Zwei-Tank-Systemen mit der gleichen Energiekapazität dimensioniert sind, im Vergleich zu Zwei-Tank-Systemen etwas weniger Strom erzeugen. Um die gleiche Menge an planbarem Strom zu erzeugen, sollte ein Thermoklinenspeicher daher so konzipiert werden, dass er unter Nennbedingungen mehr (von 5% bis 25%) Energie speichert als Zwei-Tank-Systeme, da die Energieeffizienz aufgrund des Fehlens eines perfekt geschichteten Thermoklinenspeichers geringer ist und die Schwellenwerte für die Lade- und Entladetemperatur berücksichtigt werden.

Die oben erwähnten erwarteten Einsparungen bei den Investitionskosten durch die Reduzierung der Anzahl der Tanks um zwei wurden aufgrund der erhöhten Komplexität und Kosten der Tankkonstruktion, die für die Bewältigung grösserer Gewichte und thermischer Belastungen erforderlich ist, nicht vollständig erreicht. Darüber hinaus bleiben die wirtschaftlichen Bewertungen der Kosten für Thermoklinentanks trotz eingehender struktureller Analysen unsicher, insbesondere was die Endkosten des strukturierten Füllstoffs, seine Montage im Inneren des Gefässes und die strukturellen Kosten des Tanks betrifft. Diese Unsicherheiten in der strukturellen Gestaltung und im Füllmaterial wirken sich auf die TES-Investition und damit auf die Gesamt-CAPEX-Einsparungen der Anlage aus. Von den erwarteten 5% bis 10% liegen die tatsächlichen geschätzten Einsparungen in der gesamten CSP-Anlage im Bereich von 3% bis -10% für CR-Anlagen und von 7% bis -9% für PTC-Anlagen. Negative Werte zeigen an, dass die Newcline-Systeme zu höheren CAPEX-Kosten führen als herkömmliche Zwei-Tank-Systeme. Die Spanne ergibt sich aus mehreren Kostenannahmen und Unsicherheiten.

Der entscheidende Faktor zur Reduzierung von Unsicherheiten ist die Minimierung der Unsicherheit sowohl bei der Herstellung der Füllziegel als auch bei der Montage. Während des gesamten Projekts wurden verschiedene Ziegelmodelle und chemische Zusammensetzungen auf ihre thermische Leistung sowie chemische Stabilität und Kompatibilität hin untersucht. Die mit der Massenproduktion von Ziegeln verbundenen Kosten wurden jedoch nicht vollständig untersucht. Ausserdem wurde das aktuelle Ziegelmodell für die Produktion in einer Pilotanlage entwickelt, die einen manuellen Prozess verwendet. Eine Skalierung auf eine kommerzielle Anlage würde eine grosse Anzahl von Ziegeln erfordern, was durch ein neues, wahrscheinlich grösseres Ziegelmodell verbessert werden könnte, das speziell auf den kommerziellen Einsatz zugeschnitten ist. Dies würde den Montageaufwand reduzieren und zu einer kostengünstigeren Produktion führen. Folglich wären die Entwicklung eines neuen Ziegelmodells und die Bewertung seiner Massenproduktionskosten die nächsten Schritte, um Unsicherheiten weiter zu reduzieren.

Untersucht man die Unterschiede zwischen den Investitionskosten von CR- und PTC-Systemen, so hängt der Vorteil der Salzreduzierung beim Thermoklinenkonzept mit Füllmaterialien vom Anteil der Kosten für geschmolzenes Salz an den Gesamtinvestitionen der Anlage ab. Das relative Gewicht der Salzkosten hängt weitgehend von der maximalen und minimalen Betriebstemperatur des Systems ab. Bei gleicher nomineller Speicherkapazität benötigen Systeme mit geringerer Temperaturdifferenz, wie z. B. PTC (95 K), mehr Salzmasse als Systeme wie CR mit höherer Temperaturdifferenz (265 K). Folglich profitieren Systeme mit geringerer Temperaturdifferenz wie PTC oder industrielle Anwendungen eher vom Newcline-Thermoklinenkonzept. Thermoklinensysteme weisen auch eine konstante Kosteneffizienz bei den Betriebskosten (OPEX) auf, da die Reduzierung der Anzahl der Tanks die Wartungskosten senkt.

In Bezug auf die LCOE können PTC-Systeme im Vergleich zu herkömmlichen Zwei-Tank-Systemen bis zu 6% günstiger sein, wenn man den niedrigsten Kostenwert für beide Technologien zugrunde legt. Allerdings kann das Thermoklinensystem auch eine um 10% höhere LCOE aufweisen, wenn man die höheren Kostenannahmen beider Technologien zugrunde legt, was durch die höheren Unsicherheiten beeinflusst wird, die in hohem Masse mit dem Füllmaterial zusammenhängen. Für CR-Anlagen und die in diesem Projekt angenommenen Kosten bietet die Implementierung von Thermoklinenspeichern keinen wirtschaftlichen Vorteil in Bezug auf die LCOE. Die Hauptgründe dafür sind die geringere Menge an Salzen, die im Zwei-Tank-System verwendet werden, sowie die geringere Stromerzeugung durch das Thermokline-Konzept. Letzteres könnte durch eine Vergrösserung des Thermoklinenspeichers ausgeglichen werden, aber dieser Fall wurde im Rahmen des Projekts nicht untersucht.

Insgesamt könnte das neuartige Thermoklinenspeichersystem, das im Rahmen des Newcline-Projekts entwickelt wurde, für Systeme von Vorteil sein, bei denen die Kosten für Salzschmelze einen erheblichen Teil der Gesamtinvestition ausmachen, wie z. B. bei PTC-CSP-Anlagen. Ausserdem wird erwartet, dass es für kleinere Mengen, wie hier analysiert, kostengünstiger ist. Dies erweitert die potenziellen Anwendungen von Thermoklinenkonzepten über CSP-Anlagen hinaus auf industrielle Prozesse, bei denen Hochtemperaturspeicher dazu beitragen könnten, Flexibilität zu bieten oder den Einsatz zu erweitern, wenn intermittierende Quellen wie konzentrierende Solartechnologien die wichtigste erneuerbare Quelle sind. Obwohl der Kostenvorteil bei Anwendungen, die kleiner als CSP-Anlagen sind, nachgewiesen und quantifiziert werden muss, wurden mehrere industrielle Prozesse identifiziert, die von einer solchen Speicherung profitieren könnten: Lebensmittelverarbeitung (Backen oder Kurzzeiterhitzung (HTST) bei hohen Temperaturen, Pasteurisierung und Trocknungsprozesse), chemische Industrie (Polymerisations- oder Destillationsprozesse), pharmazeutische Industrie (Sterilisations- und Trocknungsprozesse), Textilindustrie (Färben und Trocknen), Papierindustrie und Automobilindustrie u. a.

Résumé

Le projet Newcline est axé sur le développement et l'analyse d'un nouveau concept de stockage pour les centrales solaires à concentration (CSP), remplaçant les deux réservoirs de sels fondus traditionnels par un seul réservoir thermocline avec un matériau de remplissage. L'objectif est de réduire les coûts d'investissement pour le stockage de l'énergie thermique dans les centrales solaires à concentration grâce à la réduction du nombre de réservoirs et de sels fondus. Le réservoir thermocline, conçu pour minimiser le mélange des températures chaudes et froides, incorpore un nouveau matériau de remplissage en céramique structuré, ce qui réduit considérablement le volume de sels requis pour la même capacité de stockage. La diminution du volume de sels réduit les coûts d'investissement (CAPEX) et de maintenance (OPEX). Dans la proposition de projet, les économies prévues en matière de coûts d'investissement pour le sous-système de stockage ont été estimées à 40%. Il en résulterait des économies globales de CAPEX pour la centrale CSP de 5% à 10%, selon le type de centrale CSP utilisé. Deux types de centrales solaires à concentration, le récepteur central (CR) et le collecteur cylindro-parabolique (PTC), sont pris en compte dans le cadre du projet.

Le projet global a été mis en œuvre par cinq partenaires internationaux différents sous l'égide du CSP-ERANET, englobant diverses tâches, telles que le développement de matériaux de remplissage, la caractérisation CFD des processus de transfert de chaleur, le laboratoire expérimental et l'analyse de la thermocline à grande échelle, les analyses structurelles du réservoir de la thermocline et les simulations du système transitoire de l'ensemble de la centrale solaire à concentration. Les contributions spécifiques de SPF-OST ont porté sur le développement d'un cadre de simulation permettant de réaliser des simulations dynamiques afin d'intégrer ce nouveau concept de stockage dans les centrales solaires à concentration. Ce cadre de simulation est basé sur l'environnement de simulation pytrnsys, un cadre open-source pour la mise en place, la simulation et le post-traitement des simulations dynamiques TRNSYS développées au SPF (https://pytrnsys.readthedocs.io/en/latest/index.html).

SPF a développé de nouveaux modèles mathématiques représentant le comportement énergétique des principaux composants des centrales solaires et des modèles de systèmes complets pour l'ensemble des centrales CR et PTC CSP, y compris les technologies de stockage à deux réservoirs (comme cas de référence) et à thermocline. Le développement de ce cadre de simulation avait deux objectifs principaux. Premièrement, comparer la performance énergétique du système CSP thermocline avec le cas de référence utilisant deux réservoirs de sels fondus pour le stockage conventionnel. Deuxièmement, mener des études paramétriques pour explorer les capacités et les limites du système thermocline pour différents schémas et tailles afin d'optimiser son fonctionnement. Des analyses économiques, évaluant spécifiquement les CAPEX et OPEX pour déterminer le coût de l'énergie nivelé (LCOE), ont été menées pour évaluer la faisabilité technico-économique de la nouvelle technologie thermocline par rapport à la technologie de pointe à deux réservoirs.

Les simulations énergétiques réalisées avec le nouvel environnement pytrnsys indiquent un lien direct entre la performance énergétique des centrales solaires à concentration et la stratégie de contrôle du fonctionnement du réservoir thermocline. La stratégie de contrôle de la thermocline diffère de celle du système à deux réservoirs car elle dépend non seulement des capacités massiques et thermiques des matériaux et des températures maximales et minimales de fonctionnement, mais aussi des seuils de température utilisés pour contrôler les processus de chargement et de déchargement du réservoir thermocline. En modifiant ces seuils de température, il est possible de stocker plus ou moins d'énergie thermique dans le réservoir thermocline, ce qui a une influence significative sur l'énergie thermique qui pourrait être convertie en électricité.

Une analyse de sensibilité a démontré que les systèmes CSP thermocline produisent entre 70% et 100% de l'électricité par rapport aux systèmes conventionnels à deux réservoirs, en fonction des seuils de température de charge et de décharge précédents, pour une capacité nominale identique, qui peut varier en fonction de la définition des conditions nominales. Plus précisément, pour le seuil de température choisi dans cette étude, la centrale CSP CR thermocline produit 12,8% d'électricité en moins qu'une centrale CR classique à deux réservoirs, tandis qu'un système CTP produit 3,1% d'électricité en moins par rapport au système classique à deux réservoirs. En termes de facteur de capacité de la centrale CR CSP, cela représente une réduction du facteur de capacité de 71% pour le système conventionnel à deux réservoirs de sels fondus à 62% pour le réservoir thermocline, et de 45% à 43% pour le système PT CSP. Ainsi, quel que soit le cas, les systèmes thermocline dimensionnés avec la même capacité énergétique que les systèmes à deux réservoirs devraient produire un peu moins d'électricité que les systèmes à deux réservoirs. Ainsi, pour obtenir la même production d'électricité distribuable, un système de stockage thermocline doit être conçu pour stocker davantage d'énergie (de 5% à 25%) dans des conditions nominales par rapport aux systèmes à deux réservoirs, en raison de la moindre efficacité énergétique due au fait que le stockage thermocline n'est pas parfaitement stratifié et compte tenu des seuils de température de chargement et de déchargement.

Les économies de coûts d'investissement anticipées susmentionnées résultant de la réduction du nombre de réservoirs par deux n'ont pas été entièrement réalisées en raison de la complexité et du coût accru de la conception structurelle du réservoir nécessaire pour gérer des poids et des contraintes thermiques plus importants. En outre, les évaluations économiques des coûts des cuves thermoclines restent incertaines malgré une analyse structurelle approfondie, notamment en ce qui concerne le coût final du remplisseur structuré, son assemblage à l'intérieur de la cuve et le coût structurel de la cuve. Ces incertitudes concernant la conception structurelle et le matériau de remplissage ont un impact sur l'investissement dans le système de traitement des eaux usées et, par conséquent, sur les économies globales de CAPEX de l'usine. Des 5% à 10% prévus, les économies réelles estimées dans l'ensemble de la centrale CSP sont comprises entre 3% et -10% pour les centrales CR et entre 7% et -9% pour les centrales PTC. Les valeurs négatives indiquent que les systèmes Newcline entraînent des dépenses en capital plus élevées que les systèmes classiques à deux réservoirs. Cette fourchette est le résultat de plusieurs hypothèses de coûts et d'incertitudes.

Le facteur décisif pour réduire les incertitudes est de minimiser l'incertitude dans la fabrication et l'assemblage des briques de remplissage. Tout au long du projet, divers modèles de briques et compositions chimiques ont été évalués pour leur performance thermique, leur stabilité chimique et leur compatibilité. Cependant, les coûts associés à la production de masse des briques n'ont pas été entièrement étudiés. En outre, la conception actuelle des briques a été développée pour la production d'une usine pilote utilisant un processus manuel. Le passage à l'échelle d'une usine commerciale nécessiterait un grand nombre de briques, qui pourraient être améliorées grâce à un nouveau modèle de brique, probablement plus grand, conçu spécifiquement pour une utilisation commerciale importante. Cela réduirait l'effort d'assemblage et permettrait une production plus rentable. Par conséquent, l'élaboration d'un nouveau modèle de brique et l'évaluation de ses coûts de production de masse constitueraient les prochaines étapes pour réduire davantage les incertitudes.

Si l'on examine les différences entre les CAPEX des systèmes CR et PTC, l'avantage de la réduction du sel grâce au concept de thermocline avec des matériaux de remplissage dépend de la proportion du coût du sel fondu dans l'investissement total de l'usine. Le poids relatif du coût du sel dépend largement de la température thermique maximale et minimale de fonctionnement du système. Pour une même

capacité de stockage nominale, les systèmes à faible différence de température, comme le PTC (95 K), nécessitent une masse de sel plus importante que les systèmes comme le CR avec une différence de température plus élevée (265 K). Par conséquent, les systèmes à faible différence de température, tels que le PTC ou les applications industrielles, sont plus susceptibles de bénéficier du concept de thermocline de Newcline. Les systèmes thermoclines font également preuve d'une rentabilité constante en termes de dépenses d'exploitation (OPEX), car la réduction du nombre de réservoirs diminue les coûts d'entretien.

En termes de LCOE, les systèmes PTC peuvent être jusqu'à 6% plus favorables que les systèmes conventionnels à deux réservoirs, si l'on considère la valeur de coût la plus basse supposée pour les deux technologies. Toutefois, le système thermocline peut également présenter un LCOE supérieur de 10% si l'on utilise les hypothèses de coût les plus élevées des deux technologies, ce qui est influencé par les incertitudes plus élevées associées, dans une large mesure, au matériau de remplissage. Pour les centrales CR et les coûts supposés dans ce projet, la mise en œuvre de stockages thermoclines n'offre aucun avantage économique en termes de LCOE. Les principales raisons sont la plus faible quantité de sels utilisée dans le système à deux réservoirs ainsi que la plus faible quantité d'électricité produite par le concept thermocline. Ce dernier pourrait être compensé en augmentant la taille du stockage thermocline, mais ce cas n'a pas été évalué au cours du projet.

Dans l'ensemble, le nouveau système de stockage thermocline développé dans le cadre du projet Newcline pourrait être potentiellement bénéfique pour les systèmes où le coût des sels fondus constitue une part importante de l'investissement total, comme les centrales CSP PTC. On s'attend également à ce que ce système soit plus rentable pour les petits volumes tels qu'ils sont analysés ici. Cela étend les applications potentielles des concepts de thermocline au-delà des centrales solaires à concentration, aux processus industriels où les stockages à haute température pourraient contribuer à la flexibilité ou à l'extension de l'utilisation de l'exploitation lorsque des sources intermittentes telles que les technologies solaires à concentration constituent la principale source d'énergie renouvelable. Bien qu'il faille prouver et quantifier les avantages en termes de coûts pour les applications à une échelle inférieure à celle des centrales solaires à concentration, plusieurs procédés industriels ont été identifiés comme pouvant bénéficier de ce type de stockage : L'industrie alimentaire (cuisson ou pasteurisation à haute température et à court terme, et processus de séchage), l'industrie chimique (polymérisation ou processus de distillation), l'industrie pharmaceutique (stérilisation et processus de séchage), l'industrie textile (teinture et séchage), l'industrie du papier et l'industrie automobile, entre autres.

Contents

List of Acronyms

CAPEX   capital expenditures

CFD   computational fluid dynamics

CR   central receiver

CSP   concentrated solar power

DMT   dual-medium thermocline

DNI   direct normal irradiance

FVM   Finite Volume Method

GUI   graphical user interface

HCE   heat collection element

HTF   heat transfer fluid

HX   heat exchanger

LCOE   levelized cost of energy

OPEX   operating expenses

PCM   phase change material

PTC   parabolic trough collector

PV   photovoltaics

SCA   solar collector assembly

SM   solar multiple

SMT   single-medium thermocline

SOC   state-of-charge

TES   thermal energy storage

TRL   technological readiness level

1 Introduction

1.1 Motivation

While concentrated solar power (CSP) plants are promising candidates for systems converting solar power to electricity, the resulting levelized cost of energy (LCOE) when employing them still is comparably high (IRENA, 2012) respect to photovoltaics (PV). The main potential advantage of CSP compared to PV is the possibility to provide electricity in the evening hours after sunset efficiently by the use of a thermal energy storage.

Although thermal energy storage (TES) equips the CSP plant with a decisive advantage, it contributes significantly to its capital cost. A typical molten-salt two-tank storage makes up around 20 % of the capital expenditures (CAPEX) for a parabolic trough collector (PTC) CSP plant and around 10 % for a central receiver (CR) CSP plant (IRENA, 2012). Around half the cost for such a storage system is caused by the salt itself, and the majority of the remaining cost is for the storage vessel (Kolb, 2011, Kolb and Hassani, 2006, Kolb et al., 2011). Hence, using one tank instead of two and reducing the amount of salt needed for the thermal storage by replacing it with a cheaper alternative material are direct measures to reduce the LCOE of CSP plants.

Beyond CSP power plants, storing thermal energy at temperatures above 300 °C is also relevant in industrial processes. Furthermore, potential applications are the second life of steam turbines of power plants formerly fed by fossil fuels, where high temperature energy storages could be used to store excess electrical energy to be used to drive the turbine for times of high electricity demand later. Hence, the topic of molten salt storages is also interesting for industrial processes and therefore could also be employed in geographical regions with low direct normal irradiance (DNI).

1.2 State-of-the-art and previous research of TES in CSP plants

Most of CSP plants use a two-tank molten salt system for TES to decouple solar energy production from electricity generation. This approach allows for more flexible electricity generation and reduces the need for expensive power equipment, such as turbines and related components, to extract the thermal energy peak of the concentrating solar generator.

The state-of-the-art CSP storage technology consist of a two-tank TES system where hot and cold molten salts are stored separately. The molten salts are exchanged between the two tanks based on the system's operational mode. During charging, the molten salt from the cold storage tank is heated by the solar generator and transferred to the hot storage tank. Conversely, during discharging, the hot salt is cooled as it transfers heat to the power cycle before being pumped to the cold storage tank. As a result of this operation, a portion of each tank's volume is always unused (typically filled with an inert gas), requiring a storage container with a volume capacity approximately twice of the total volume of molten salts.

In order to reduce the unnecessary volume of the two-tank system, the concept of a *thermocline* storage tank was introduced in previous research by various authors (Herrmann and Kearney, 2002, Kolb and Hassani, 2006, Pacheco et al., 2001). The word thermocline refers to the temperature gradient which forms naturally between the hot and the cold fluid due to density gradients. A thermocline tank stores both hot and cold molten salt in the same vessel. This approach reduces the need for additional storage volume and lowers costs by eliminating the need for a second tank, though it requires careful management to prevent mixing between different temperatures and maintain efficiency. Storing the hot and cold heat transfer medium in the same vessel is not a new idea. Most thermal energy storages, e.g. water storages for building applications, use the same concept. However, a significant difference exist as explained below.

There are two main thermocline molten salt TES concepts: the single-medium thermocline (SMT), when the tank uses only fluid, like molten salt; and the dual-medium thermocline (DMT), where a cheap filler material is placed inside the vessel. As stated in Boubou et al. (2021), the evaluation by means of numerical simulation shows a higher thermal performance of the molten salt SMT than the dual-medium thermocline (DMT). Nevertheless SMT molten salt tank are more sensible to flow disturbances than DMT. Furthermore, DMT has an additional key benefit compared to the SMT concept: the filler material reduces the quantity of molten salts required, which typically are more expensive. That results in DMT as a more promising technology and consequently, current research and developments are focused in this technology.

The filler material used in most of the previous dual-medium thermocline (DMT) research activities is based on stones. The vessel is packed with these stones and therefore the storage concept is known as *packed-bed* thermocline storage. The resulting heat storage capacity of the DMT is that from the solid stones and from the liquid heat transfer medium flowing between them. In Angelini et al. (2014) a finite-difference numerical model, validated with previous experimental results of Pacheco et al. (2002), was developed to predict the performance of the thermocline storage with a quartzite-rock packed-bed. In this analysis the thermocline storage shows an overall storage efficiency between the charging and discharging process of 64.2 % and a cost reduction of 33 % is stated. In Flueckiger et al. (2012), a detailed CFD simulation of a packed-bed thermocline tank was performed to evaluate mechanical stresses and thermal ratcheting potential. Different operation strategies of packed-bed thermocline tanks operation in CSP plants were analysed in Biencinto et al. (2014). As a general conclusion of this analysis it was stated that the annual electricity yield of a solar thermal power plant with a thermocline tank is slightly lower than with the conventional two-tank molten salt TES system because, despite both cases have the same nominal storage capacity, *«the thermocline tanks develop a temperature profile that disminishes the available thermal energy at maximum temperature, and hence the useful energy that can be extracted»*. In Bruch et al. (2014), a pilot-scale for a oil/rock thermocline thermal energy storage was experimentally studied and a 1-D model for the dual-medium thermocline was developed and validated. Mira-Hernández et al. (2014) analysed two types of molten-salt thermocline with and without packed bed (quartzite rock) by means of CFD. In Galione et al. (2015), the packed bed concept was extended to a multilayered solid-PCM (consisting of a thermocline tank combining layers of solid and phase change filler materials) which would result in lower thermocline degradation throughout consecutive charging and discharging cycles. In Hoffmann et al. (2016), two different models, one considering an homogeneous medium and a second, distinguishing between the solid and continuous and flowing through the void fraction, were compared.

There are several benefits of thermocline tank technologies compared to two-tank molten salt systems by the fact of reducing to the half the number of tanks:

- Reduction of heat losses (e.g. only one instead of two tanks).

- Reduction of ancillary equipment to tanks.

- Simpler handling of the gas on top of the molten salt (less losses, easier control).

- Utilisation of lower cost short shaft pumps (compared to long shaft pumps) which also leads to the possibility to increase the height of the tank.

- Reduction of the unused sump salt volume.

- Reduced ground space required.

1.3 Innovation and progress of Newcline

The state-of-the-art of TES in CSP plants relies on the two-tank molten salt storage as storage system. Recent research, however, has been exploring thermocline TES storage, which primarily includes two types: single-medium and dual-medium thermocline systems (employing packed-bed as solid filler medium). Dual-medium envisaged the following benefits over the single medium thermocline storage tanks for CSP, becoming the most promising thermocline technology:

- Large cost reduction potential if inexpensive filler material can replace molten salt which is the major aspect for TES CAPEX cost reduction.

- Significant reduction of the size of the second drainage/repair tank due to the small salt fraction.

- Minor influences in stratification regarding flow inlet-outlet disturbances.

The Newcline project, on the basis of the dual-medium thermocline technology, introduces an innovative approach by incorporating a cost-effective ceramic structured filler, replacing the rocky packed-bed approach

used in the previous research for DMT, and an additional complementary PCM layer concept. This novel concept is expected to achieve a higher reduction of CAPEX for the TES compared to the conventional two-tank molten salt (Klasing et al., 2020).

The energetic performance and cost-effectiveness of thermocline packed-bed storages depend on several characteristics, e.g. density, specific heat and particle size of the packed-bed. The flexible design of the Newcline's structured fillers allows the optimisation of all these factors within the same ceramic structured filler design process. Within Newcline's project, an innovative refractory material filler, the so-called *thermocline filler checker* (TCF-checker)[1] has been developed with additional advantages compared to packed-bed filler concept of previous research:

- Significant further reduction of the volume fraction of salt by refractory checker geometry design with low void fraction (e.g., channel design).

- Adjustable flow distribution by checker geometry design.

- Defined chemical composition of refractory checkers (e.g. compared to natural stone) which allows on-site quality control in the construction phase.

- Reduction of thermal stress between filler and tank wall (thermal ratcheting) due to refractory checker rather than the previous experienced packed-bed design.

- Simpler opening of side tank walls for repair.

- Potential for using waste materials as raw material for the checker's manufacture as circular economy.

Prior to this project, lab-scale validation (unpublished) confirmed the compatibility of Solar Salt with both the novel filler material developed by the consortium partner Kraftblock and other slag-based materials, achieving a Technology Readiness Level (TRL) of 4.

To validate the dual-medium thermocline technology based on the ceramic structured filler developed within Newcline project, different models at various scales and experimental setups have been developed. computational fluid dynamics (CFD) models for the structured filler material were developed and experimentally validated by the consortium's partner Universitat Politècnica de Catalunya (UPC). The Deutsches Zentrum für Luft- und Raumfahrt (DLR) developed an energetic model of the thermocline tank in Matlab validated through pilot-scale experiments at the DLR's thermal energy storage molten salt facility TESIS. To our knowledge, a thermocline tank with structured ceramic material has never before been experimentally tested at the size and capacity of the TESIS facility bringing this new technology to TRL 5.

Complementary, SPF has developed the simulation framework for the whole CSP plants in which the thermocline tank technology is integrated. This pytrnsys simulation framework has enabled the assessment of the energy performance of the thermocline technology, developed within the Newcline's project, integrated into the CSP plant. This simulation framework was used to compare the energy performance of the state-of-the-art two-tank storage system with the NewCline's termocline development for CSP plants. Moreover, by modelling the complete CSP plan using the pytrnsys simulation framework, it has been found that the performance of thermocline systems is influenced not only by the capacity or design of the thermocline tank and its filler, as was stated in previous research, but also by the temperature threshold limits imposed during the thermocline's charging and discharging processes during the operation. Those temperature thresholds impact the operational storage capacity, and consequently the thermal energy stored and eventually converted into electricity. By means of system simulations these effects have been quantified for at the system level for the first time.

---

[1]A checker is a structured refractory ceramic element, which is resistant to heat/chemical decomposition, employed as heat storage or exchange element used in regenerative furnaces such as those found in some industries, improving the thermal efficiency of the furnace.

2 Project framework and objectives

2.1 Project objective

The overall objective of the European *ERA-NET Newcline* (`http://www.newcline.eu/`) is to develop new thermocline concepts, able to reduce the storage capital costs up to 40 % compared to the conventional two molten salt storage tanks, that can be applied to different CSP plants (parabolic trough collector, central receiver, linear Fresnel). Two concepts will be explored. The first concept involves the use of innovative structured ceramic filler. The other one is an innovative combination of solid filler material (the ceramic one is the preferred option) with specially selected encapsulated PCM located at the top and bottom regions of the tank.

Both concepts will be tested in a lab-scale setup, and their Technological readiness level (TRL) will be increased from TRL 4 to TRL 6 through demonstrations at a relevant pilot scale of 4 MWh with at least 50 charge/discharge cycles. Finally, both concepts will be evaluated and optimized in terms of system integration and LCOE savings on a CSP system level and up-scaling for CSP target applications. This last step is where *SPF* is involved by developing the simulation framework and optimizing the operation of new thermocline concepts into the CSP plant.

2.2 SPF Specific objectives

The specific objectives of SPF's contribution for the *ERA-NET Newcline* project are:

- Extend the existing *TRNSYS* simulation framework *pytrnsys* to feature a CSP system including its components.

- Develop/extend *TRNSYS types* to simulate a total of four cases: parabolic trough and central receiver plants, each with two tank solutions and both single tank thermocline concepts.

- Implement and validate a thermocline storage tank *type* in *TRNSYS*.

- Optimize the integration of the thermocline solutions through system simulation studies.

- Conduct a techno-economic analysis of the simulation results to assess the LCOE reduction potential of the thermocline single-tank solution with the two approaches. The target value for this is at least 5 % to 10 % LCOE reduction compared to the two-tank solution.

2.3 Consortium

Newcline project, which consortium is formed by Universitat Politècnica de Catalunya-BarcelonaTech (UPC), the Deutsches Zentrum für Luft- und Raumfahrt e. V. / German Aerospace Center (DLR), SPF Institute for Solar Technology - Eastern Switzerland University of Applied Sciences (OST), Kraftblock GmbH (KB) and Empresarios Agrupados Internacional, S.A. (EAI), is supported by the European Commission within the EU Framework Programme for Research and Innovation HORIZON 2020 (Cofund ERA-NET Action, N° 838311).

Hereafter, a brief description of the other four European partners involved in the consortium *CSP ERANET Newcline*:

- *Universitat Politècnica de Catalunya (UPC)* is a Catalan university located in Terrassa (Barcelona). Within the UPC, the technological center of heat and mass transfer (CTTC) is leading the whole project. Their main expertise is on computational fluid dynamics in the relevant field.

- *Empresarios Agrupados (EAI)* is a Spanish engineering firm with a strong experience in thermal storage systems for CSP plants and provides support in the engineering and design aspects of the project.

- The *Thermal Process Technology* department of the *German Aerospace Center DLR* has been involved in the development of high-temperature thermal energy storage over decades. *Newcline* will employ the institution's testing facility *TESIS* in Cologne to demonstrate its two filler concepts on a pilot scale.

- *Kraftblock* is a German company founded in 2014 that develops and sells high-temperature (up to 1300 °C) energy storage systems. It follows a sustainable approach using 85 % recycled raw materials. *Kraftblock's* task within *Newcline* is the material development.

2.4 Report structure

This report deals with the developments and works carried out only by SPF, in the framework of *Newcline* project.

This report will be organised into 3 main sections which cover the main three tasks in which SPF is in charge. Section 3 covers the development of the simulation framework of CSP plants in the *pytrnsys* environment. In section 4 we report on the energy system performance and LCOE analyses of the new thermocline concept in CSP Plants. Finally, in section 5 we analyse different plant schemes and sizes an its influence in the LCOE of CSP Plants.

3 Simulation framework development for CSP plants

3.1 Introduction

The development of the simulation framework is carried out on the well-known dynamic simulation environment for dynamic simulations *TRNSYS* (Klein et al., 2010). In this regard, SPF has developed the *pytrnsys*[2], an open source python framework specific for *TRNSYS* which allows for a user-friendly way to set up, execute and process *TRNSYS* simulations. A graphical user interface (GUI) coupled with a flow solver supports the creation of hydraulic schemes and allows visualisation of the mass flow rates and temperatures determined by the simulations. This simulation framework has been adapted to support the simulation of CSP plants in the framework of the *Newcline* project.

In order to do that, as a first step, several new models representing different components or subsystems of CSP plants have been developed in the *TRNSYS* environment. Two of these nine new models have been developed by means of fitting functions, using data from other simulation softwares, i.e. *THERMOFLEX*[3] and *SAM*[4].

- *SAM*, is a dynamic simulation software developed by the U.S. Department of Energy's National Renewable Energy Laboratory (NREL), which can model many different renewable energy systems, among them, parabolic trough collector (PTC) and central receiver (CR) CSP systems (but no thermocline storage is included among them).

- *THERMOFLEX* is a software used to model and simulate power plants by means of heat and mass balances in steady-state conditions. The software includes different component models for all types of power plants, including steam and combined cycles as well as renewable energy plants.

In section 3.2, there is a description of the models especially developed for the *Newcline* project. As a second step, and using the aforementioned developed *TRNSYS* component models, different CSP plants have been modelled featuring both the reference system (with the conventional two-tank molten salt energy storage) and the new thermocline concepts.

In section 4, there is a description of the CSP system models developed for the *Newcline* project. The comparison between the state-of-the-art two-tank and the thermocline storage solutions in CSP plants is one of the main targets of the system simulations within the *Newcline* project. Thus, setting up a reliable simulation framework of a CR and a PTC system with two-tank storages is a vital part of this task. Consequently, the reference systems using the two-tanks developed in *pytrnsys* are compared with the numerical simulations provided by *EAI* using by *SAM* with an hourly resolution for a whole year. These results are provided in sections 4.1.3 and 4.2.3 for the CR and PTC respectively.

3.2 Development of energetic models

TRNSYS has an extended library of different components of thermal systems. However, most of them are based on the assumption of constant fluid's thermophysical properties. However, when modelling a CSP systems, it becomes necessary to account for variant thermophysical properties due to the significant temperature variations involved. For this reason, the *STEC TRNSYS* library was developed during 1998-2006 as a *SolarPACES*[5] activity. This library consists of a collection of TRNSYS models especially developed to simulate solar thermal power generation. Unfortunately, these models correspond to earlier versions of TRNSYS, almost 20 years old that were difficult to update to new TRNSYS version. Consequently, the developed simulation framework in *pytrnsys* predominantly employs newly developed components with temperature-dependant properties for density and heat capacity. Only the PTC component was derived from an existing type (from the *TESS* library[6]), also with temperature dependant properties. The rest of TRNSYS components were developed from scratch by *SPF* for the *ERA-NET Newcline* project.

---

[2]https://pytrnsys.readthedocs.io
[3]https://www.thermoflow.com/products_generalpurpose.html
[4]https://sam.nrel.gov/concentrating-solar-power.html
[5]https://sel.me.wisc.edu/trnsys/trnlib/stec/stec.htm
[6]http://www.trnsys.com/tess-libraries/index.html

An overview of the various components can be found in Tab. 1.

component	type	model
Central receiver (CR)	-	fitting functions*
PTC field	2257	modified *TESS* type1257
Power Block	-	fitting functions*
Heat exchanger	991	new *TRNSYS* type
Molten salt tank	2261 2262	new *TRNSYS* type
Thermocline tank	2263	new *TRNSYS* type
CR control	897	new *TRNSYS* type
PTC control	898	new *TRNSYS* type
HX control	899	new *TRNSYS* type

Table 1: Overview of the main TRNSYS components that are used for the simulations within the current project. * fitting functions are implemented as equations in the deck file.

Since the core of this project is the thermal storage employed in CSP plants, we tried to decrease the complexity of models of other components as much as possible. In particular, we aimed at representing the CR and the power block of both CSP plants investigated through simple linear and quadratic functions (see section 3.2.1 and 3.2.3). These functions were fit to simulation data from *SAM* and *THERMOFLEX* simulation environments provided by *Empresarios Agrupados* (*EAI*) (Spain).

3.2.1 Central receiver

The central receiver operates at a fixed output temperature $T_{rec, out} = 565\,°C$. To achieve this output temperature for varying solar irradiance levels impinging on the mirror field, the mass flow rate through the central receiver is varied. By analysing the data from *SAM* simulations, the response of the receiver mass flow rate to the normal irradiance was parameterised. As can be seen in Fig. 1, the dependency of these two terms falls into two regimes.
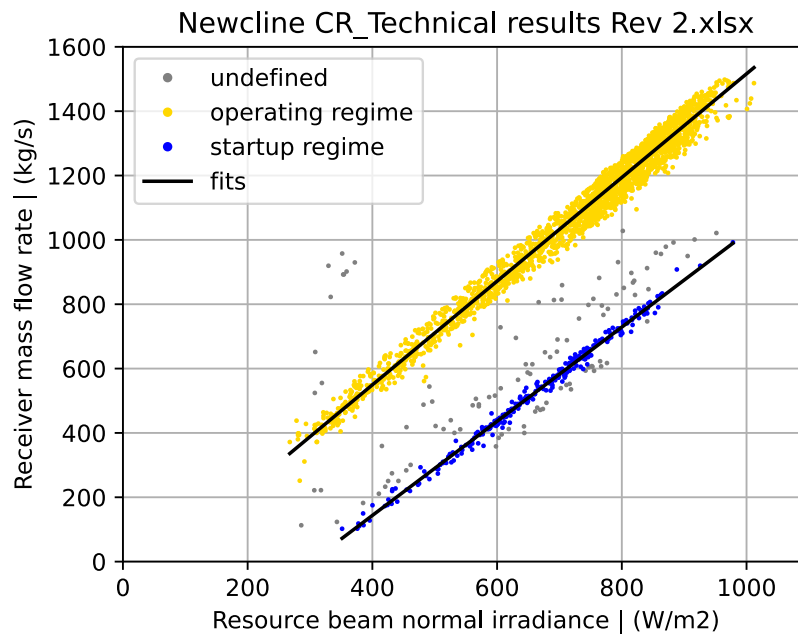

Figure 1: Fitting the mass flow rate through the central receiver in dependence of the normal irradiance. Two separate regimes were fitted with a linear function, as described in the text.

The regime marked in yellow is the regime of normal operation, while the one in blue is composed of points during the startup process. The few remaining points are shown in grey. Each regime is represented through a linear function of the form.

$$\dot{m}_{rec} = c \cdot (I - I_0) \tag{1}$$

Here $\dot{m}_{rec}$ is the mass flow rate through the receiver, c the linear coefficient, I the beam normal irradiance and I_0 the respective beam radiance offset.

The best fit values for both regimes can be found in the table Tab. 2:

regime	parameter	value
operating	c	1.611 kg m^2/(s W)
regime	I_o	59.051 W/m^2
startup	c	1.463 kg m^2/(s W)
regime	I_o	301.923 W/m^2

Table 2: Fit values for the different regimes for the central receiver parameterized curve.

This parameterization is referred to a solar field consisting of 15941 heliostats, each with an area of 96.3 m^2, resulting in a total mirror surface area of 1.535 million square meters. Parametric analyses for other sizes have been scaled accordingly based on this total mirror surface area.

3.2.2 Parabolic trough collector

The parabolic trough collector (PTC) is modelled based on the *TRNSYS TESS* type1257 which models one or more concentrating parabolic trough solar collectors connected in series. The model calculates the energy yield based on the energy absorption, heat losses, and fluid properties based on the work of Patnode (2006) among others. As thermo-physical properties of the fluid are temperature-dependent, an iterative numerical algorithm, using the Runge-Kutta method, is used.

The net energy collected by the PTC, $Q_{collected}$, is:

$$Q_{collected} = Q_{absorbed} - Q_{losses,HCE} \tag{2}$$

where $Q_{absorbed}$ is the solar radiation absorbed by the receiver tubes, the heat collection elements (HCEs), and $Q_{losses,HCE}$ are the thermal losses along the HCE.

The solar irradiation absorption is calculated based on the following equation:

$$Q_{absorbed} = DNI \cdot cos\theta \cdot IAM \cdot f_{RowShadow} \cdot f_{EndLoss} \cdot \eta_{field} \cdot \eta_{HCE} \cdot f_{SF,avail} \tag{3}$$

where DNI is the direct normal irradiance, θ is the angle of incidence, the IAM is the incidence angle modifier, $f_{RowShadow}$ is a performance factor that accounts for losses due to mutual shading of parallel collector rows, $f_{EndLoss}$ the performance factor that accounts for losses from collector's ends and $f_{SFAvail}$ is the fraction of the solar field that is operable and tracking the sun. The term η_{field} represents the field efficiency that accounts for losses due to mirror optics and imperfections. Specifically, it considers the twisting and tracking error, the geometric accuracy of the collector mirrors, the mirror reflectivity and its cleanliness. The efficiency term η_{HCE} accounts for losses due to HCE optics and imperfections and includes losses due to shading of HCE by dust on the glass envelope, the losses from shading due to the bellows, the transitivity of the glass envelope and the absorptance of the HCE selective coating. Other miscellaneous performance factors could be applied.

The receiver heat loss, $Q_{losses,HCE}$ is calculated using a linear regression heat loss model by means of the following equation:

$$Q_{losses,HCE} = a_0 + a_1 \cdot T + a_2 \cdot T^2 + a_3 \cdot T^3 + DNI \cdot (b_0 + b_1 \cdot T^2) \tag{4}$$

where T is the fluid bulk temperature, and a,b coefficients are provided for different vacuum levels in Patnode (2006).

Additionally to the original code from TESS, which was written originally by Jeff Thornton, a limiting operating temperature, simulating an idealistic solar collector field defocussing strategy, has been implemented in this type in order to avoid the overheating of the system.

3.2.3 Power block

The power block is a component of both the CR as well as the PTC system. For each of these two systems it operates, however, in quite different regimes. Hence, the power block is modelled separately for each system. Two types of functions are used to represent the power block. A linear one:

$$y = a \cdot x + y_0 \tag{5}$$

and a quadratic one:

$$y = a_0 + a_1 \cdot x + a_2 \cdot x^2 \tag{6}$$

Here, x is the argument of the function, y its value, a the slope of the linear function and y_0 the offset at $x = 0$. In the quadratic function a_0 denotes the constant, a_1 the linear and a_2 the quadratic coefficient.

The power block receives a certain mass flow rate $\dot{m}_{PB}$ of a heat transfer fluid at a certain temperature $T_{PB, in}$. Depending on these two variables the electrical power output to the grid $P_{el, grid}$ and the output temperature $T_{PB, out}$ vary. To fit equations 5 and 6 over the two input dimensions the fitting process was split into two steps. First, $\dot{m}_{PB}$ was fixed and the fits for $P_{el, grid}$ and $T_{PB, out}$ were done over $T_{PB, in}$. Then, another round of fits for the resulting coefficients a and y_0 or a_0 to a_2 respectively were done over $\dot{m}_{PB}$. All fits were done with the python *curve_fit*[7] routine.

Power block for CR system

For the power block of the CR system, *EAI* provided steady state simulation data generated through the software *THERMOFLEX* at three values for $\dot{m}_{PB}$ at four values of $T_{PB, in}$ each. First, each set for a fixed $\dot{m}_{PB}$ was treated separately. The electric power to the grid was fitted with:

$$P_{el, grid} = a \cdot T_{PB, in} + P_{el, 0} \tag{7}$$

and the outlet temperature with:

$$T_{PB, out} = a_0 + a_1 \cdot T_{PB, in} + a_2 \cdot T_{PB, in}^2 \tag{8}$$

The resulting fitted coefficients are shown in Figs 2 and 3. The evolution over different mass flow rates $\dot{m}_{PB}$ is shown in Fig. 2 a) for a, in Fig. 2 b) for $P_{el, 0}$ and in Fig. 3 a) to c) for a_0 to a_2. The error bars indicate the confidence intervals resulting from the fits. These coefficients were then again fitted with equation 5 over $\dot{m}_{PB}$, as shown by the black lines in the respective plots. This leads to the following equations mapping $P_{el, grid}$ and $T_{PB, out}$ over $\dot{m}_{PB}$ and $T_{PB, in}$:

$$P_{el, grid} (\dot{m}_{PB}, T_{PB, in}) = a (\dot{m}_{PB}) \cdot T_{PB, in} + P_{el, 0} (\dot{m}_{PB}) \tag{9}$$

$$T_{PB, out} (\dot{m}_{PB}, T_{PB, in}) = a_0 (\dot{m}_{PB}) + a_1 (\dot{m}_{PB}) \cdot T_{PB, in} + a_2 (\dot{m}_{PB}) \cdot T_{PB, in}^2 \tag{10}$$

Figs. 2 c) and 3 d) show the *THERMOFLEX* data (stars), *SAM* data (dots) and the results of the fitted functions for $P_{el, grid}$ and $T_{PB, out}$ respectively. For $P_{el, grid}$ shown in Fig. 2 the multilinear function corresponds well to both the *THERMOFLEX* and the *SAM* data. Deviations with respect to the *THERMOFLEX* data, which are significant but still below 10 %, can only be seen for points at which $\dot{m}_{PB}$ and $T_{PB, in}$ are low simultaneously. For $T_{PB, out}$ shown in Fig. 3, the fitted function deviates from the *THERMOFLEX* data by 1.3 % in the worst case. The deviation of the fitted function is worse for the comparison to the *SAM* data, especially for the lowest $\dot{m}_{PB} = 175$ kg/s. But even there, the deviation is less than 3 %.

---

[7]https://docs.scipy.org/doc/scipy/reference/generated/scipy.optimize.curve_fit.html

Figure 2: Fitting of the electric power-to-grid output of the power block of the CR system. Scaling factor a for various mass flow rates in a) and offset values in b). The results of the multilinear function (solid lines) are shown in comparison to the *THERMOFLEX* (TF) data (stars) over which the fits were done and in comparison to the *SAM* data (dots) in c). The mass flow rates are color-coded.
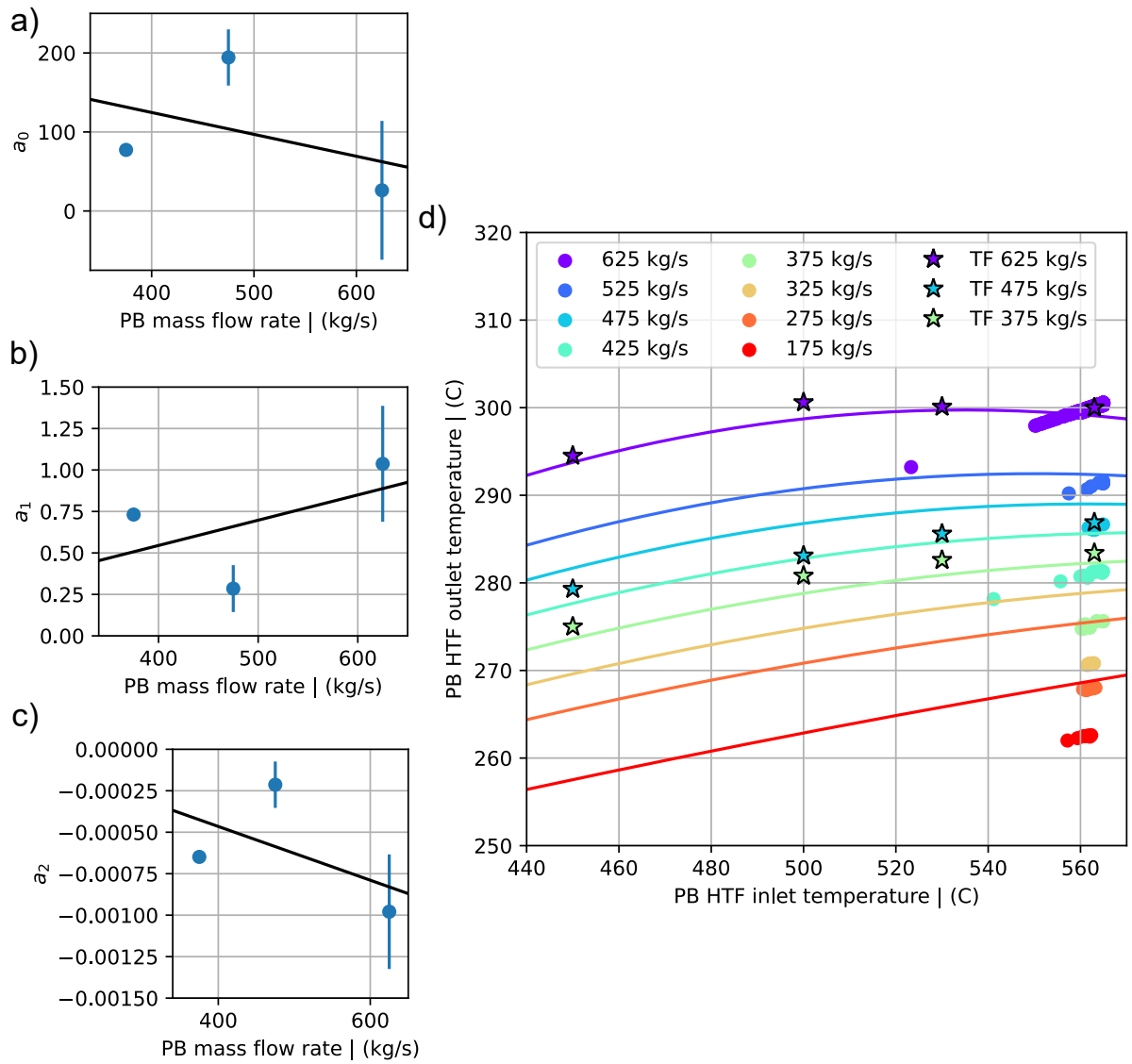
Figure 3: Fitting of the output temperature of the power block of the CR system. Coefficients of the quadratic function in a), b) and c). The results of the functions (solid lines), which are quadratic in $T_{PB, in}$ and linear in $\dot{m}_{PB}$, are shown in comparison to the *THERMOFLEX* (TF) data (stars) over which the fits were done and in comparison to the *SAM* data (dots) in d). The mass flow rates are color-coded.

Since it was not possible to attain *THERMOFLEX* simulation data for the power block of the PTC system, the *SAM* data were used to fit equation 5 for $P_{el, grid}$ and $T_{PB, out}$. In a first step the *SAM* data was separated into several bins in $\dot{m}_{PB}$ with a width of $50\,t/h$. The electric power to the grid was fitted with:

$$P_{el, grid} = a \cdot T_{PB, in} + P_{el, 0} \tag{11}$$

and the outlet temperature with:

$$T_{PB, out} = a \cdot T_{PB, in} + T_{out, 0} \tag{12}$$

The fitted scaling factors a for different $\dot{m}_{PB}$ are shown in panels a) and the offset values in panels b) of Figs. 4 and 5 respectively. The error bars indicate the confidence intervals resulting from the fits. These coefficients were then again fitted with equation 5 over $\dot{m}_{PB}$, as shown by the black lines in the respective plots. This leads to the following equations mapping $P_{el, grid}$ and $T_{PB, out}$ over $\dot{m}_{PB}$ and $T_{PB, in}$:

$$P_{el, grid}\left(\dot{m}_{PB}, T_{PB, in}\right) = a\left(\dot{m}_{PB}\right) \cdot T_{PB, in} + P_{el, 0}\left(\dot{m}_{PB}\right) \tag{13}$$

$$T_{PB, out}\left(\dot{m}_{PB}, T_{PB, in}\right) = a\left(\dot{m}_{PB}\right) \cdot T_{PB, in} + T_{out, 0} \tag{14}$$

The results of these fitted functions are compared to the *SAM* data in panels c) of Figs. 4 and 5. The largest deviation of the function from a data point for $P_{el, grid}$ is less than $3\,\%$. Furthermore, the multi-linear function corresponds well to the *SAM* data for $T_{PB, out}$.
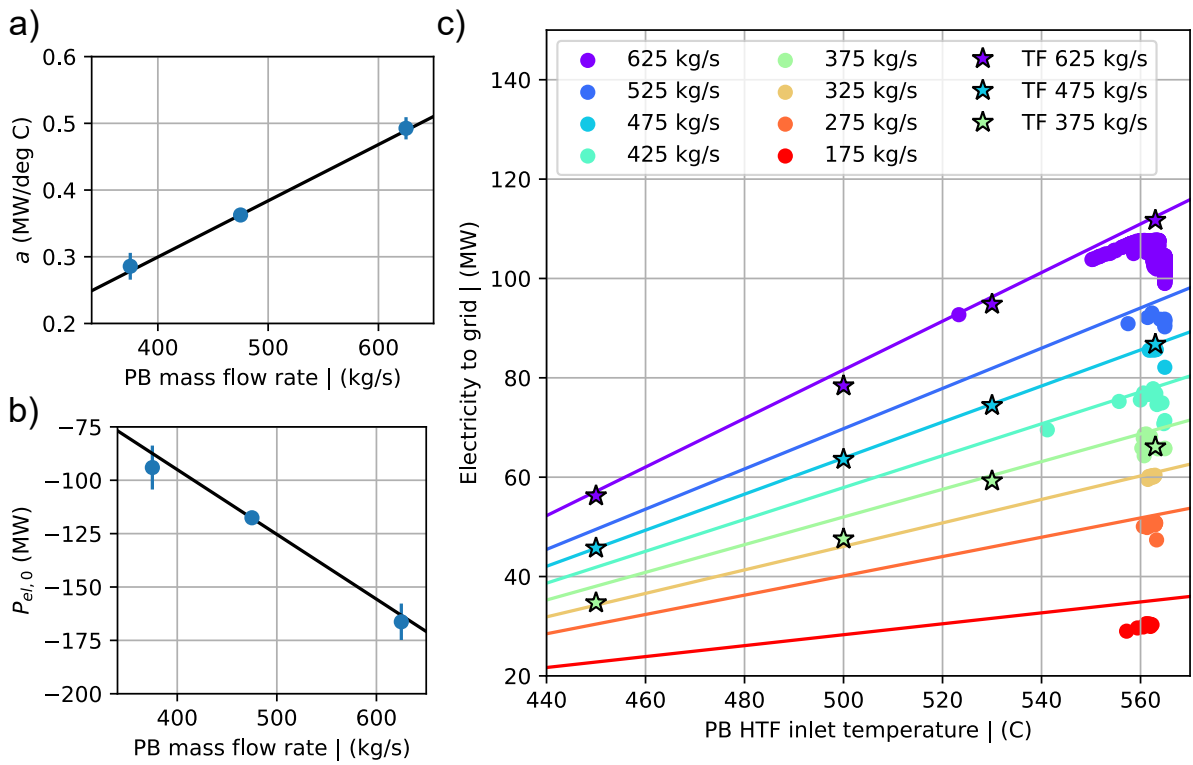

Figure 4: Fitting the electric power-to-grid output of the power block of the PTC system. Scaling factor a for various mass flow rates in a) and offset values in b). The multi-linear fit (solid lines) is shown in comparison to the data (dots) in c), where the respective mass flow rates are color-coded.
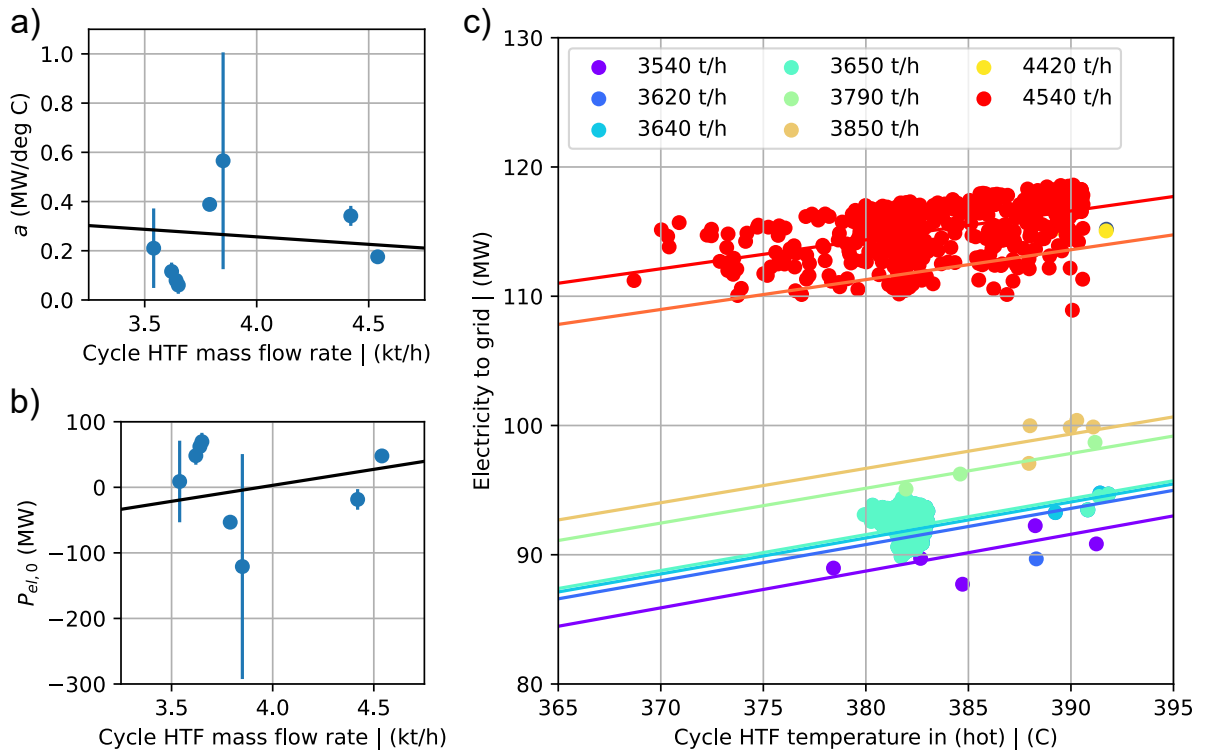
Figure 5: Fitting the output temperature of the power block of the PTC system. Scaling factor a for various mass flow rates in a) and offset values in b). The multilinear fit (solid lines) is shown in comparison to the data (dots) in c), where the respective mass flow rates are color-coded.
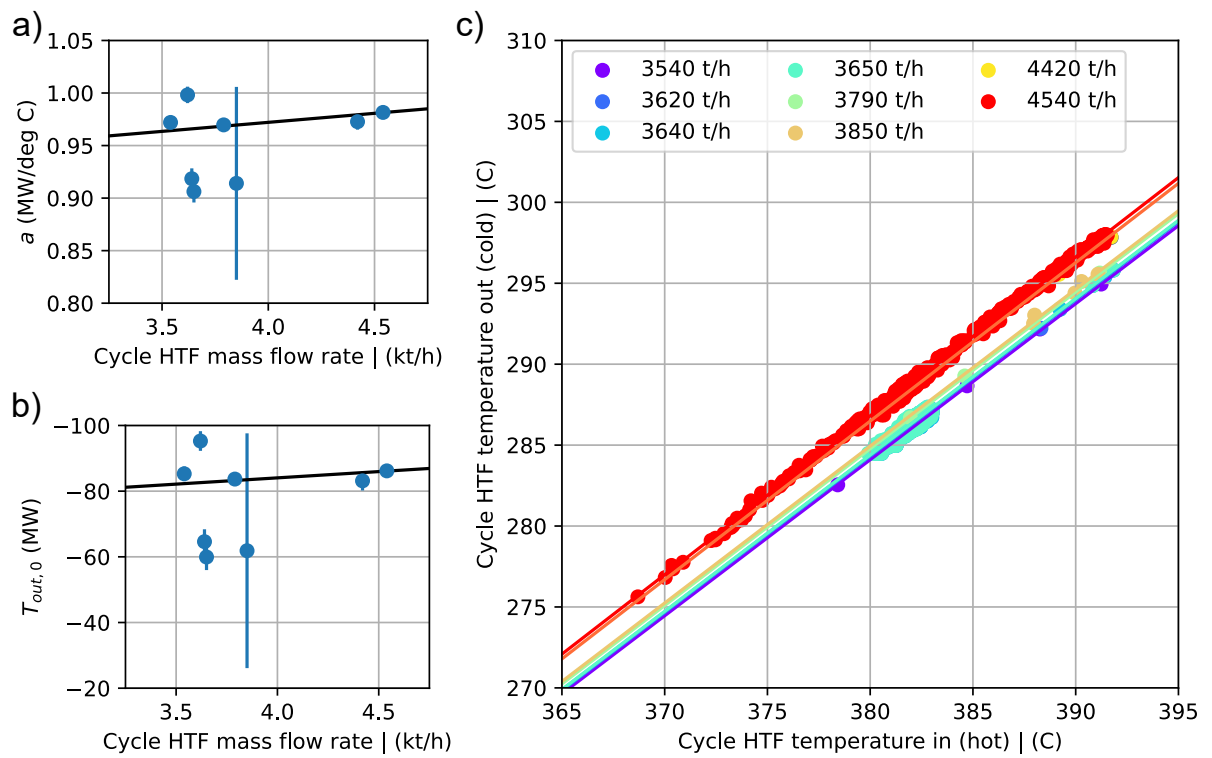
3.2.4 Physical Properties

The two heat transfer fluids (HTFs) have different physical properties that are computed using Eqs 15-16.

$$\rho(T) = a_0 + a_1 T + a_2 T^2 \tag{15}$$

$$C_p(T) = b_0 + b_1 T + b_2 T^2 \tag{16}$$

$$\overline{C_p} = \frac{1}{2}(C_p^{hot} - C_p^{cold}) \tag{17}$$

Here, a_i and b_i, are the coefficients for the given fluid, T, is the temperature of the fluid, $\overline{C_p}$, is the average heat capacity of the given fluid when the temperature drops (e.g. in the HX), C_p^{hot} and C_p^{cold}, are the heat capacities at the higher and lower temperature, respectively, i.e. $C_p^{hot} = C_p(T^{hot})$.

Table 3: Thermo-physical properties of the two HTFs. a_i are density coefficients (Eq. 15) and b_i are heat-capacity coefficients (Eq. 16)

Fluid	a_0 kg/m^3	a_1 kg/(m^3 °C)	a_2 kg/(m^3 °C^2)	b_0 J/kg	b_1 J/(kg °C)	b_2 J/(kg °C^2)
Oil	1074	-0.6367	-7.762e-4	1496.4	1.5247	-2.8485e-4
Salt	2090.24	-0.640386	0	1447.5	0.171826	0

3.2.5 Molten-Salt Tanks

The molten-salt storage tank TRNSYS Type is used to model the two different storage tanks that store molten salt at different temperature levels in the conventional CSP reference plant. In the PTC plant, the salt at cold tank is at ∼290 °C, whereas the hot tank stores salt at ∼385 °C. Likewise, in the CR plant, the cold tank salt is at ∼300 °C, whereas the hot tank stores salt at ∼565 °C.

The developed zero-dimensional TRNSYS type representing either the cold or hot storage molten salt tank calculates the instantaneous mixing of the introduced fluid (when charging), with the previous available fluid contained in the tank. This requires the calculation of the new stored mass, m_f, (Eq. 18) and the heat capacities (Eq. 16) of both the stored fluid, $C_p(T_f^{i-1})$, and the introduced fluid, $C_p(T_{in})$.

$$m_f = m_f^{i-1} + m_{f,in} - m_{f,out} \tag{18}$$

where m_f^{i-1} is the fluid mass of the previous time step, $m_{f,in}$ and $m_{f,out}$ are the added mass and removed mass during the current time step respectively.

The overall general energy balance reads:

$$Q_{in} - Q_{out} - \Delta Q - Q_{losses} = 0 \tag{19}$$

where subscript in and out denote the energy flows going in and out of the storage tank. With this convention, positive term increase the energy stored in the vessel and negative terms decrease the energy stored. The term ΔQ include not only the change of sensible energy, but also mass dependent energy, since the storages are open vessels with changes in mass over time, as it is shown in 20.

$$\Delta Q = \frac{1}{\Delta t}\left(m_f \cdot h_f - m_f^{i-1} \cdot h_f^{i-1}\right) \tag{20}$$

where h_f is the enthalpy of the fluid in timestep i, and h_f^{i-1} is the enthalpy in the previous timestep.

The losses to the ambient, Q_{losses}, are evaluated with the following expression, where UA is the global heat transfer coefficient of the tank, and T_{amb}, the ambient temperature.

$$Q_{losses} = UA \cdot (T_f - T_{amb}) \tag{21}$$

With, Q_{losses}, Q_{in} and Q_{out}, energy flowing into and out of the tank through the inflow and outflow, respectively, and ΔQ, the change in stored energy, energy fluxes of the tank are defined.

Lastly, Eqs. 22 and 23 provide other information required to control operation modes (see Sections 3.2.7 and 3.2.8).

$$V_f = \frac{m_f}{\rho_f} \tag{22}$$

$$V_{ratio} = \frac{V_f}{V_t} \tag{23}$$

where ρ is the density and V the volume. The subscripts f and t refer to fluid and tank, respectively.

3.2.6   Heat Exchanger

The reference PTC plant uses two HTFs: a molten salt for the storage loop and an oil for the main loop including the power block and PTCs (see Section 4.2). A heat exchanger (HX) connects the two loops allowing heat transfer between the two HTFs. When charging the storage (see Section 3.2.5), colder molten salt moves from the cold storage, through the HX where it is heated, to the hot tank. At the same time, hot oil moves from the PTCs to the HX, where it is cooled down, and back to the PTCs. When discharging the storage, molten salt moves from the hot storage tank, through the HX, where it is cooled down, to the cold storage tank. At the same time, cold oil moves from the power block, through the HX, where it is heated, and back to the power block, where the heat is ultimately used.

The HX uses an iterative algorithm to solve for the temperature-dependent thermo-physical properties. The mode (charging or discharging) defines two of the input temperatures to the HX: one each for each of the fluids. The other two fluid temperatures are calculated using Eqs. 24 and 25.

$$(\dot{m} \cdot C_p)_{min} = min(\dot{m}_{salt} \cdot \overline{C_{p,salt}}, \dot{m}_{oil} \cdot \overline{C_{p,oil}}) \tag{24}$$

$$Q = \epsilon \cdot (\dot{m} \cdot C_p)_{min} \cdot (T_{hot} - T_{cold}) \tag{25}$$

where, $\overline{C_p}$ are the average heat capacities of the inlet and outlet for each fluid (Eq. 17). The term $\dot{m}$ is the mass flow rate of the given fluid, Q is the transferred heat, ϵ is the HX effectiveness and T_{hot} and T_{cold} are the hot and cold temperatures of a given fluid, respectively.

3.2.7   CR Control

For the CR system, a unified control strategy to manage the whole system has been developed. This control strategy, embedded in a new TRNSYS type, evaluates (1) the conditions for operating the central receiver, (2) the status of the power block, and (3) the storage state-of-charge (SOC). As an output, the mass flow rates of the central receiver, the power block, and the resulting mass flow rates for the hot and cold molten salt storage tanks are given.

For operating the CR, it must be first preheated. Preheating is the first step of the CR operation in which the CR receiver is set to its minimum operational temperature. In this, mode the heat transfer medium is recirculated only through the CR in order to heat it with the solar radiation. This preheating starts only when the CR is not operating and two additional conditions have been met: the beam normal irradiance is above a threshold value and there is a need of heat, either by the storage tank, that could be charged, or by the power block, that should be in operation. When there is no heat demand, or when there is not a minimum irradiance value, the solar system switches off and does not start operation, including preheating.

In order to decide whether to ramp up or down the power block the control considers the status of the CR (if there is enough solar power) and the storage (if there is enough energy stored). Once the operation

conditions of the CR and the power block are set regarding the previous conditions, the resulting mass flow rates of the storage tanks are evaluated.

The control algorithms for both the thermocline system and the two molten salt tank CSP systems are identical. However, they differ in how they assess the state-of-charge (SOC) of the storage system. In the case of the two molten salt tanks the SOC is calculated using the volume ratio, representing the level of molten salt in the hot and cold tanks. On the other hand, for the thermocline tank, the SOC is obtained using the temperature sensors across different levels, including the outlet. The SOC is then used to assess the feasibility of charging or discharging.

3.2.8 PTC Control

The PTC system requires a control strategy to manage the whole system: the parabolic trough collector (PTC) solar field, the power block and the storage. In order to do this, a new type has been developed which considers, (1) the conditions for operating the parabolic trough solar field, (2) the actual status of the power block, and (3) the SOC of the storage. As an output, the mass flow rates of the PTC, the power block, and the resulting mass flow rates for the hot and cold molten salt storage tanks are given.

For operating the PTC, it must be preheated. This preheating, similar to the CR control described in section 3.2.7, starts only when two conditions have been met: a minimum beam normal irradiance above a threshold value and the request of heat demand, either from the storage tank, that could be charged, or from the power block, that should be in operation. When none of the heat demand requirement conditions are met, or when there is not a minimum irradiance value, the solar system switches off and does not start operation, including preheating.

Similarly to the CR control, to decide whether to ramp up or down the power block the control considers the status of the PTC (if there is enough solar power) and the storage (if there is enough energy stored).

Once the operation conditions of the PTC and the power block are set regarding the previous conditions, the resulting mass flow rates of the storage tanks and in bith side of the heat exchanger are evaluated.

3.2.9 Thermocline Tank

The reference system consist of two separate tanks, i.e. the hot and the cold storages, which are filled and emptied using roughly twice the storage volume to accommodate the salt needs. In comparison, a thermocline tank has only one vessel, which is always full, leading to space and cost savings by compacting two vessels into one. Further cost reductions are achieved in this component by adding a solid filler, which reduces the required amount of salt. Clearly, the filler material cost must be lower than that of the solar salt, to achieve cost savings.

The thermocline concept is based on the moving gradient between the two temperatures. The thermocline is thus a very important part of the component, as its "sharpness" governs the volumes of high and low temperature fluid in the tank. As soon as the thermocline approaches the tank exit, the desired temperature is no longer reached, i.e., in discharging mode the hot side produces lower temperatures, whereas on the cold side (when charging), the fluid gets hotter as the thermocline leaves the tank. For this reason, the tank needs to be completely recharged every so often.

Eq. 26 and Eq. 27 show the governing equations for the fluid and filler (solid), respectively (modified from Odenthal et al., 2017, 2019, 2023, Xie et al., 2022). These coupled partial-differential equations have been implemented using the Finite Volume Method (FVM). Each term has the units of W/m³.

$$\epsilon \cdot \rho_f \cdot C_{p,f} \cdot \left(\frac{\partial T_f}{\partial t} + u_f \cdot \frac{\partial Tf}{\partial z} \right) = \frac{\partial}{\partial z} \cdot \left(\lambda_{f,eff} \cdot \frac{\partial Tf}{\partial z} \right) + h_{sf,eff} \cdot a_s \cdot (T_s - T_f) + Q_{wall} \tag{26}$$

$$(1 - \epsilon) \cdot \rho_s \cdot C_{p_s} \frac{\partial T_s}{\partial t} = \frac{\partial}{\partial z} \cdot \left(\lambda_{s,eff} \cdot \frac{\partial Ts}{\partial z} \right) + h_{sf,eff} \cdot a_s \cdot (T_f - T_s) \tag{27}$$

In these equations, variables with subscript f belong to the fluid, and variables with subscript s belong to the solid (filler). Here, ϵ denotes the filler void fraction, ρ the density, A_c the tank's cross-sectional area, V the tank's volume, C_p the heat capacity, T the temperature, t the time, u the fluid velocity, z the vertical tank height, λ the thermal conductivity, $h_{sf,eff}$ the effective heat-transfer coefficient between fluid and filler, a_s

the surface-to-volume factor for the fluid-solid heat transfer, and Q_{wall} the heat flux to the ambient through the wall.

Eq. 28 shows the surface-to-volume factor, a_s [m²/m³], for the fluid-solid heat transfer (e.g. Xie et al., 2022):

$$a_s = 6\frac{(1-\epsilon)}{d_p} \tag{28}$$

where d_p is the characteristic diameter of the packed bed particles.

Instead of fluid velocities, the thermocline type is provided with mass flow rates, $\dot{m}$. Eq. 29 shows the fluid velocity relative to the tank height, $u_{f,tank}$, whereas Eq. 30 shows the interstitial fluid velocity, $u_{f,int}$:

$$u_{f,tank} = \frac{\dot{m}}{A_c\rho_f} \tag{29}$$

$$u_{f,int} = \frac{\dot{m}}{\epsilon A_c\rho_f} \tag{30}$$

With regard to our purposes, the implementations of the governing Eqs. (cf. our Eqs. 26 and 27) in Xie et al. (2022) and Odenthal et al. (2023) mainly differ in three aspects: the implementation of the thermal conductivities, the heat transfer coefficient between the solid and the filler, and the implementation of the heat flux to the ambient.

Though many different implementations have been proposed for the thermal conductivity values, the most common approach in the literature is described in Odenthal et al. (2023). The thermal resistance of the packed-bed/fluid combination is modelled as a thermal resistance in series, adjusted for using the filler's porosity (Eq. 31 and Eq. 32). This implementation was chosen, because the authors of Odenthal et al. (2023) provide the validation data for the EU-ERANET Newcline project.

$$\lambda_{f,eff} = \left(\frac{1-\epsilon}{\lambda_s} + \frac{\epsilon}{\lambda_f}\right)^{-1} \tag{31}$$

$$\lambda_{s,eff} = 0 \tag{32}$$

The effective heat transfer coefficient between the fluid and the filler is calculated using the Nusselt number, Nu, the Reynolds number, Re, and the Prandtl number, Pr (Odenthal et al., 2023):

$$h_{sf,eff} = \left(\frac{1}{h_{sf}} + \frac{5d_p}{2\lambda_s}\right)^{-1} \tag{33}$$

$$h_{sf} = \frac{\lambda_s Nu}{d_p} \tag{34}$$

$$Nu = 2 + 1.1Pr^{\frac{1}{3}}Re^{0.6} \tag{35}$$

$$Re = \frac{\rho_f u_f d_p}{\mu} \tag{36}$$

$$Pr = \frac{\mu C_{p,f}}{\lambda_f}, \tag{37}$$

where h_{sf} is the surface film heat transfer coefficient and μ the dynamic fluid viscosity.

As thermal losses are estimated to be less than 1% of the overall thermal energy input of CSP plants, these are not accounted for in this version of the component.

3.2.10 Thermocline tank validation

The validation of the thermocline model is done in several incremental steps against the already validated tool used in Odenthal et al. (2023). By working incrementally, the amount of effort required to fix any issues is greatly reduced.

The first validation case described in Table 4 considers a charging process of the thermocline storage, where the thermo-physical properties of the solar salt and filler material are considered to be constant and the storage losses trough the wall are neglected.

Table 4: Values used for the temperature-invariant validation case without wall fluxes.

| variable	symbol	value	variable	symbol	value
tank height [m]	L	10	filler porosity [-]	ϵ	0.4
tank diameter [m]	D	24.72	mass-flow rate [kg/s]	$\dot{m}$	300
tank volume [m³]	V	4800	fluid density [kg/m³]	ρ_f	1819.7
cross-sectional area [m²]	A_c	480	fluid heat capacity [J/kgK]	$C_{p,f}$	1517
fluid therm. cond. [W/(mK)]	λ_f	0.5233	dyn. fluid viscosity [kg/(ms)]	μ	0.0016
solid density [kg/m³]	ρ_s	2992	solid heat capacity [J/(kgK)]	$C_{p,s}$	1038.3
solid therm. cond. [W/(mK)]	λ_s	1.6005	filler particle diameter [mm]	d_p	10
initial temperature both [°C]	T_{init}	290	fluid temperature inflow [°C]	T_f^{in}	555
wall flux [W]	Q_{wall}	0	heat tran. coeff. [W/(m²K)]	$h_{sf,eff}$	53.4
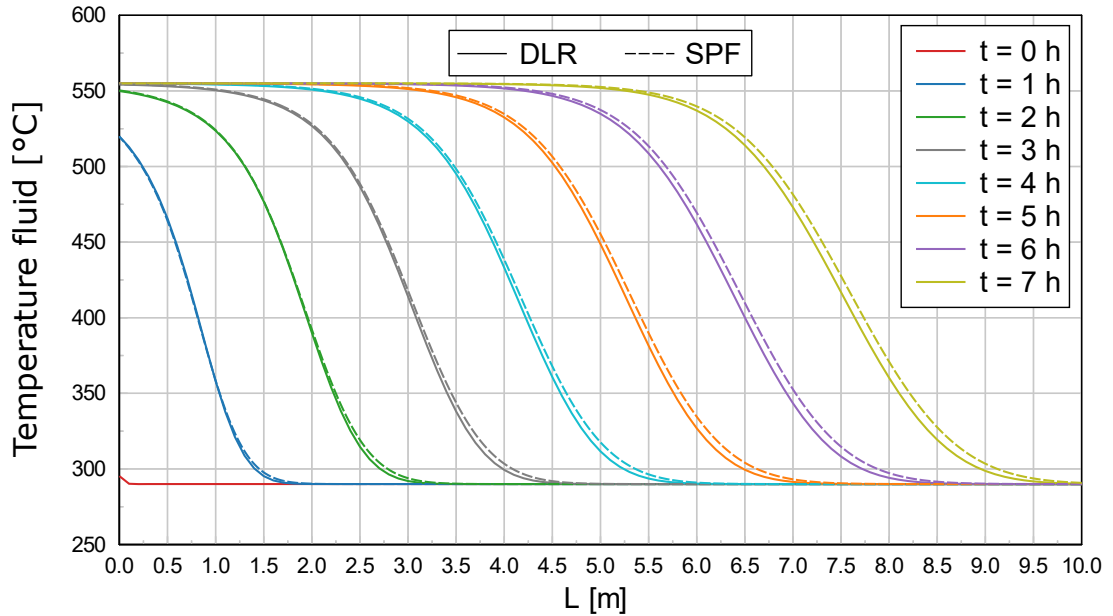
Figure 6: Validation results: comparison of the new type's results with numerical data provided by DLR using the model validated in Odenthal et al. (2023). The x-axis corresponds to the vertical axis of the thermocline tank z, with 0 m corresponding to the top of the tank.

Fig. 6 shows the simulation results from both the model developed at DLR and the one developed at SPF. At t=0 h, the whole storage is at T_{init}=290 °C. Afterwards, we are entering 300 kg/s of solar salt at the top of the storage (z=0 m) at 560 °C. However, since there is a volume layer that buffers the inlet and outlet of the thermocline storage, it takes around 3 h until the temperature at z=0 m is exactly at 560 °C. This volume layer, of 0.6 m height, is assumed to be fully mix and thus modelled as one control volume.

As time passes on, the thermocline moves towards the bottom of the storage at z=10 m. The thermocline starts to move outside of the storage tank at t=7 h. For this example, this is signalled by the storage's outlet temperature (at z=10 m) increasing to above the cold target temperature of 290 °C. Fig. 6 shows a small difference between the two models at the end of the thermocline. With increasing time, the differences increase, and it seems like the deviations move from the end of the thermocline to the beginning of it. This might be due to a different implementation of the convective term. Nevertheless, besides this small difference, the results look very close to each other and we consider both models are in good agreement.

3.3 Development of economic models

The main relative economic indicators are capital expenditures (CAPEX), operating expenses (OPEX) and levelized cost of energy (LCOE). CAPEX or investment cost, refers to all up-front costs (construction, financing, etc). OPEX considers all operation and maintenance costs incurred to operate the CSP plant. The LCOE is techno-economical indicator to measure the lifetime cost of generating the electricity of the power plant including both investment and operation cost. The LCOE during the lifetime period is used to evaluate and compare the cost-effectiveness of different energy system alternatives.

The LCOE formula is:

$$\text{LCOE} = \frac{I_0 \cdot (1 - DR) + \sum_{t=1}^{n} \frac{M_t \cdot (1+i)^t + F_t \cdot (1+i)^t + D_t}{(1+d)^t}}{\sum_{t=1}^{n} \frac{E_t}{(1+d)^t}}$$

Where:

- I_0 is the initial investment expenditure.

- M_t are the operations and maintenance costs in year t.

- F_t other fixed costs (i.e. insurance) in year t.

- D_t are the debt payments in year t, $D_t = I_0 \cdot DR \cdot r_D$, where DR is the debt ratio and r_D is the debt interest rate.

- E_t is the energy produced in year t.

- d is the discount rate, that could be real discount rate d_r, which excludes inflation, or d_n is the nominal discount rate, which includes it.

- i is the inflation rate.

- n is the lifetime of the project.

The main economic parameters used for the evaluation of the LCOE are shown in Tab. 5.

Table 5: Main economic parameters used for the economic analysis.

parameter	unit	value
Plant Lifetime, n	years	25
Inflation Rate, i	%	2
Real Discount Rate, d_r	%	7.5
Nominal Discount Rate, d_n	%	9.65
Debt percent, DR	%	70
Deb interest rate, r_D	%	8.72
Debt tenor, n_D	years	25
Insurance Rate (vs Investment)	%	0.5

NOTE: *Economic models were developed by Empresarios Agrupados (EAI) and are subjected to confidentiality policy. Consequently, this report abstains from presenting absolute economic values, but rather focuses on relative economic indicators for the comparative analysis.*

4 Energy system performance and LCOE analyses of CSP plants

4.1 Central receiver two-tank CSP plant

4.1.1 Description of the system

The definition of the hydraulic scheme of the CR two-tank plant and its main components was proposed by Empresarios Agrupados (EAI). The CR plant consists of:

- thermal energy storage (TES) which consists of two molten salt storage tanks, one for the hot and the other for the cold molten salt.

- a solar field, which comprises thousands of heliostats arranged in concentric circles around the central tower, at the top of which is located the central receiver (CR).

- a power block which encompasses the main and auxiliary equipment for transforming the thermal energy into electricity.

- auxiliary equipment, pipes, valves, pumps, insulation, etc.

The hydraulic scheme of the CR plant used in the system simulations with *pytrnsys* is shown in Fig.7.
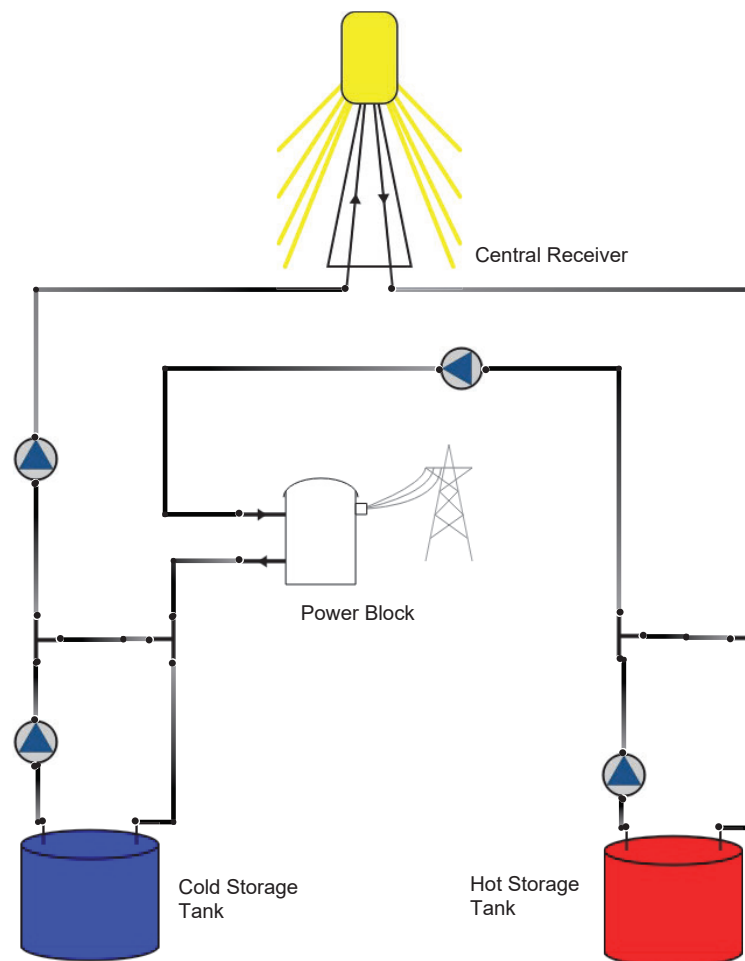

Figure 7: Hydraulic scheme of the CR two-tank plant simulated with *pytrnsys*.

The CR two-tank plant has mainly two operation modes and loops:

- *The charging operational mode*: here the solar central receiver generation loop, which collects energy from the sun and, either stores heat it in the molten salt storage tank, delivers it directly to the power block or both.

- *The discharging operational mode*: where the power block generates electricity using the molten hot salt coming either from the storage tanks and/or directly from the central receiver.
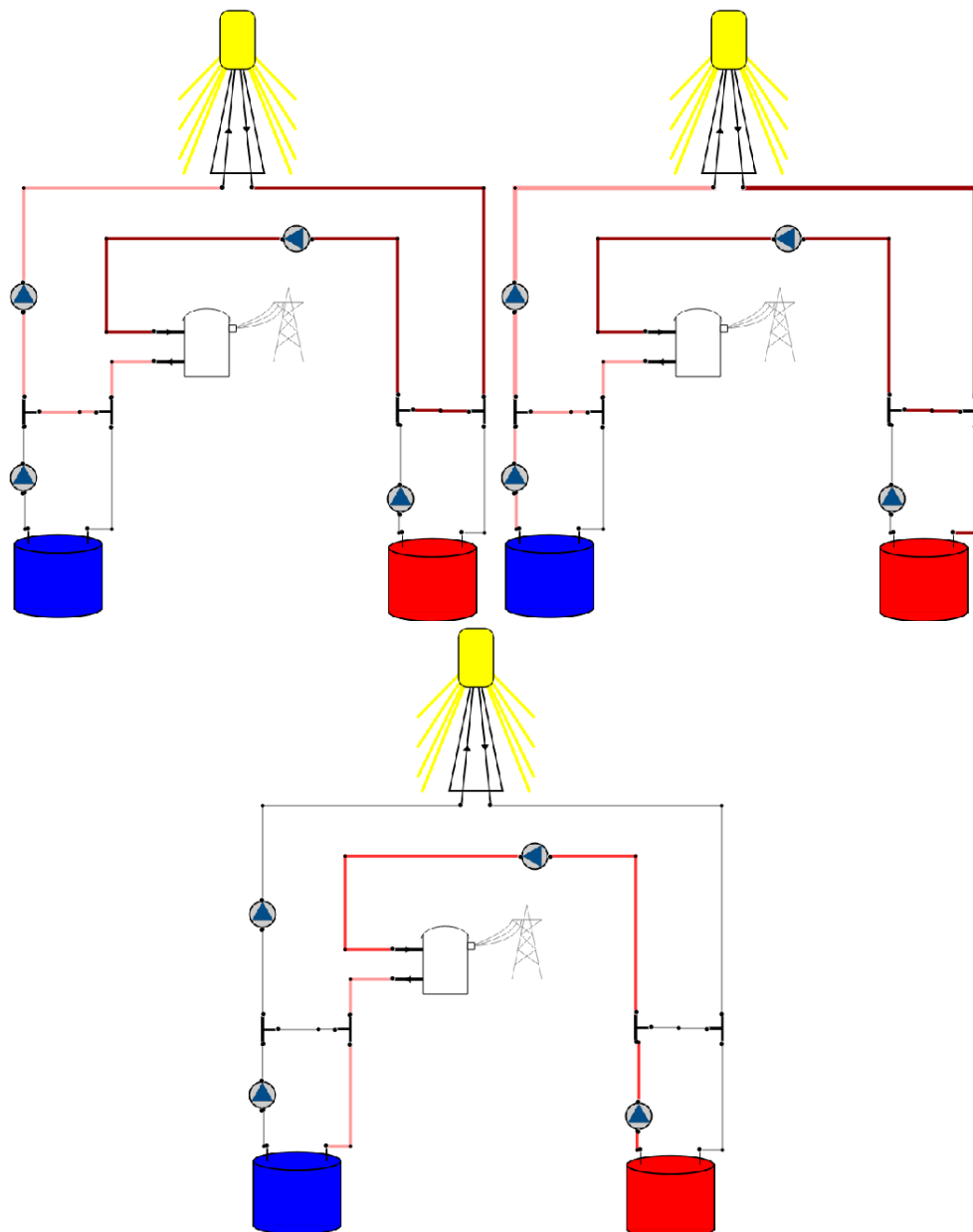

Figure 8: Three different operation modes represented by means of *pytrnsys* flow visualiser. *Left top:* Charging operational mode, from the central receiver to the power block. *Right top:* Charging operational mode, from the central receiver to the power block and molten salt tank. *Bottom:* Discharging operational mode.

Depending on the balance between the central receiver and power block mass flow rates, the hot and cold tank pumps are respectively operated. The central receiver is enabled when there is enough normal irradiance and when the power block is in operation or there is enough cold salt volume to be heated. The power block is activated whenever the central receiver is in operation or there is enough energy in the storage tank, which implies that regardless of the instantaneous irradiance, it can operate in the evening or at night.

4.1.2   Energy system performance of the reference plant

A reference plant, with a specified location and comparable size, is set forth to facilitate the comparative analysis of the different technologies. The main characteristics of this proposed CR CSP reference plant are:

- Coordinates: 37.244N, 2.982W, Province of Granada (Spain).

- Hot storage at 565 °C and cold storage at 300 °C with a volume of 21×10^3 m^3 each and a required amount of molten salts of ca. 40×10^3 ton, resulting in a nominal thermal capacity of 3545 MWh.

- A total heliostat mirror surface of $1\,535\,611$ m^2 and a central receiver with a thermal power of 787.5 MW

- A gross/net electrical power: 115/100 MW.

As it is shown in Tab. 6 the CR annual energy yield CSP reference plant is 1458.6 GWh, equivalent to 950.17 kWh/m^2. With an annual electricity production of 620.3 GWh, this indicates an average power block performance of 42.8 %. In the subsequent section, an energy performance comparison analysis between the results from *pytrnsys* and *SAM* is conducted, providing additional insights into the energy fluxes in monthly and hourly values.

4.1.3   Comparison of *pytrnsys* with *SAM* results of the reference plant

In Fig. 9, Fig. 10 and Fig. 11 simulation results of *pytrnsys* and SAM for the CR CSP reference plant for different periods of the year are presented. Fig. 9 shows the thermal energy yield of the CR for different weeks (1/10/20/40) of the year. Despite there are slight differences between the results of both simulation environments, the hourly energy yield is very similar.

The predictions of the thermal input to the power block for both simulation environments are depicted in Fig. 10.

Fig. 11 shows the electrical outlet power for both tools. Slight discrepancies are noticeable, possibly associated with inertia and the optimization algorithm controlling the power block power. Additionally, the preceding variations of the energy yield of the CR may accumulate.

The monthly energy balances for both *SAM* and TRNSYS simulations are shown in Fig. 12 and Tab. 6. The positive side of the energy balance refers to the input energy to the system, which is composed by the thermal output energy of the CR, while the negative side consist on two components. The first one is the electricity provided to the grid, the second one is the thermal losses and consumption of the solar system and power block, which is the difference between the energy provided from the central receiver and its electrical output.

Results of both simulation programs are compared in Fig. 12 and Tab. 6: the thermal output of the CR obtained with *TRNSYS* is 2.1 % lower than that obtained with SAM. The system and power block losses and consumption obtained with *TRNSYS* is 4.1 % lower than that of SAM. These differences lead to generated electricity predicted by *TRNSYS* being 0.7 % higher than that of the generated electricity obtained with SAM.

In conclusion it can be stated that there is a good agreement between the results from the SAM simulation environment and the new TRNSYS environment for the CR CSP plant developed in *pytrnsys*.
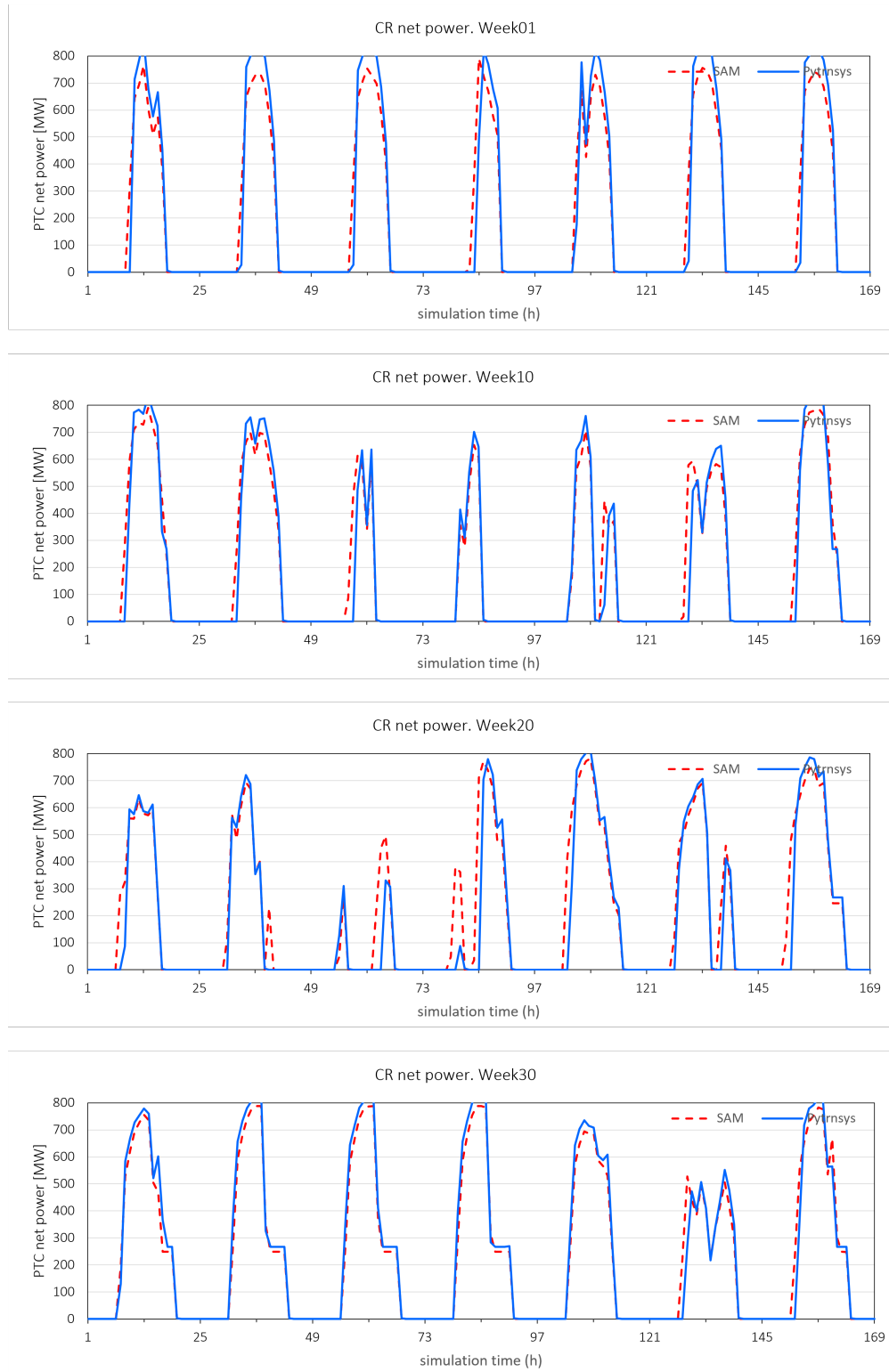
Figure 9: Central receiver thermal energy yield results obtained with *pytrnsys* and SAM for different weeks of the year.
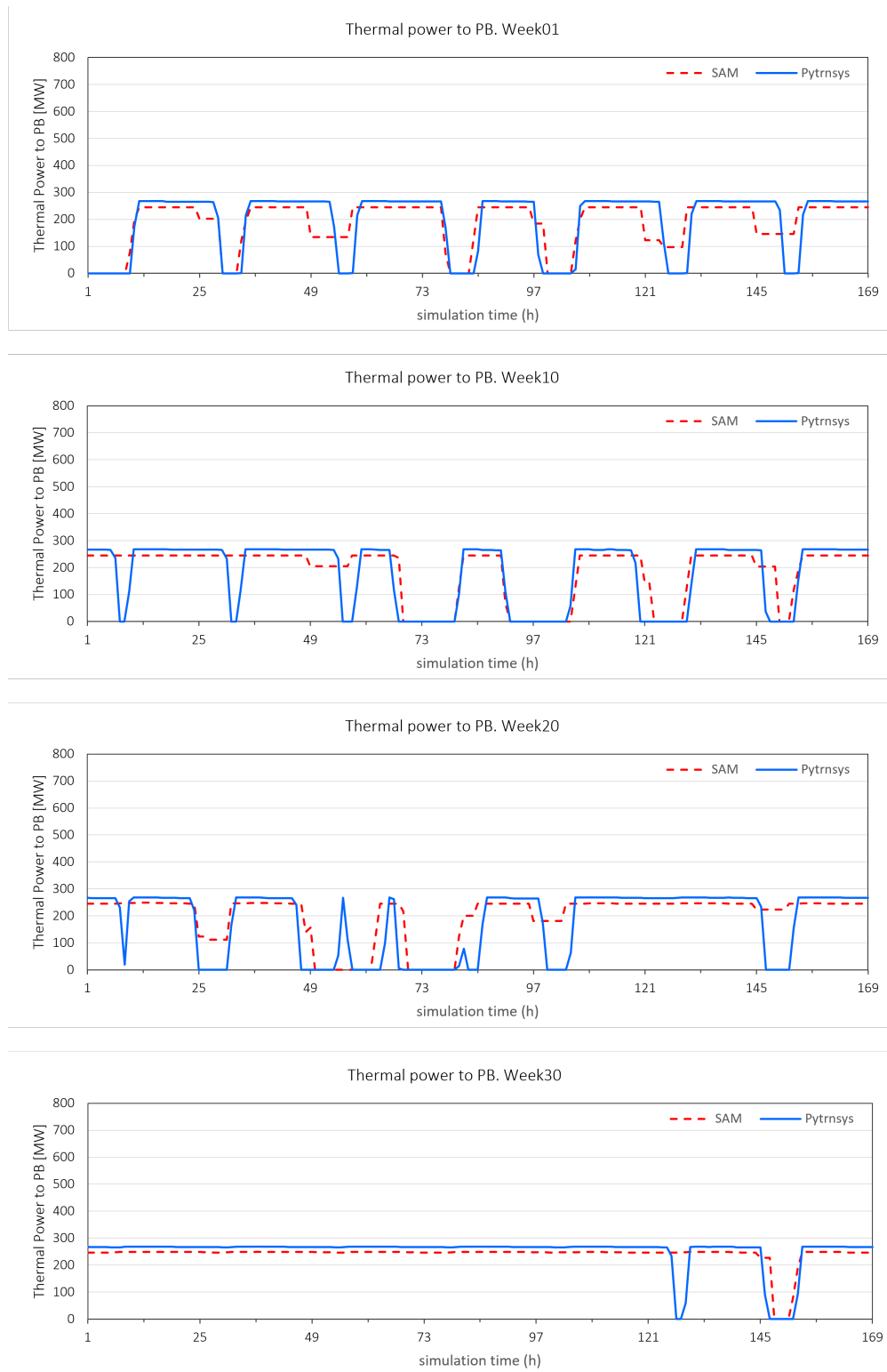
Figure 10: Thermal energy entering to the power block results obtained with *pytrnsys* and SAM for different weeks of the year.
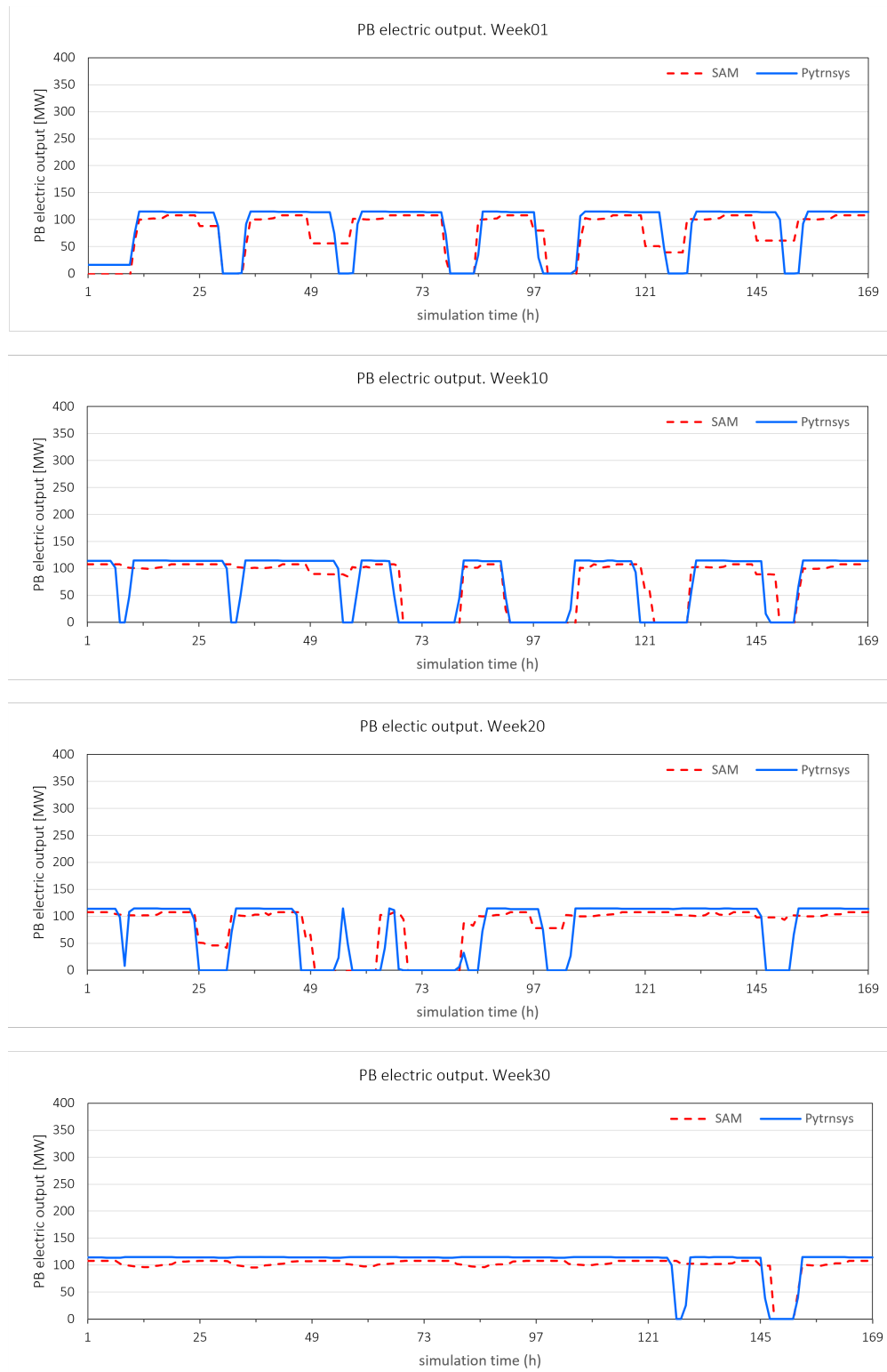
Figure 11: Electricity produced by the power block results obtained with *pytrnsys* and SAM results for different weeks of the year.
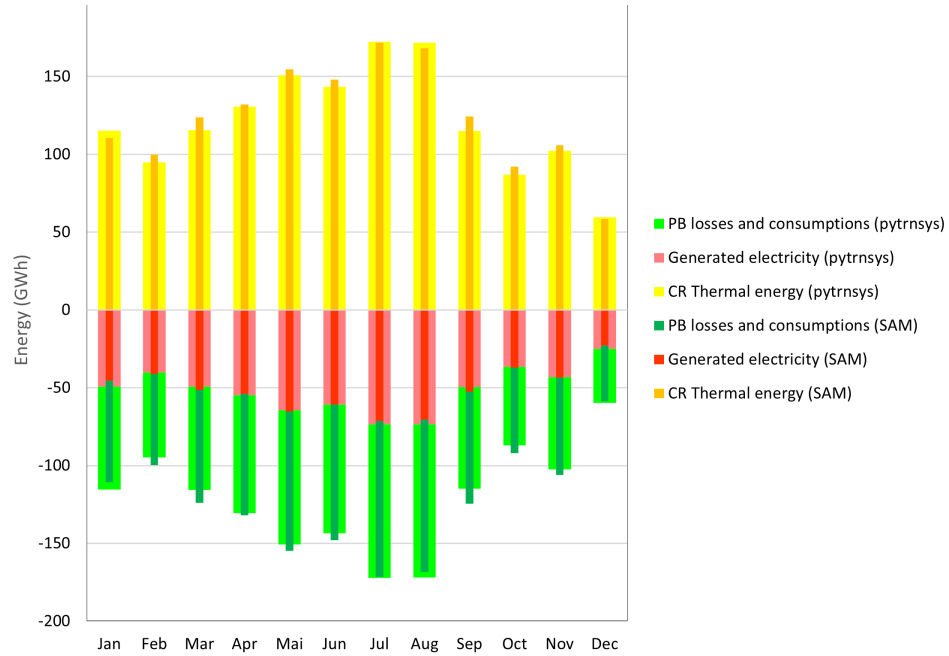
Figure 12: Monthly energy balances of the *pytrnsys* (wider lighter bars) and *SAM* (smaller darker bars) simulations for the central receiver CSP solar plant.

Table 6: Comparison between the monthly energy balances of the *SAM* and the *TRNSYS* simulations for the central receiver CSP solar plant. A positive values in Difference indicates the value predicted by pytrnsys is larger than that of SAM

	CR Thermal energy		PB looses and cons.		Gen. Electricity	
	SAM	pytrnsys	SAM	pytrnsys	SAM	pytrnsys
	GWh	*GWh*	*GWh*	*GWh*	*GWh*	*GWh*
Jan	110.6	115.3	-65.3	-66	-45.3	-49.3
Feb	99.8	94.8	-58.6	-54.6	-41.2	-40.3
Mar	123.8	115.6	-72.3	-66.4	-51.5	-49.1
Apr	132	130.7	-78	-75.9	-54	-54.7
Mai	154.8	150.7	-89.5	-86.2	-65.3	-64.5
Jun	148	143.4	-87.2	-82.6	-60.9	-60.8
Jul	171.7	172.3	-100.4	-98.8	-71.3	-73.5
Aug	168.3	171.8	-97.9	-98.4	-70.4	-73.4
Sep	124.5	114.9	-71.8	-65.2	-52.7	-49.7
Oct	92.1	87	-54.9	-50.4	-37.2	-36.6
Nov	106	102.4	-62.5	-59.2	-43.5	-43.2
Dec	58.6	59.7	-35.7	-34.6	-22.9	-25.1
Total	1490.3	1458.6	-874.1	-838.3	-616.2	-620.3
Difference	-2.1%		-4.1%		+0.7%	

4.2 Parabolic trough two-tank CSP plant

4.2.1 Description of the systen

The definition of the hydraulic scheme of the PTC two-tank plant and its main components was proposed by Empresarios Agrupados (EAI). The PTC plant consists of:

- thermal energy storage (TES) which consists of two molten salt storage tanks, one for the hot and the other for the cold molten salt.

- a parabolic trough field, which comprises thousands of parabolic trough collectors arranged in rows.

- a power block which encompasses the main and auxiliary equipment for transforming the thermal energy into electricity.

- a heat exchanger (HX) that hydraulically separates the oil-based loop for the Parabolic Trough and Power Block from the molten salt loop used for the storage system.

- and auxiliary equipment, pipes, valves, pumps, insulation, etc.

The hydraulic scheme of the PTC plant used in the system simulations with *pytrnsys* is shown in Fig.13.
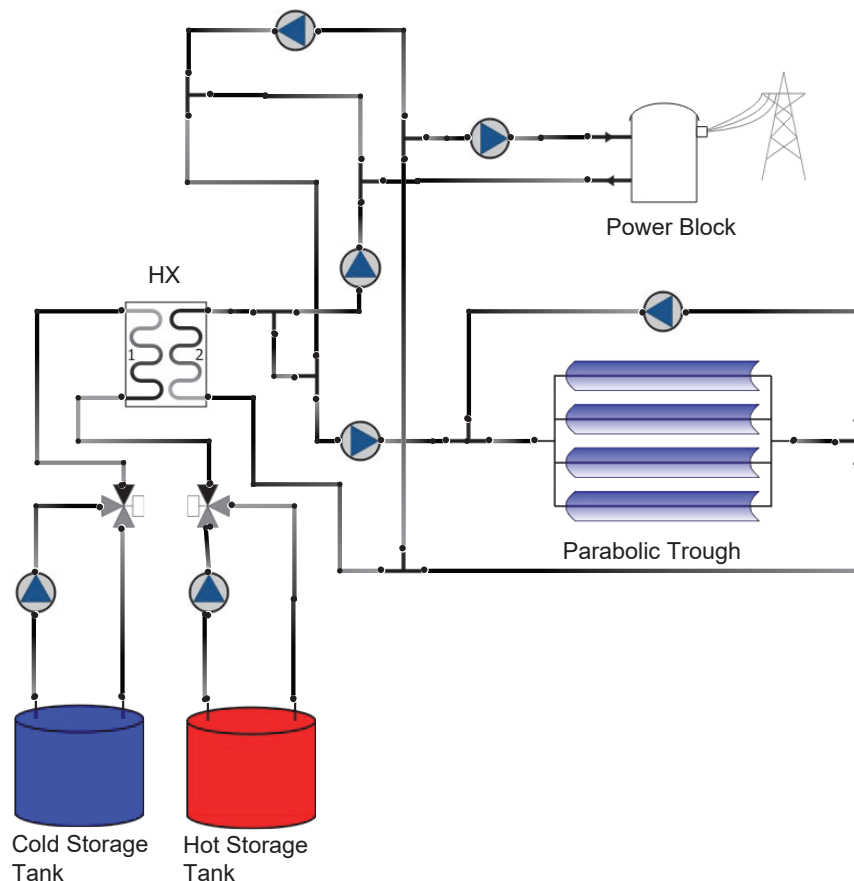

Figure 13: Hydraulic scheme of the PTC two-tank plant simulated with *pytrnsys*.

The PTC two-tank CSP plant has five different operation modes:

- *Heat transfer from the solar field to the power block and TES non-operative.* In this mode, the PTC will operate only with the power block.

- *Heat transfer from the solar field to the power block and TES in parallel.* In this mode, the PTC will feed both the power block and the TES.

- *Mode heat transfer from the TES to the power block.* In this mode, the thermal energy stored in the hot molten salt will be used to operate the power block.

- *Mode heat transfer from the solar field to the TES.* In this mode, the PTC will only feed the TES.

- *Mode heat transfer from the solar field and from the TES in parallel to the power block.* When there is not enough solar radiation for operating power block with the the PTC alone, the TES provides the additional energy needs.
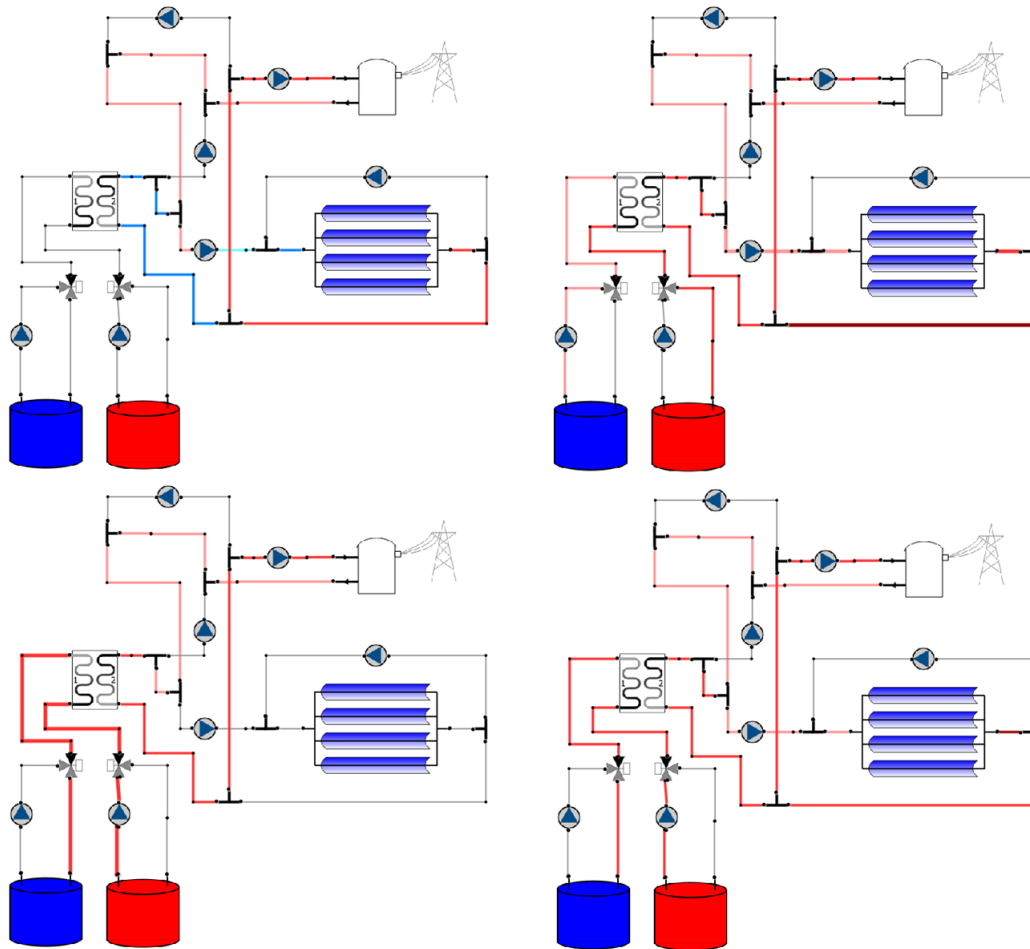
Figure 14: Four different operation modes represented by means of *pytrnsys* flow visualiser. *Left top:* Heat transfer from the solar field to the power block and TES non-operative. *Right top:* Heat transfer from the solar field to the power block and TES in parallel. *Left bottom:* Mode heat transfer from the TES to the power block. *Right bottom:* Mode heat transfer from the solar field and from the TES in parallel to the power block.

These five different operation modes are considered in the TRNSYS type used to control the PTC plant described in section 3.2.8.

4.2.2 Energy system performance of the reference plant

A reference plant, with a specified location and comparable size, is set to facilitate the comparative analysis of the different technologies. The main characteristics of the proposed CSP reference plant with PTC are:

- Location and coordinates: 37.244N, 2.982W, Province of Granada (Spain).

- Two hot and two cold storage tanks with a volume of $21 \times 10^3 \, m^3$ each, operated at 385 °C and 290 °C respectively. This results in a total volume of $42 \times 10^3 \, m^3$ and a required amount of molten salts of ca. 80×10^3 ton, resulting in a nominal thermal storage capacity of 2679 MWh. Despite doubling the volume compared to the CR, the storage capacity is lower due to the smaller thermal difference between the hot and cold storage.

- A solar field comprised of 375 loops, each one made up of 4 solar collector assembly (SCA). Each SCA with an aperture area of 817.5 m^2. Hence, a total aperture area of $1\,226\,250 \, m^2$.

- A gross/net electrical power: 115/100 MW.

As it is shown in Tab. 7 the PTC annual energy yield CSP reference plant is 1204.8 GWh, equivalent to 982.5 kWh/m^2. With an annual electricity production of 392.7 GWh, this indicates an average power block performance of 34.7 %, lower than CR CSP plant due to a lower power block operating temperature. In the subsequent section, an energy performance comparison analysis between the results from *pytrnsys* and *SAM* is conducted, providing additional insights into the energy fluxes in monthly and hourly values.

4.2.3 Comparison of *pytrnsys* with *SAM* results of the reference plant

Simulation results used to compare *pytrnsys* and SAM for different periods of the year are presented in Fig. 15, Fig. 16 and Fig. 17.

Fig. 15 shows the thermal energy yield of the PTC solar field for different weeks (1/10/20/40) of the year. Despite there are slight differences between the results of both simulation environments, the hourly energy yield is very similar. The predictions of the thermal input to the power block are depicted in Fig. 16. Fig. 17 shows the electrical outlet power for both tools. Slight discrepancies are noticeable during winter, possibly associated with inertia and the optimisation algorithm controlling the power block power. Additionally, the preceding variations of the energy yield of the PTC may accumulate. However, the overall impact of these differences on the global objectives of the project remains minimal, as the objective is to compare, not both softwares (SAM and TRNSYS), but to compare the new thermocline concepts with the reference cases in pytrnsys.

The monthly energy balances for both *SAM* and *pytrnsys* simulations are shown in Tab. 7 and Fig. 18. The positive side of the energy balance is composed of the thermal output energy of the PTC only, while the negative side is composed by two terms. The first one is the electricity provided to the grid, and the second one is the system and power block losses and consumption, which is the difference between the thermal energy provided by the parabolic trough and its electrical output.

Comparing the simulation results between SAM and *pytrnsys* we can state that the thermal output of the PTC obtained with *TRNSYS* is 1.0 % lower than obtained with SAM. The TES losses calculated with *TRNSYS* are 0.5 % higher than those calculated with SAM. The generated electricity obtained with *TRNSYS* is 3.8 % lower than the one obtained with SAM.

Consequently, it can be stated that there is a good agreement between the results from the SAM simulation environment and the new TRNSYS environment for the PTC CSP plant developed in *pytrnsys* for the *Newcline* project.
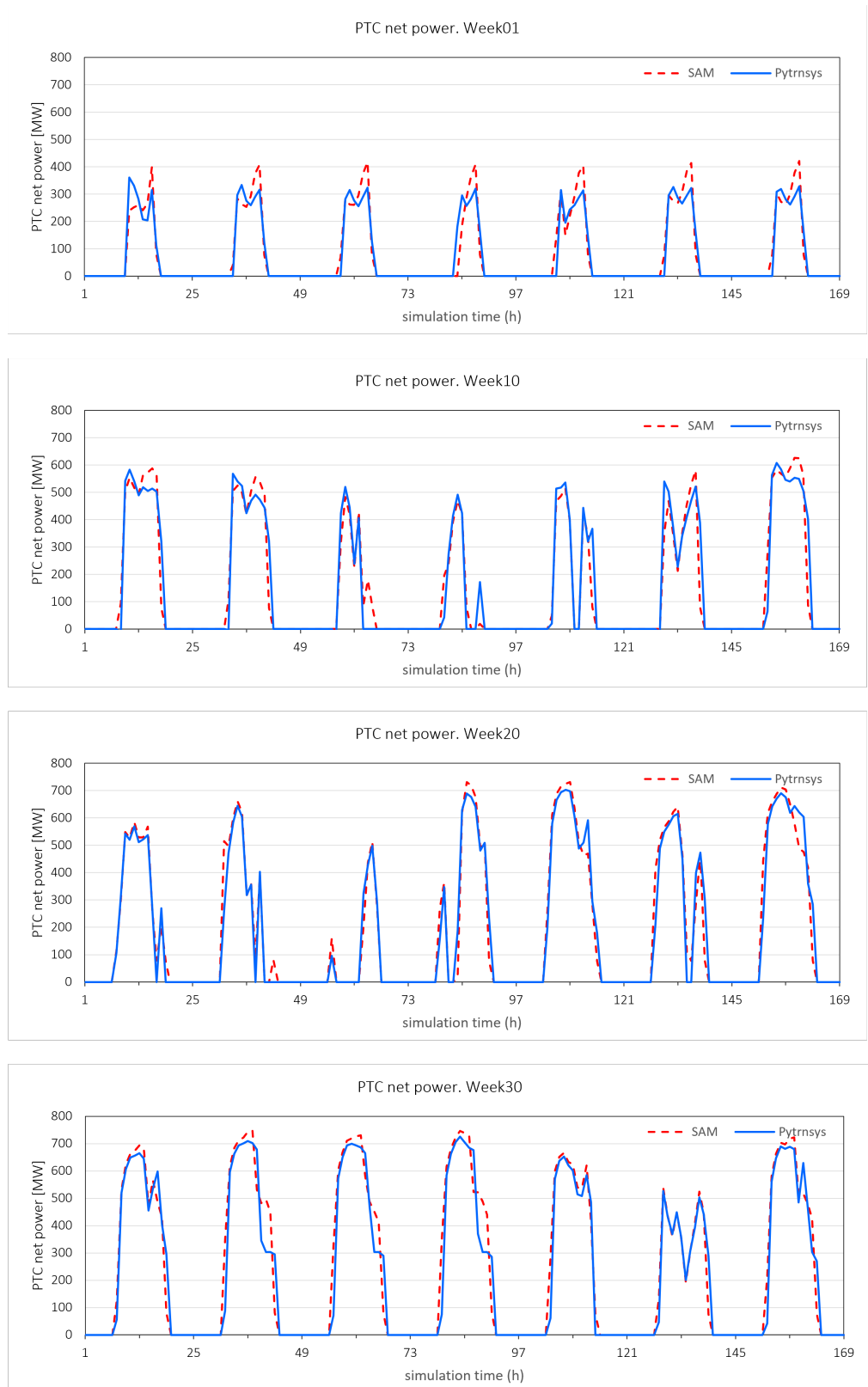
Figure 15: Parabolic trough thermal energy yield results obtained with *pytrnsys* and SAM for different weeks of the year.
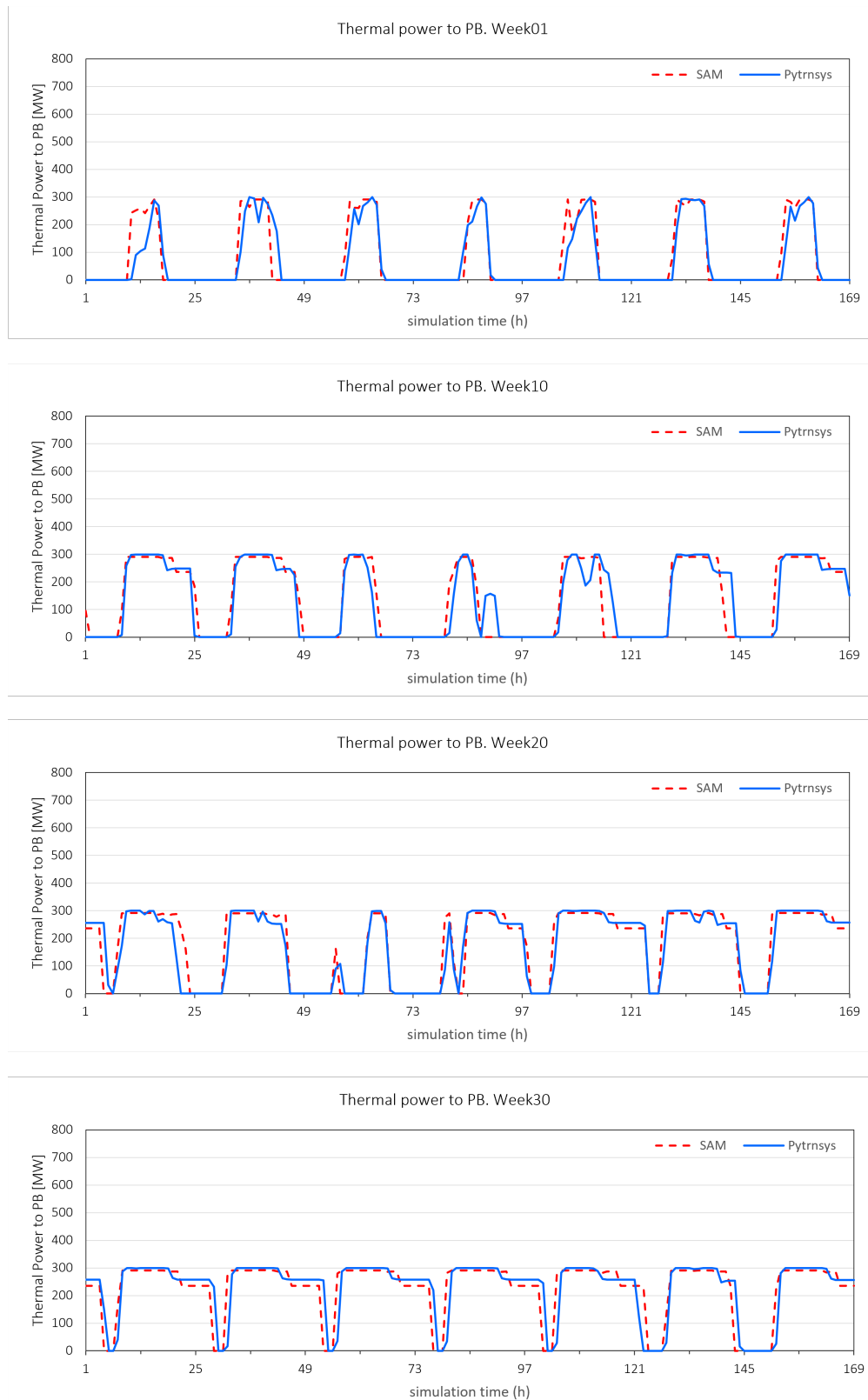
Figure 16: Thermal energy entering to the power block results obtained with *pytrnsys* and SAM for different weeks of the year.
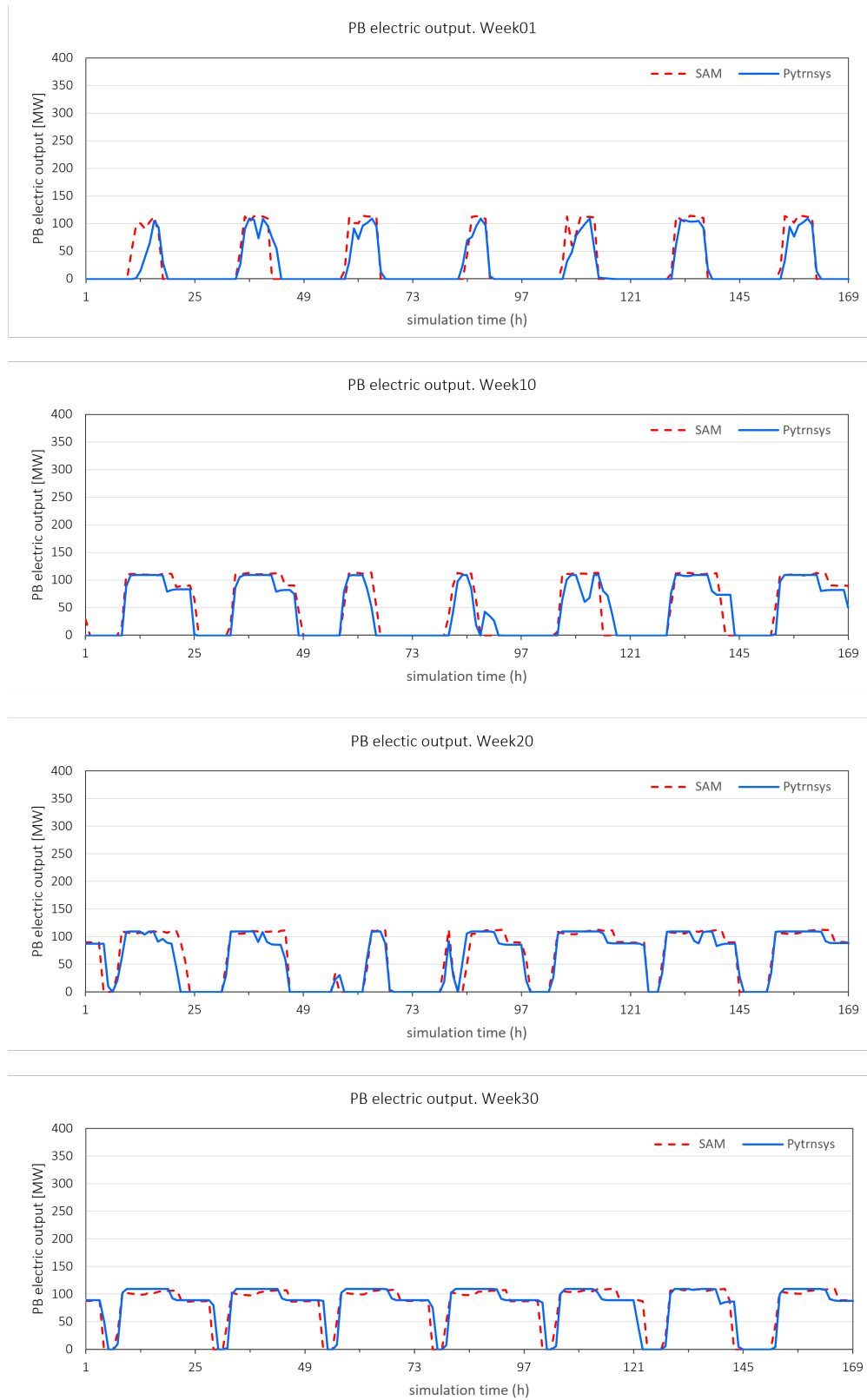
Figure 17: Electricity produced by the power block results obtained with *pytrnsys* and SAM results for different weeks of the year.
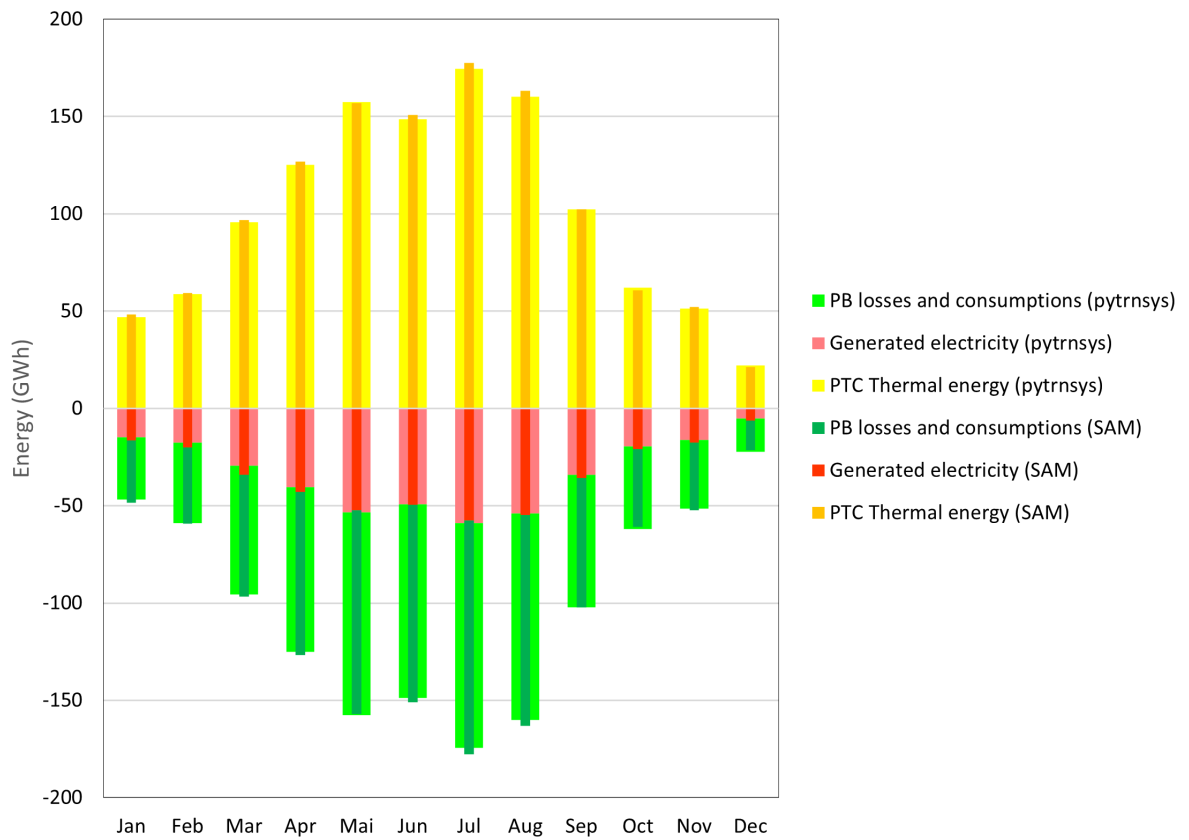
Figure 18: Monthly energy balances of the *pytrnsys* (wider lighter bars) and *SAM* (smaller darker bars) simulations for the parabolic trough CSP solar plant.

Table 7: Comparison between the monthly energy balances of the *SAM* and the *TRNSYS* simulations for the PTC CSP solar plant. A positive values in Difference indicates the value predicted by pytrnsys is larger than that of SAM.

	PTC Thermal energy		PB looses and cons.		Gen. Electricity	
	SAM	pytrnsys	SAM	pytrnsys	SAM	pytrnsys
	GWh	*GWh*	*GWh*	*GWh*	*GWh*	*GWh*
Jan	48.4	46.9	-31.8	-32.1	-16.6	-14.7
Feb	59.2	58.8	-39.2	-41.2	-20	-17.6
Mar	96.7	95.6	-62.7	-66.1	-34	-29.5
Apr	126.7	125.1	-83.7	-84.6	-43	-40.5
Mai	156.9	157.5	-104.6	-104.1	-52.3	-53.4
Jun	150.9	148.7	-101.2	-99.4	-49.7	-49.3
Jul	177.6	174.5	-120.2	-115.6	-57.4	-58.9
Aug	163.2	160.1	-108.4	-106	-54.8	-54.1
Sep	102.3	102.2	-66.7	-68.1	-35.6	-34.1
Oct	60.7	62.1	-39.9	-42.7	-20.8	-19.4
Nov	52.2	51.3	-34.5	-35.2	-17.6	-16.2
Dec	21.4	22.1	-15.2	-17	-6.2	-5.1
Total	1216.4	1204.8	-808.3	-812.1	-408.1	-392.7
Difference	-1.0%		0.5%		-3.8%	

4.3 Central receiver thermocline CSP plant

4.3.1 Description of the system

The CR thermocline CSP plant, similar to the two-tank CSP plant, consist of:

- a solar field, which comprises thousands of heliostats arranged in concentric circles around the central tower, at the top of which is located the CR,

- a power block which encompasses the main and auxiliary equipment for transforming the thermal energy into electricity,

- auxiliary equipment, pipes, valves, pumps, insulation, etc.

The difference lies in the thermal energy storage (TES) which consists of the thermocline concept tank developed within the *Newcline* project. A tank with a solid phase, based on structured bricks, and a liquid phase, the molten salts, in which the bricks are embedded. In 4.3.2, there is a more detailed description of the thermocline tank developed within the *Newcline* project.

The hydraulic scheme of the CR plant, where the thermocline tank is integrated, is shown in Fig.19.

Central Receiver

Power Block

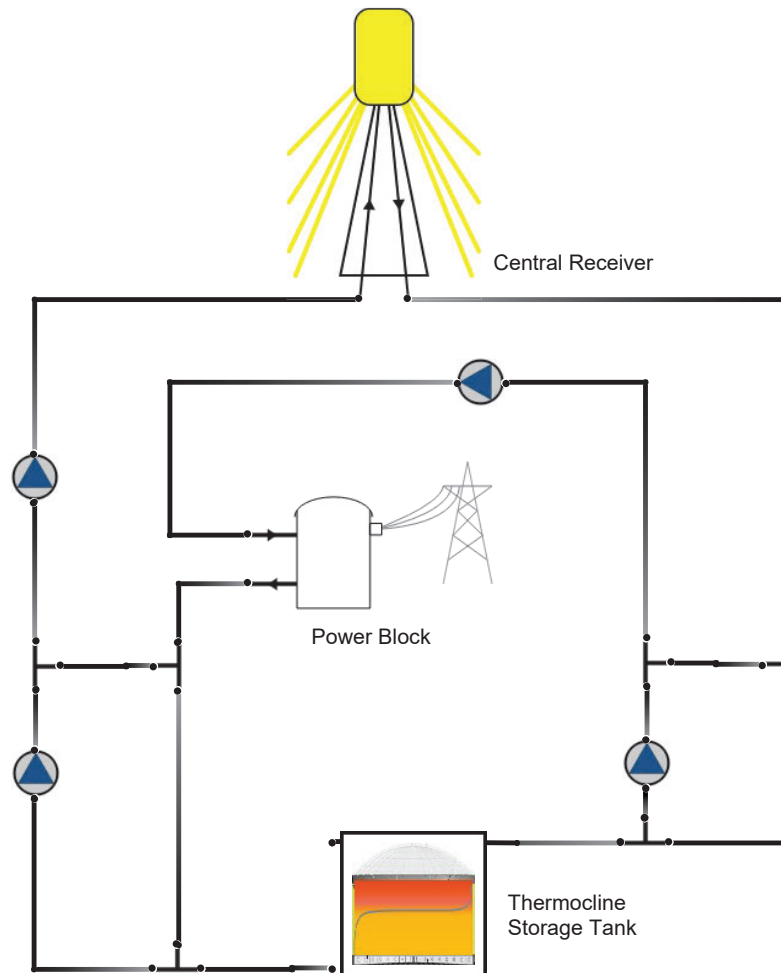Thermocline
Storage Tank

Figure 19: Hydraulic scheme of the CR thermocline plant simulated with *pytrnsys*.

The CR thermocline CSP plant operation modes are similar to the two-tank CSP system:

- the *charging operational mode*, where the solar central receiver generation loop, which collects energy from the sun and stores it in the thermocline tank or delivers it directly to the power block,

- the *discharging operational mode*, where the power block, either from the thermocline tank and/or directly from the central receiver, consumes thermal energy to generate electricity.

Depending on the balance between the central receiver and power block mass flow rates, the hot and cold tank pumps are respectively operated consequently charging the thermocline tank, in a hotter molten salts flow from the top to the bottom, displacing the thermocline downwards, or discharging it, in the opposite direction, in a flow of cooler molten salts from the bottom to the top, displacing the thermocline upwards. The central receiver and the power block are operating under the same criteria as the two molten salt tank CSP plants.

4.3.2 Description of the thermocline tank

The main components of the thermocline tank, apart from the molten salts, are:

- Metallic structure of the tank, composed of the roof, the walls, and the base structure,

- Ceramic blocks which fill the volume of the tank,

- Hydraulic distributor rings on top and at the bottom for the hot and cold areas,

- Insulation and fiberglass filler.
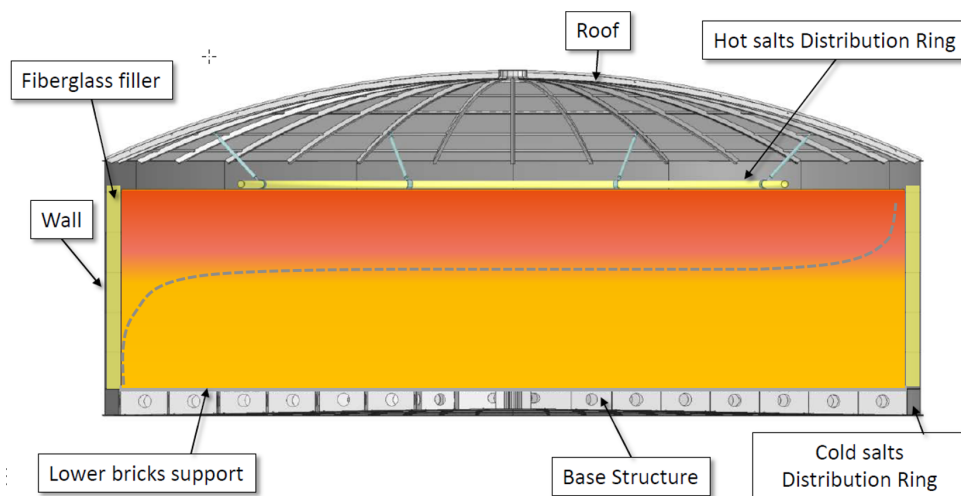
Figure 20: General scheme of the Thermocline tank. Source: *Empresarios Agrupados*.

As it is shown in 20 hot and cold molten salts are stored in the same tank, and the thermocline tank and the filler bricks are designed so as to ensure that operational conditions prevent both zones from a high mixing ratio. Indeed the thermocline concept is based on a high separation (low mixing) of the hot and cold zones inside the same tank. These hot and cold temperatures depend on the hot and cold plant operational temperatures. In the CR CSP plant, the hot salt temperature is 565 ºC while the cold salt temperature is 300 ºC. In the PTC CSP plant, the hot salt temperature is 385 ºC while the cold salt temperature is 290 ºC.

In Fig. 21 the structured solid phase composed by individual ceramic bricks is shown. Those bricks rely on internal channels where the liquid phase, the molten salts, is able to circulate trough. The structured solid phase is then, embedded in the molten salt liquid phase which rises above the upper row of bricks up to the hot salts distribution ring shown in Fig. 20, resulting in a upper buffer zone. The down buffer zone is the flooded volume below the downer row of bricks and the basement, connecting to the cold salts distribution ring shown in Fig. 20.

In Fig. 22, there is a scheme of the hot and cold distributors ring which facilitates the inlet and outlet of the molten salts into the thermocline tank.

Figure 21: Internal scheme of the Thermocline tank with the structured filler blocks. Source: *Empresarios Agrupados*.

Figure 22: Hydraulic ring distributors for charging and discharging of the Thermocline tank. Source: *Empresarios Agrupados*.

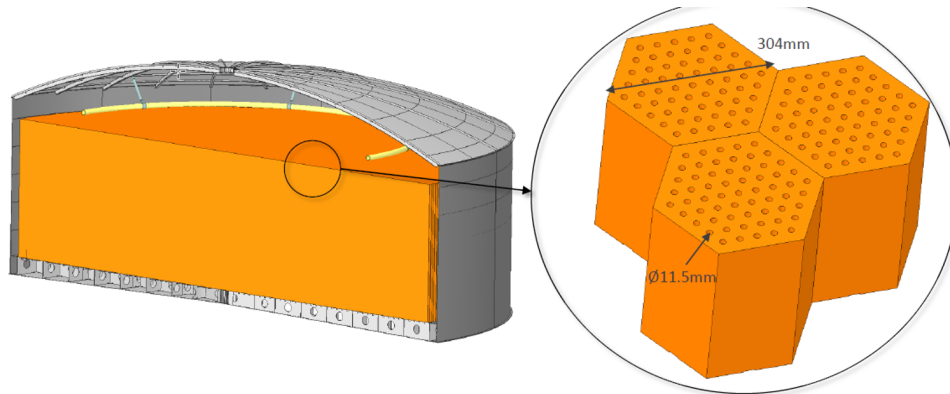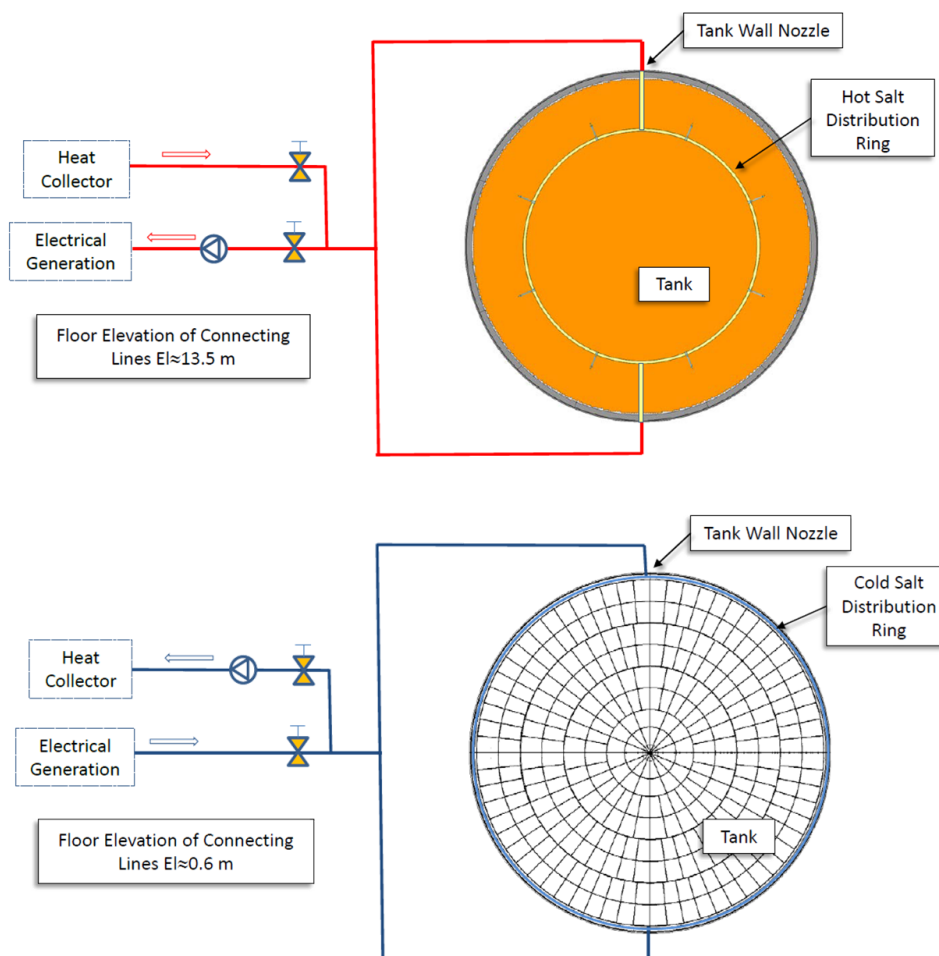### 4.3.3 Energetic performance comparison CR thermocline versus two-tank reference system

The main characteristics of the proposed CR thermocline CSP reference plant, with similar nominal storage capacity and equally solar CR aperture area, are:

- same location and coordinates: 37.244N, 2.982W, Province of Granada (Spain).

- a unique thermocline tank with similar external dimensions but a lower amount of molten salts compared to the two-tank molten salt reference plant, ca. 18×10^3 ton. The *Newcline* thermocline storage, despite having less molten salts, only 45 %, achieves a similar nominal storage capacity of 3532 MWh as the two-tank reference plant (3545 MWh), thanks to being partially filled with the structured bricks through which the molten salts circulate.

- same heliostat mirror surface of $1\,535\,611\,\text{m}^2$ and a central receiver with a thermal power of 787.5 MW.

- same gross/net electrical power: 115/100 MW as the two-tank reference system.

Energetic performance comparison CR thermocline versus two-tank reference system for different periods of the year are presented in Fig. 23, Fig. 24 and Fig. 25. Fig. 23 shows the thermal energy yield of the CR solar field for different weeks (1/10/20/40) of the year. Despite the energy yield profile is similar, there are small differences in the first but mainly in the last hours of the CR daily operation. These differences may come from the thermocline storage tank availability to be charged and to be discharged.

The predictions of the thermal input to the power block are depicted in Fig. 24. Here deviations between the behaviour of the thermocline CR CSP and the two-tank molten salts CSP plant are exhibited. The main differences arise during the final hours of daily operation, where the thermocline tank provides fewer lasting hours than the two-tank molten salts CSP plant with an equivalent nominal storage capacity. This implies that the thermocline tank, despite having a similar nominal storage capacity, may not be fully available for charging or discharging depending on the selected charging and/or discharging control. (Specifically depending on the temperature thresholds as it is outlined in section 5.6). Nonetheless, the differences between the two CR CSP systems are minimal. Fig. 25 shows the electrical outlet power for both systems. The previous differences observed in the thermal energy input to the power block are clearly transferred to the electrical output.

In Tab. 9 the comparison between the main parameters and results of both system is shown.

Comparing the simulation results between two-tank molten salt and thermocline we can state that the thermal output of the CR likewise the thermal input to the power block and the electricity produced by the CR thermocline CSP plant is 13.2 % to 12.8 % lower than obtained with the two-tank molten salt CSP plant. These results depend, as it is shown in section 5.6 on the control strategy for charging or discharging, which could even improve the performance and harnessing of the thermocline storage.
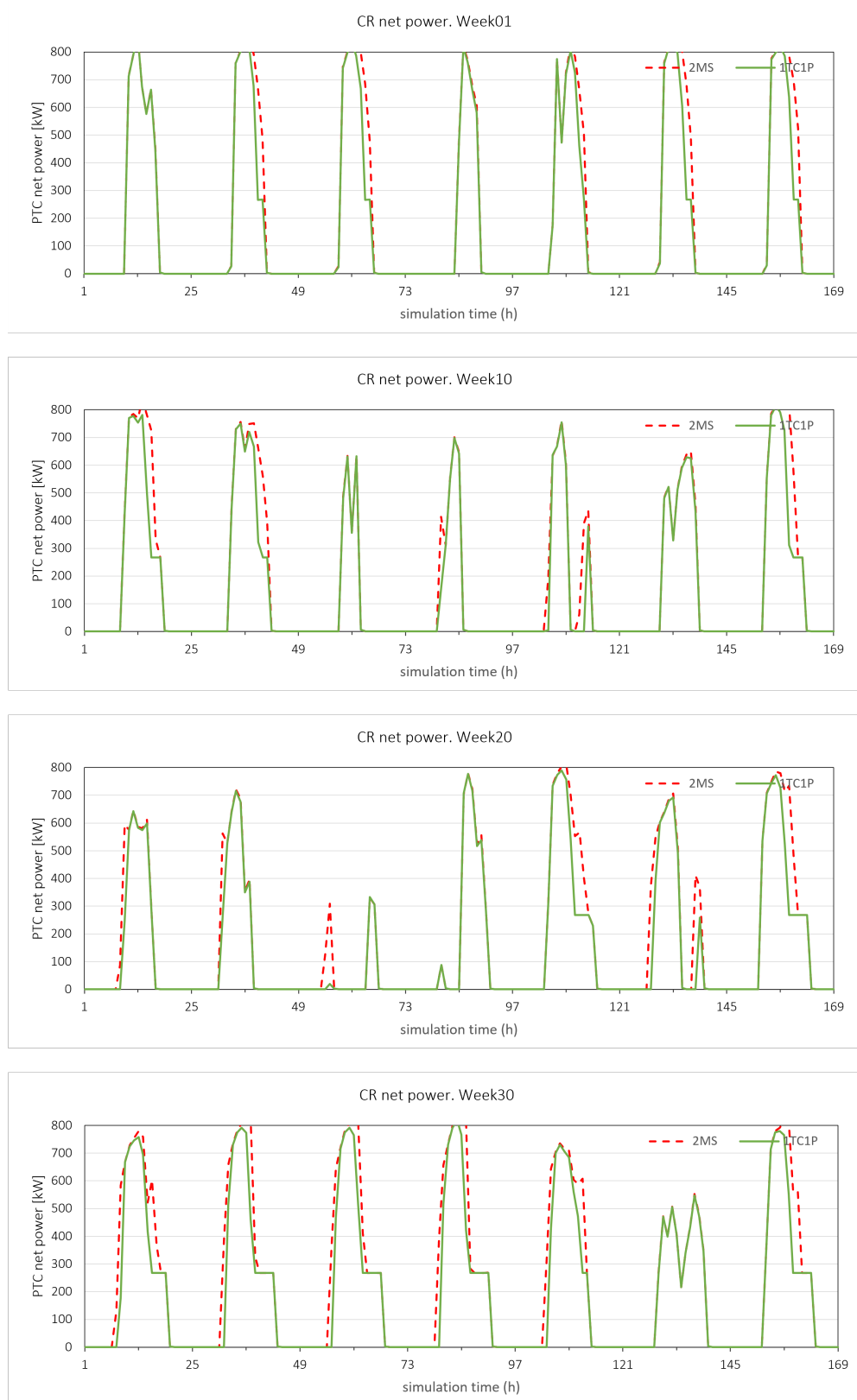
Figure 23: Central receiver thermal energy yield for the thermocline CSP plant (1TC1P), in continuous green line, compared with the two-molten salts CSP plant (2MS), in dashed red line, for different weeks of the year.
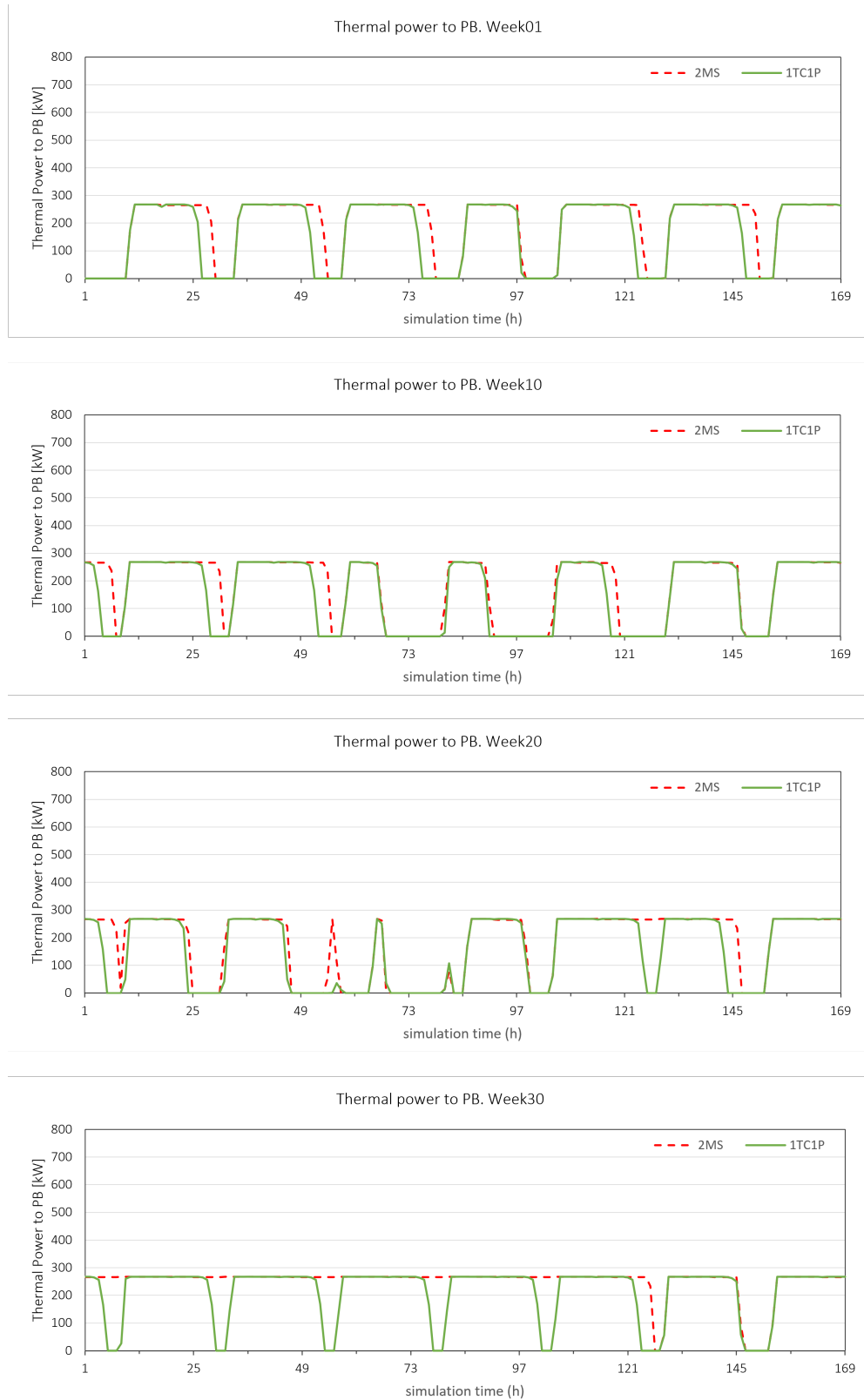
Figure 24: Thermal energy entering to the power block for the thermocline CSP plant (1TC1P), in continuous green line, compared with the two-molten salts CSP plant (2MS), in dashed red line, for different weeks.
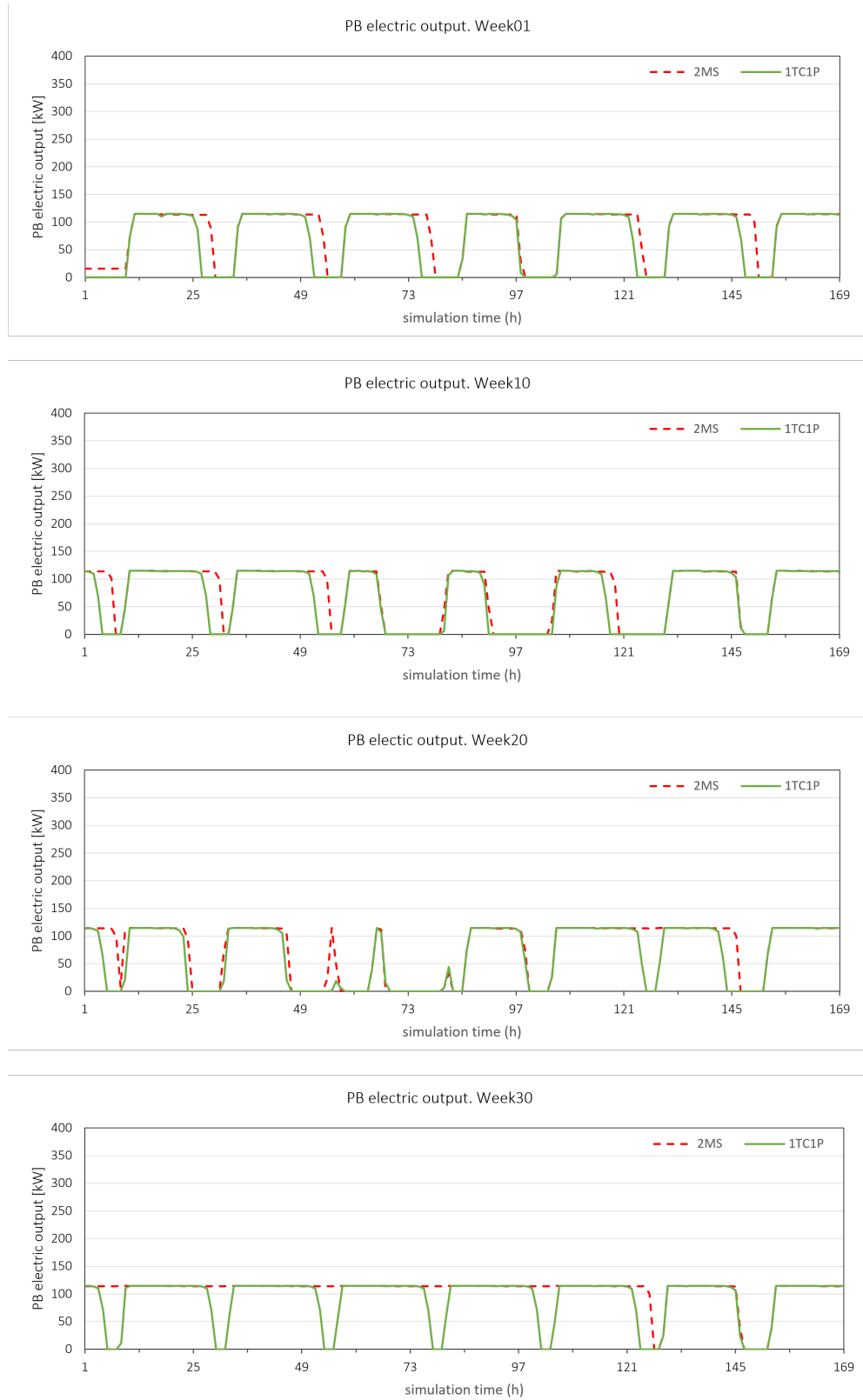
Figure 25: Electricity produced by the power block for the thermocline CSP plant (1TC1P), in continuous green line, compared with the two-molten salts CSP plant (2MS), in dashed red line, for different weeks.

Table 8: Comparison between two-tank molten salt and thermocline CR CSP solar plant. Where η_{system} is the thermal energy input to the power block divided by the solar thermal energy yield and the $\eta_{\text{power}-\text{block}}$ is the generated electricity divided by the thermal energy input to the PB.

	units	Two-tank 2MS	Thermocline 1TC	Difference
Reference conditions:				
Aperture area	m^2	1 535 611		0 %
Gross/net electrical power	MW	115/100		0 %
Storage Capacity	MWh	3545	3532	-0.4 %
Molten salts	ton	40×10^3	18×10^3	-55 %
Storage temperature (T$_{\text{hot}}$/T$_{\text{cold}}$)	°C	565/300		
Results from Simulations:				
Solar thermal energy yield	kWh/m^2	950.17	824.83	-13.2 %
Thermal energy input to power block	kWh/m^2	944.24	823.65	-12.8 %
η_{system}	%	99.4	99.9	
Electricity	kWh/m^2	404.08	352.21	-12.8 %
$\eta_{powerblock}$	%	42.8	42.8	

4.3.4 LCOE comparison CR thermocline versus two-tank reference system

As mentioned in section 3.3, the LCOE is a metric used to evaluate and compare the cost-effectiveness of different energy generation technologies. It represents the cost of projecting, financing, constructing and operating a generation plant over a period of time per energy demand provided. Therefore, the evaluation of the capital expenditures (CAPEX) and operating expenses (OPEX) are previously required.

For reasons of confidentiality, the investment and operating costs as well as the corresponding LCOE values will be shown in relative percentages. Relative compared values, named as *Difference*, are calculated by the difference between the thermocline value and the two-tank value, divided by the two-tank value.

As evidenced by the comparative analysis presented in Table 9, for the CR CSP technology, the thermocline system, depending on whether the economic investment assumptions are met or not, could potentially be more costly (up to 10%). However, it could also lead to investment cost savings of up to 3%. Nevertheless, this cost savings might not result in a reduction in the LCOE as the electricity produced by the thermocline CR CSP is 12.8 % lower than the electricity produced by the two-tank molten salt CR CSP (as it is shown in section 4.3.3). This means that the 12.8% reduction in electricity production in the case of the CR is not offset by the possible savings in investment costs of 3%. A higher electricity production could be achieved by the thermocline by means of optimizing the threshold temperatures as it will be shown in 5.6.

Table 9: Comparison between two-tank molten salt and thermocline CR CSP solar plant.

Variable	units	Difference
CAPEX	%	-3 % to +10 %
OPEX	%	-9 % to -10 %
LCOE	%	+9 % to +23 %

As a conclusion, the anticipated investment cost savings for the thermocline are not achieved for the CR CSP plant. The reduction in the number of tanks does not translate into an economic competitive advantage; the fact that the tank has to handle a higher weight (the filler plus molten salts), in addition to higher thermal and, consequently, mechanical stresses, requires of a more complex and expensive structural design to ensure the tank's integrity and safety. As a result, the cost savings from having one tank instead of two, might be offset by the increased costs associated with the enhanced design and the additional amount of metal of the thermocline tank required to withstand the higher stresses. In addition, the advantage of a 55 % salt reduction is not very significant for the CR case in absolute terms and it is not enough benefit alone to contribute to potential cost savings. The main difference between the CR and the PTC case, in terms of salt savings, is the higher temperature difference of the CR case, that demands less amount of salt for the same energy stored. Consequently, the savings of reducing the salt are not that relevant for the CR. Thus, in terms of LCOE, the thermocline CR CSP does not appear to be more economical than the conventional two-tank CR CSP. Depending on the assumed cost, the thermocline system is expected to be between 9 % to 23 % more expensive.

4.4 Parabolic Trough thermocline CSP plant

4.4.1 Description of the system

The PTC thermocline CSP plant, similar to the two-tank CSP plant, consist of:

- a parabolic trough field, which comprises thousands of parabolic trough collectors arranged in rows.

- a power block which encompasses the main and auxiliary equipment for transforming the thermal energy into electricity.

- a heat exchanger (HX) that isolates the oil-based loop for the Parabolic Trough and Power Block from the molten salt loop used for storage.

- auxiliary equipment, pipes, valves, pumps, insulation, etc.

The difference lies is the thermal energy storage (TES) which consists of the same thermocline tank presented in the previous subsection 4.3.2, developed within the *Newcline* project. A tank with a solid phase, based on structured bricks, and a liquid phase, the molten salts. Hot and cold molten salts are, therefore, stored in the thermocline tank. The solid filler material prevents the mixing between the hot and the cold molten salt.

The hydraulic scheme of the PTC thermocline plant used in the system simulations with *pytrnsys* is shown in Fig.26.
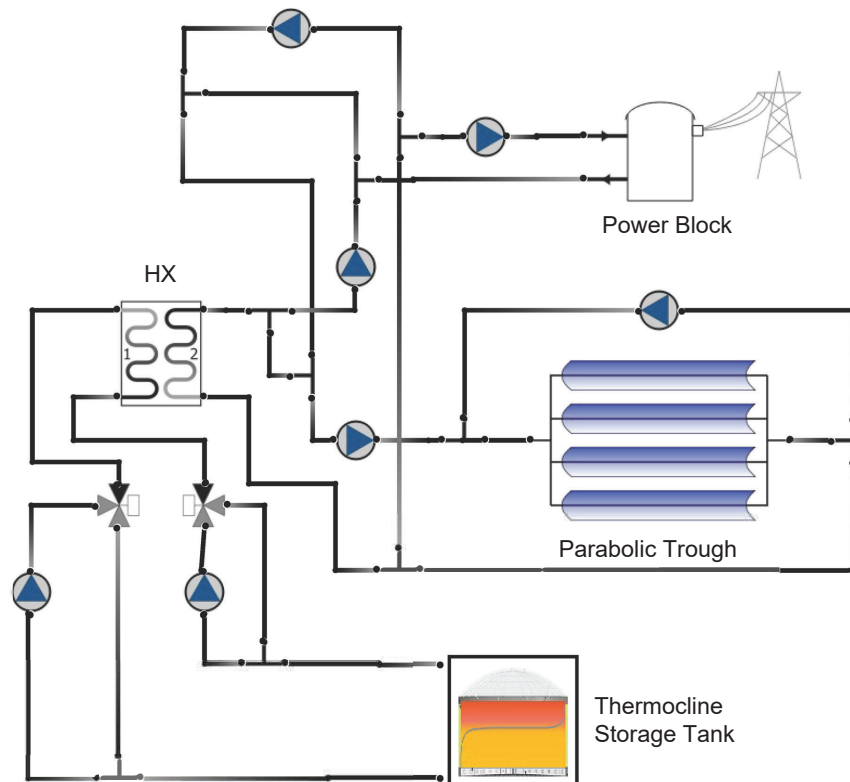
Figure 26: Hydraulic scheme of the PTC thermocline plant simulated with *pytrnsys*.

Similar to the CR, depending on the balance between the PTC and power block mass flow rates, the hot and cold tank pumps are operated to charge and discharge the thermocline tank respectively. In charging mode, the hot molten salts flow from the top to the bottom, displacing the thermocline downwards. In discharge mode, the cold molten salts flow from the bottom to the top, displacing the thermocline upwards.

The parabolic trough and the power block are operating using the same criteria applied to the two molten salt tank CSP plants.

4.4.2 Energetic performance comparison PTC thermocline versus two-tank reference system

The main characteristics of the proposed PTC thermocline CSP reference plant, with similar nominal storage capacity and equally solar PTC aperture area, are:

- same location and coordinates: 37.244N, 2.982W, Province of Granada (Spain),

- two thermocline tank with similar external dimensions but a lower amount of molten salts as the PTC two-tank molten salt reference plant, ca. 36×10^3 ton. The *Newcline* thermocline storage, despite having less molten salts, only 45 %, achieves a similar nominal storage capacity of 2584 MWh as the two-tank reference plant (2679 MWh), thanks to being partially filled with the structured bricks through which the molten salts circulate.

- the same solar field comprised of 375 loops, each one made up of 4 solar collector assembly (SCA). Each SCA with an aperture area of 817.5 m^2. Hence, a total aperture area of 1 226 250 m^2,

- same gross/net electrical power: 115/100 MW as the two-tank reference system.

Energetic performance comparison PTC thermocline versus two-tank reference system for different periods of the year are presented in Fig. 27, Fig. 28 and Fig. 29. Fig. 27 shows the thermal energy yield of the PTC solar field for different weeks (1/10/20/40) of the year. Despite the energy yield profile is similar, there are small differences in the last hours of the PTC daily operation. These differences may come from the thermocline storage tank availability to be charged.

The predictions of the thermal input to the power block are depicted in Fig. 28. Here deviations between the behaviour of the thermocline PTC CSP and the two-tank molten salts CSP plant are exhibited. The main differences arise during the final hours of daily operation, where the thermocline tank provides fewer lasting hours than the two-tank molten salts CSP plant with an equivalent nominal storage capacity. This implies that the thermocline tank, despite having a similar nominal storage capacity, may not be fully available for charging or discharging depending on the selected charging and/or discharging temperature thresholds. A more detailed explanation of this phenomenon is depicted in section 5.6. Nonetheless, the differences between the two PTC CSP systems are small. Fig. 29 shows the compared electrical outlet power for both systems. The previous differences observed in the thermal energy input to the power block are clearly transferred to the electrical output.

In Tab. 11 the comparison between the main parameters and results of both systems is shown. Comparing the simulation results between two-tank molten salt and thermocline we can state that the thermal output of the PTC, the thermal input to the power block and the electricity produced by the PTC thermocline CSP plant, are in the range of 3.1 % to 4.6 % lower than obtained with the two-tank molten salt CSP plant. These results depend, as will be shown in section **??**, on the control strategy for charging or discharging.
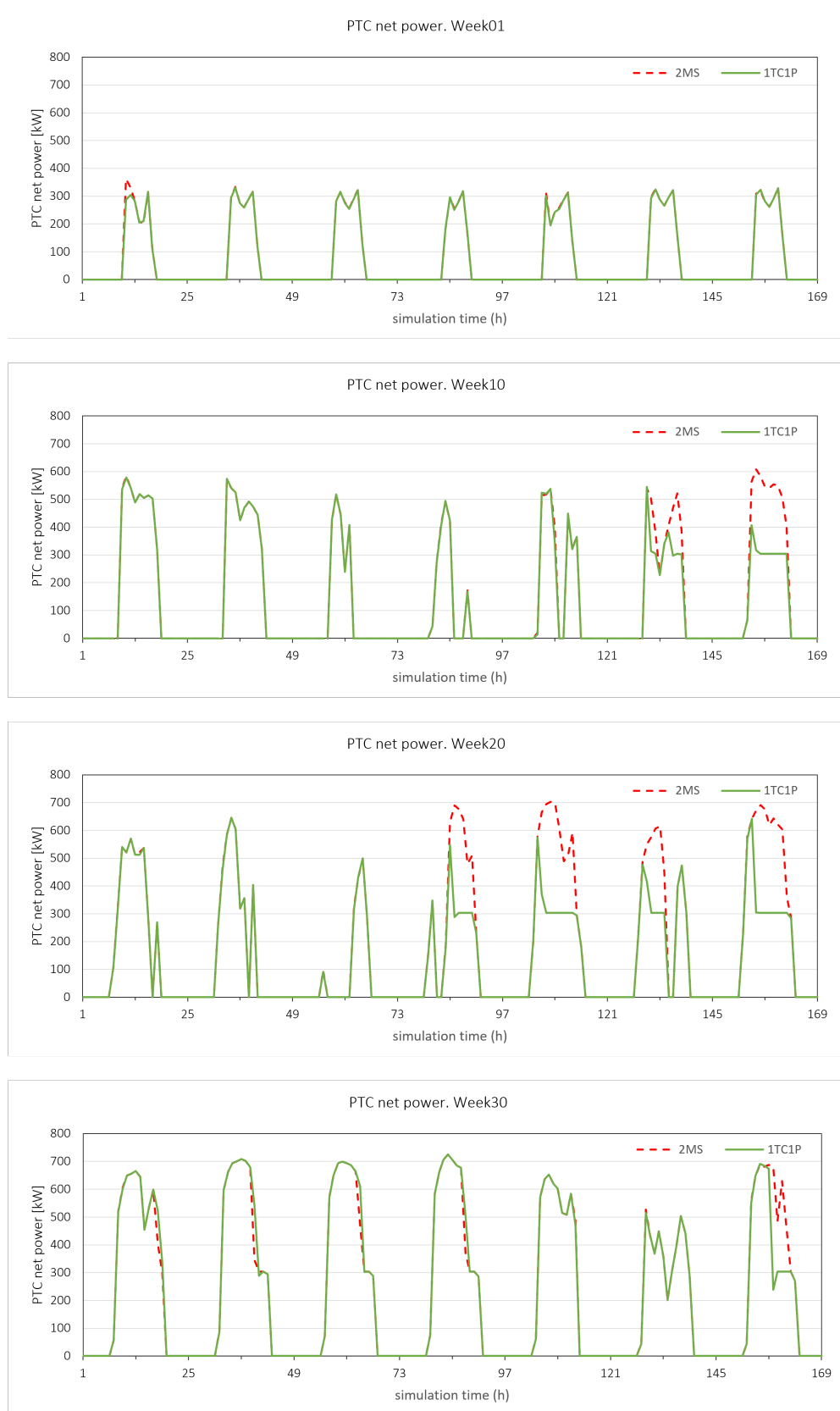
Figure 27: Parabolic Trough thermal energy yield for the thermocline CSP plant (1TC1P), in continuous green line, compared with the two-molten salts CSP plant (2MS), in dashed red line, for different weeks of the year.
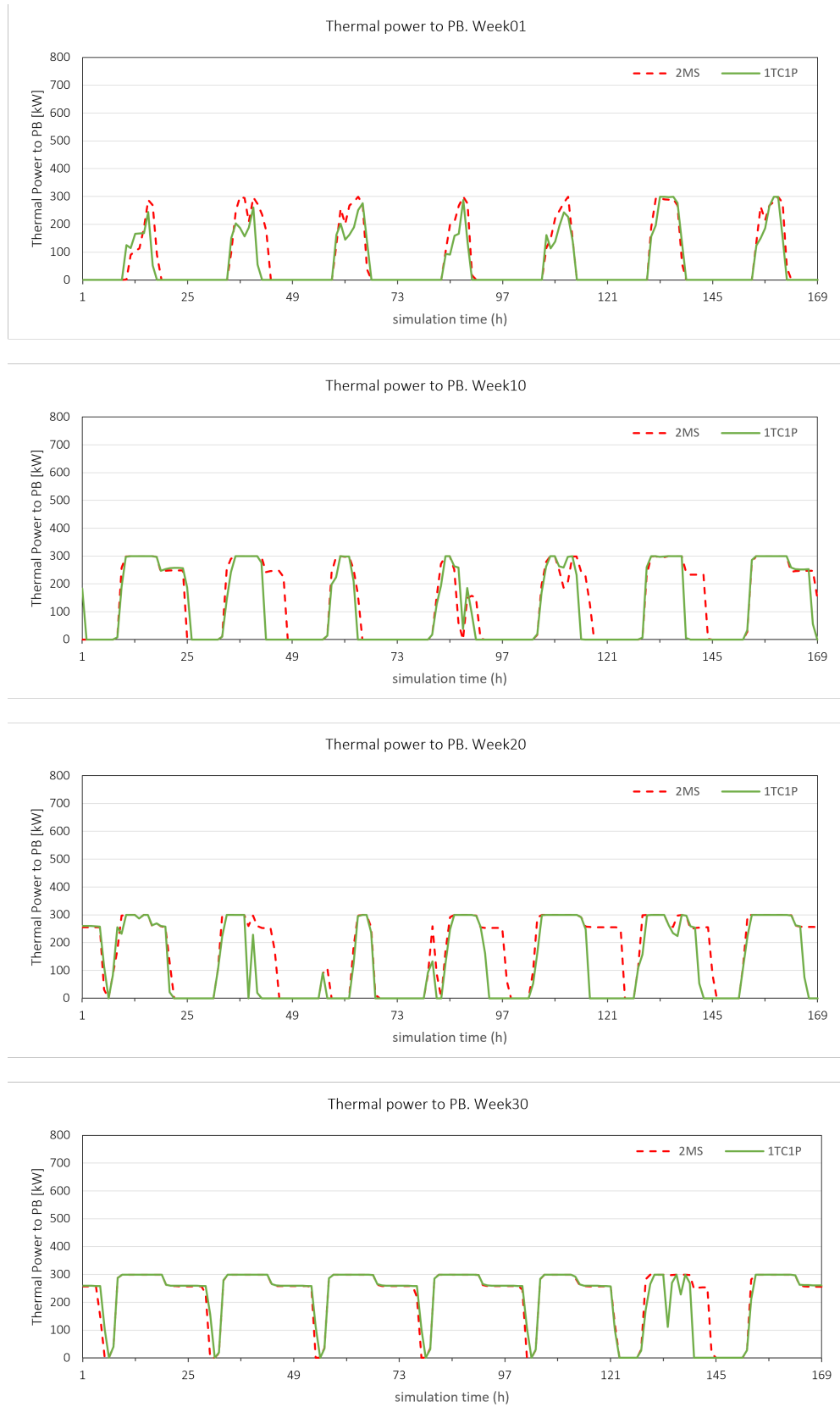
Figure 28: Thermal energy entering to the power block for the thermocline CSP plant (1TC1P), in continuous green line, compared with the two-molten salts CSP plant (2MS), in dashed red line, for different weeks.
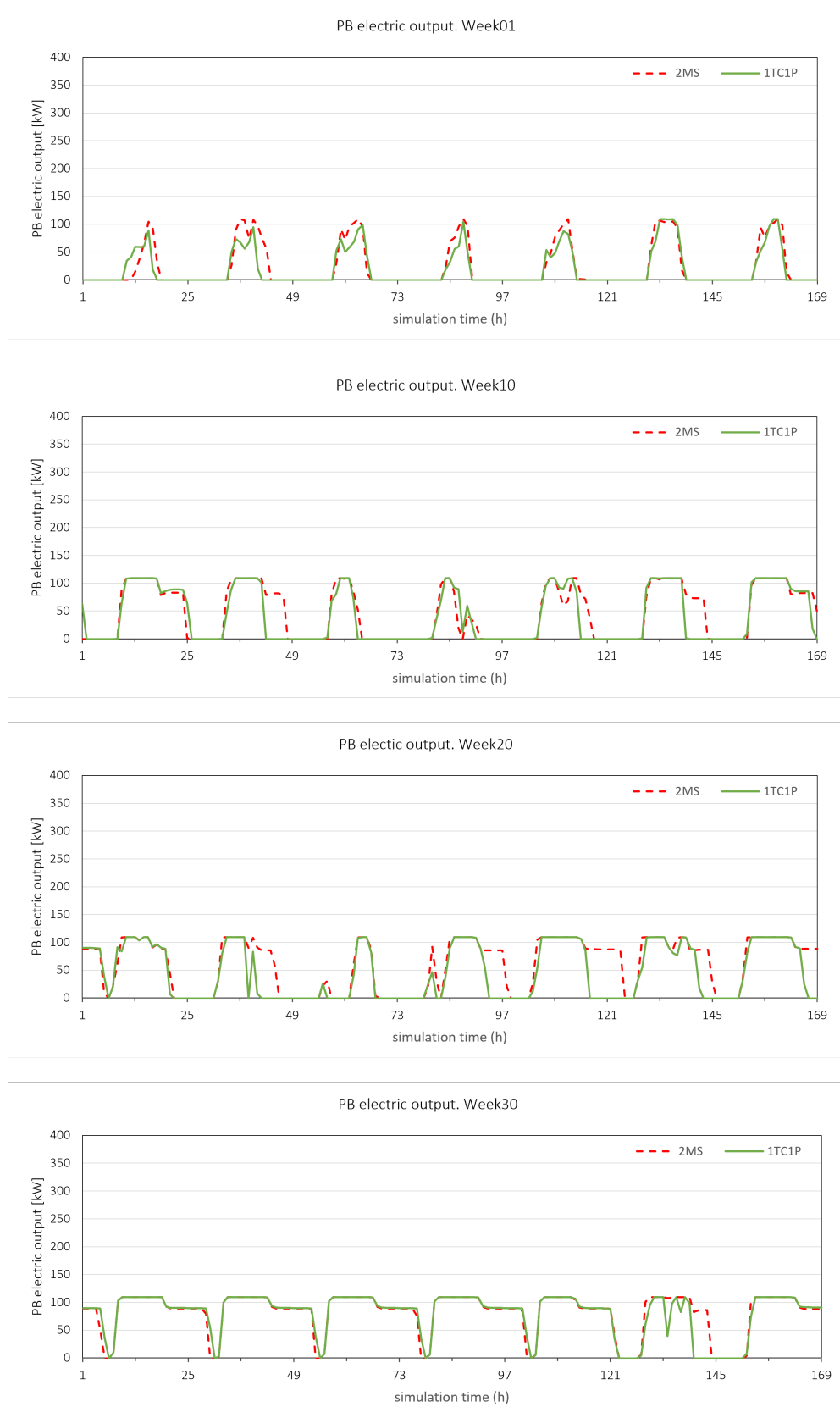
Figure 29: Electricity produced by the power block for the thermocline CSP plant (1TC1P), in continuous green line, compared with the two-molten salts CSP plant (2MS), in dashed red line, for different weeks.

Table 10: Comparison between two-tank molten salt and thermocline PTC CSP solar plant. Where η_{system} is the thermal energy input to the power block divided by the solar thermal energy yield and the $\eta_{power-block}$ is the generated electricity divided by the thermal energy input to the PB.

	units	Two-tank 2MS	Thermocline 1TC	Difference
Reference conditions:				
Aperture area	m^2	1 226 250		0 %
Gross/net electrical power	MW	115/100		0 %
Storage Capacity	MWh	2679	2584	-3.6 %
Molten salts	ton	81×10^3	36×10^3	-55 %
Storage temperature (T_{hot}/T_{cold})	°C	385/290		
Results from Simulations:				
Solar thermal energy yield	kWh/m^2	982.50	944.94	-3.8 %
Thermal energy input to power block	kWh/m^2	923.73	881.47	-4.6 %
η_{system}	%	94.0	93.3	
Electricity	kWh/m^2	320.24	310.36	-3.1 %
$\eta_{power-block}$	%	34.7	35.2	

4.4.3 LCOE comparison PTC thermocline versus two-tank reference system

Table 11 shows the comparative analysis for the PTC CSP technology between the two-tank and the thermocline system. Depending on the economic investments assumptions, which include a range for the uncertainty associated, the CAPEX of the thermocline system could potentially be 9 % higher or 7 % lower. For the evaluation of the LCOE, the electricity produced by the thermocline system, which is 3.1 % lower as the electricity produced by the two-tank molten salt PTC CSP (shown in section 4.4.2) has a significant impact. The LCOE might be either 6 % lower or 10 % higher compared to the two-tank molten salt CSP plant. A higher electricity production could be achieved by the thermocline by means of optimizing the threshold temperatures as it will be shown in **??**.

Table 11: Comparison between two-tank molten salt and thermocline PTC CSP solar plant.

Variable	units	Difference
CAPEX	%	-7 % to +9 %
OPEX	%	-17 % to -8 %
LCOE	%	-6 % to +10 %

As a conclusion, depending on the economic assumptions, the anticipated investment cost savings for the thermocline could be achieved for the PTC case. However, the economic benefits are within the uncertainty range and it could also well be that the thermocline system would be more expensive.

The potential investment cost advantage of implementing a thermocline storage in PTC compared to CR, steams from the difference in the relative weight of the cost of salts in the total CSP plant's investment cost. As shown in Tab. 11 and Tab. 9, a two-tank plant requires 40 000 ton of salts, whereas an equivalent PTC power plant, with even lower storage capacity, requires 81 000 ton of molten salts. Consequently, the share of the cost of salts in the total investment cost of the CSP plant is much higher for the PTC than for the CR. Although this is a disadvantage for the PTC two-tank conventional storage systems, it becomes an advantage for the PTC thermocline storage, whose primary objective is to reduce the amount of salts, thereby proportionally reducing the investment cost.

5 Analysis of different plants schemes

5.1 Introduction

A parametric analysis of different power block and storage capacities has been carried out to assess the differences in the energetic performance and levelized cost of energy (LCOE) between the two-tank molten salt and the thermocline storage CSP plants. CSP plants able to provide 50 MW, 100 MW and 150 MW of electricity including storages capacities between 6 h to 14 h have been reported in the following sections. These hours represent the total operating hours that the storage can provide to the power block, in other words, the energy accumulated by the storage divided the the thermal energy input of the power block in nominal conditions.

The dimensioning criteria for sizing the power block, the solar aperture area, and the nominal equivalent storage hours of these CSP plants have been established to optimise the overall plant's operation. As a result, the specific solar energy yield and the amount of energy produced by the power block, both relative to the solar aperture area, are expected to remain within a similar range. Therefore, the dominant factor in the comparative analysis of the LCOE will be primarily the influences of the economies of scale of the CAPEX and OPEX. This is because larger-scale energy projects typically benefit from reduced per-unit costs in both the construction and operational phases.

Additionally, a sensibility analysis of the thermocline charging and discharging threshold temperatures in thermocline systems has been performed with the aim to assess the influence in operational storage capacity and energy performance of the CSP plant.

5.2 Energetic performance of different CR thermocline versus two-tank CSP plants

In the following Tab. 12 the resulting values obtained from the pytrnsys simulation framework for CR solar energy yield, power block thermal input, and electricity for the CR two-tank compared with the thermocline CSP for different nominal power plants and storage, is shown.

As the solar multiple (SM) criteria for dimensioning the solar aperture area with respect to the power block's power, and the nominal equivalent storage hours, has been established to optimize the overall plant's operation, the specific solar energy yield of all plants relative to the solar aperture area remains in a limited range between $894\,\mathrm{kWh/m^2}$ to $971\,\mathrm{kWh/m^2}$, the power block thermal input in the range between $889\,\mathrm{kWh/m^2}$ to $964\,\mathrm{kWh/m^2}$, and the electricity produced by the power block between $381\,\mathrm{kWh_e/m^2}$ to $412\,\mathrm{kWh_e/m^2}$. For the thermocline CR CSP plant, the specific solar energy yield of all plants relative to the solar aperture area remains in a constrained range between $797\,\mathrm{kWh/m^2}$ to $843\,\mathrm{kWh/m^2}$, the power block thermal input in the range between $796\,\mathrm{kWh/m^2}$ to $842\,\mathrm{kWh/m^2}$, and the electricity produced by the power block between $340\,\mathrm{kWh_e/m^2}$ to $360\,\mathrm{kWh_e/m^2}$.

The differences in the solar energy yield between the two-tank (2MS) and thermocline (1TC) are for the CR in the range of -14 % to -8 %. In terms of the power block thermal input and electricity produced, these differences are transferred in a similar range, resulting in equivalent differences. These differences, as depicted in section 4.3.3 come from a slightly lower thermocline storage capacity, which in turn is influenced by the control criteria for charging and discharging. The control strategy will be investigated in section 5.6.

Table 12: Energetic performance comparison between different two-tank molten salt (2MS) and thermocline (1TC) CR CSP solar plant. Compared values (Diff.) are the difference between the thermocline values and the two-tank values, divided by the two-tank value. In **bold** the reference case presented in section 4.3.3

PB Power MW	Storage Capacity h	CR Solar Thermal yield			PB Thermal input			Electricity		
		2MS kWh/m^2	1TC kWh/m^2	Diff. %	2MS kWh/m^2	1TC kWh/m^2	Diff. %	2MS kWh/m^2	1TC kWh/m^2	Diff. %
50	6.0	919	830	-10%	913	828	-9%	391	354	-9%
	10.0	934	827	-11%	928	826	-11%	397	353	-11%
	14.2	971	843	-13%	964	842	-13%	412	360	-13%
100	6.0	910	832	-9%	905	831	-8%	388	355	-8%
	10.0	927	829	-11%	922	828	-10%	395	354	-10%
	14.2	**950**	**825**	**-13%**	**944**	**824**	**-13%**	**404**	**352**	**-13%**
150	6.0	902	826	-8%	898	825	-8%	384	353	-8%
	10.0	894	797	-11%	889	796	-11%	381	340	-11%
	14.2	933	803	-14%	927	802	-13%	397	343	-14%

5.3 Energetic performance of different PTC thermocline versus two-tank CSP plants

Tab. 13 shows the results obtained from the pytrnsys simulation framework for PTC solar energy yield, power block thermal input, and electricity for the PTC two-tank compared with the thermocline system for different nominal power plants and storage capacities.

Similar to the CR case, the solar multiple (SM) has been calculated depending on the nominal equivalent storage hours to optimise the overall plant's operation, the specific solar energy yield of all two-tank molten salt PTC CSP plants remains in a narrow range of 978 kWh/m^2 to 995 kWh/m^2, the power block thermal input in the range between 910 kWh/m^2 to 936 kWh/m^2, and the electricity produced by the power block between 314 kWh$_e$/m^2 to 324 kWh$_e$/m^2. For the thermocline PTC plant, the specific solar energy yield relative to the solar aperture area remains in a narrow range between 912 kWh/m^2 to 958 kWh/m^2, the power block thermal input in the range between 839 kWh/m^2 to 901 kWh/m^2, and the electricity produced by the power block between 295 kWh$_e$/m^2 to 317 kWh$_e$/m^2.

Table 13: Energetic performance comparison between different two-tank molten salt (2MS) and thermocline (1TC) PTC CSP solar plant. Compared values (Diff.) are the difference between the thermocline values and the two-tank values, divided by the two-tank value. In **bold** the reference case presented in section 4.4.2

PB Power MW	Storage Capacity h	PTC Solar Thermal yield			PB Thermal input			Electricity		
		2MS kWh/m^2	1TC kWh/m^2	Diff. %	2MS kWh/m^2	1TC kWh/m^2	Diff. %	2MS kWh/m^2	1TC kWh/m^2	Diff. %
50	6.0	993	934	-6%	928	861	-7%	318	301	-5%
	9.3	995	956	-4%	936	893	-5%	323	313	-3%
	12.5	988	957	-3%	932	900	-3%	322	316	-2%
100	6.0	982	933	-5%	914	860	-6%	315	302	-4%
	9.3	**982**	**945**	**-4%**	**924**	**881**	**-5%**	**320**	**310**	**-3%**
	12.5	987	958	-3%	931	901	-3%	323	317	-2%
150	6.0	978	912	-7%	910	839	-8%	314	295	-6%
	9.3	988	944	-4%	928	881	-5%	323	311	-4%
	12.5	985	944	-4%	929	889	-4%	324	314	-3%

The differences in the solar energy yield between the two-tank (2MS) and thermocline (1TC) are in the range of -7 % to -3 % for the different cases analyzed. In terms of the power block thermal input and electricity produced, these differences are transferred in a similar range, resulting in equivalent differences. These differences, as explained in section 4.4.2, come from a slightly lower thermocline storage capacity, which in turn is influenced by the control criteria for charging and discharging.

5.4 LCOE of different CR thermocline versus two-tank CSP plants

Parallel to the energetic performance analyses, economic analyses of the different CR CSP plants to evaluate their respective CAPEX and OPEX have been performed. The relative values, comparing those CAPEX, OPEX and resulting LCOE, between the two-tank molten salts (2MS) and the thermocline (1TC) are shown in Tab 14. Relative compared values are calculated by the difference between the thermocline value and the two-tank value, divided by the two-tank value.

In terms of investment, analogous to the reference case shown in section 4.3, the investment cost (CAPEX Diff.) varies between -4% to 10%. Thus CAPEX tends to be higher for the thermocline storage system. Thus the foreseen savings for the thermocline CR CSP plant CAPEX are difficult to achieve.

Regarding the OPEX, thermocline CR CSP plants are more economical to operate (-19% to -2%.) than two-tank molten salt plants.

In the same way as for the reference case shown in 4.3.4, taking into account not only the thermocline trend towards higher CAPEX, but also slightly lower electricity production, the resulting LCOE is higher (between 5% to 23%) compared to the two-tank conventional storage CR plant.

Table 14: CAPEX, OPEX and LCOE comparison between different two-tank molten salt and thermocline CR CSP solar plant. In **bold** the reference case presented in section 4.3.3

PB Power MW	Storage Capacity h	CAPEX Diff. %	OPEX Diff. %	LCOE Diff. %
50	6	-2 to 9 %	-12 to -2 %	6 to 19 %
	10	-3 to 9 %	-14 to -4 %	8 to 21 %
	14.2	-4 to 9 %	-19 to -10 %	8 to 22 %
100	6	-3 to 9 %	-12 to -2 %	5 to 17 %
	10	-3 to 9 %	-14 to -4 %	6 to 19 %
	14.2	**-3 to 10 %**	**-18 to -10 %**	**9 to 23 %**
150	6	-3 to 9 %	-12 to -2 %	5 to 17 %
	10	-4 to 9 %	-14 to -4 %	6 to 20 %
	14.2	-4 to 9 %	-19 to -10 %	9 to 23 %

5.5 LCOE of different PTC thermocline versus two-tank CSP plants

In this section, economic analyses of the different PTC CSP plants to evaluate their respective CAPEX and OPEX have been performed. The relative values, comparing those CAPEX, OPEX and resulting LCOE, between the two-tank molten salts (2MS) and the thermocline (1TC) are shown in Tab 15.

In terms of investment, analogous to the reference case shown in section 4.4, the relative investment cost (CAPEX Diff.) shows a tendency of the thermocline PTC CSP plant of slightly lower CAPEX. The anticipated CAPEX savings of 10 % for the thermocline PTC system could be achieved as the difference in CAPEX of the thermocline is between (-7% to 9%) depending on the economic assumptions.

Regarding the OPEX, thermocline PTC CSP plants are more economical to operate (-20% to -4%) than two-tank molten salt plants, as reducing the number of tanks from two to one decreases the maintenance costs of the adjacent equipment to them (i.e. valves, pipes).

In the same way as for the reference case shown in 4.4.3, taking into account not only the thermocline CAPEX, but also the slightly lower electricity production of the thermocline system, the resulting LCOE could be lower for the thermocline system (-7% to 13%) compared to the two-tank conventional storage system.

Table 15: CAPEX, OPEX and LCOE comparison between different two-tank molten salt and thermocline PTC CSP solar plant. In **bold** the reference case presented in section 4.4.2

PB Power MW	Storage Capacity h	CAPEX Diff. %	OPEX Diff. %	LCOE Diff. %
50	6 9.3 12.5	-7 to 7 % -7 to 9 % -7 to 9 %	-13 to -4 % -18 to -8 % -20 to -11 %	-3 to 11 % -6 to 10 % -7 to 9 %
100	6 **9.3** 12.5	-7 to 7 % **-7 to 8 %** -6 to 10 %	-13 to -4 % **-17 to -8 %** -20 to -11 %	-4 to 10 % **-6 to 10 %** -6 to 9 %
150	6 9.3 12.5	-6 to 8 % -7 to 9 % -7 to 9 %	-13 to -4 % -17 to -8 % -20 to -11 %	-1 to 13 % -5 to 11 % -5 to 10 %

5.6 Sensibility analysis of the Thermocline Charging and Discharging threshold temperatures in thermocline CSP sytems

5.6.1 Introduction

The utilisation and availability of the thermocline storage capacity largely depends not only on the geometric and physical parameters of the tank design, but also on the control and operational parameters. In other words, the same tank with the same dimensions, filler and molten salt composition, and physical properties, having the same *nominal* storage capacity, can have different *operational* storage capacities. In practice this means that the nominal capacity might not be exploited fully if control is not optimal. This is based on the fact that, unlike the case of the two molten salt tanks where the tanks are loaded or unloaded to their maximum operational limits defined by a level control, the thermocline tank is charged or uncharged based on predetermined *outlet* control temperatures.

Let us illustrate this with the example of thermocline PTC CSP operating between 385 °C and 290 °C.

Charging process and threshold temperatures

During the charging process of a thermocline PTC CSP system, the flow of molten salts enters from the top of the thermocline storage at a temperature of 385 °C, displacing the thermocline towards the bottom of the tank and extracting the cold molten salt from the bottom section, starting at 290 °C. This process is shown in the left-side schemes in Fig. 30. While this process takes place, the thermocline itself moves to the bottom. At some point, when the thermocline approaches the bottom, the tank's outlet temperature progressively increases. The control temperature, starting from the cold temperature at 290 °C, at which the charging process will decide to stop, varies the amount of energy that can be loaded. When we limit the outlet temperature to 300 °C in the charging process, we have a lower charging capacity than if we limit the outlet temperature to 320 °C or to 385 °C, which would mean to the thermocline to "leave" the tank from the bottom. Although this fact would enable 100 % tank charging, it would likely entail modifications to the system design, thereby its CAPEX, as the return "cold" temperatures to the PTC might be too high.
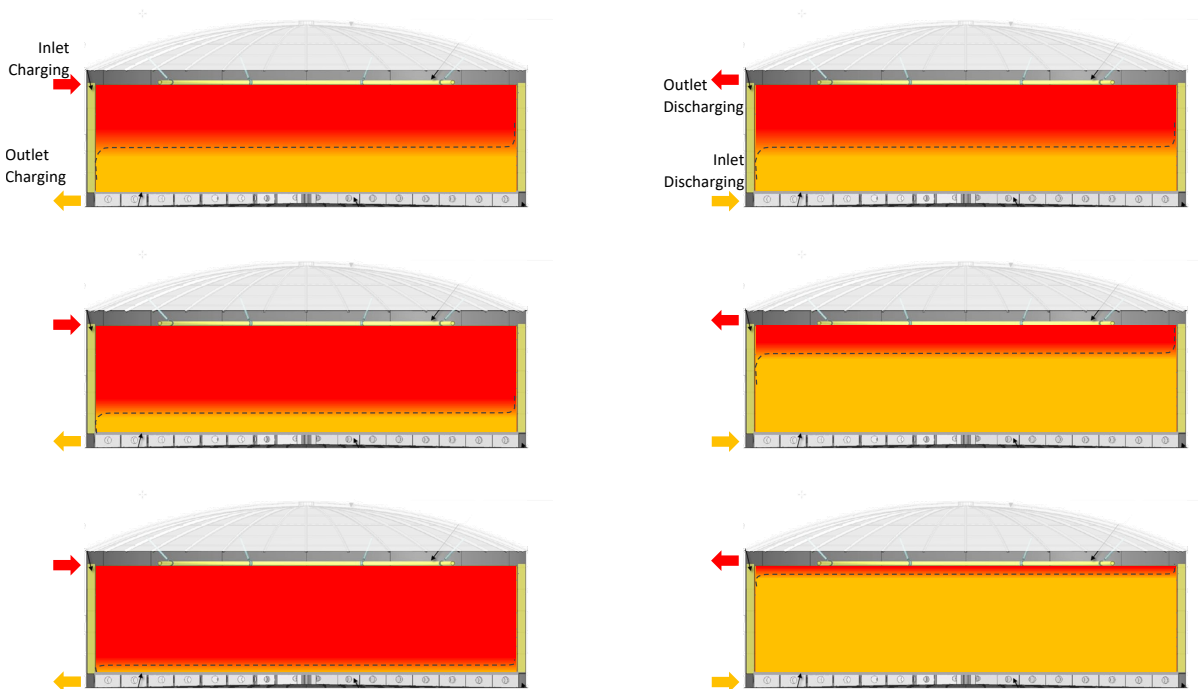

Figure 30: Thermocline storage charging (left) and discharging (right) processes.

This thermocline storage charging percentage resulting from threshold temperatures significantly affects solar energy production because having a lower storage capacity reduces solar energy yield.

Discharging process and threshold temperatures

Similarly, following the example of the PTC, during the discharging process, the flow of molten salts enters at an approximate temperature of 290°C from the bottom (coming from the power block) and exits from the top of the thermocline at its upper temperature (assuming around 385 °C if previously charged), as it is shown in the right-side schemes of Fig. 30. In the discharging process, the thermocline displaces upwards, and the same decision must be made about which threshold temperature below the nominal (385 °C) we should continue discharging the storage (for feeding the power block). In case we reach the 100% of discharging, the thermocline would leave from above, this time from the top of the tank, resulting in an outlet temperature of 290 °C. Depending on this discharging control temperature, we can extract almost all the available energy from the tank. The lower this control temperature, the greater the energy, but there is an operational limit for the power block because it cannot operate within an unlimited temperature range.

5.6.2 Sensibility analysis of the Thermocline Charging and Discharging threshold temperatures

Based on these operational parameters, a sensibility analysis of the energy performance of the system has been carried out as a function of these operational thresholds. Tab. 16 and Tab. 17 show the variation in the solar energy yield and the electricity produced for both operational limits for the CR case. Very similar results are obtained in both cases due to the storage capacity resulting from threshold temperatures affects solar energy production and consequently to electricity production.

As hot and cold temperatures for CR and PTC and different, in order to compare their results, two parameters have been defined, r_{char} and r_{disc} :

$$r_{char} = \frac{(T_{Threshold,char} - T_{cold})}{\Delta T_{hot-cold}} \tag{38}$$

$$r_{disc} = \frac{(T_{hot} - T_{Threshold,disc})}{\Delta T_{hot-cold}} \tag{39}$$

where $\Delta T_{hot-cold}$ is the temperature difference between T_{hot} hot and T_{cold} cold temperatures, and $T_{Threshold,char}$ and $T_{Threshold,disc}$ represent the threshold temperatures for charging and discharging processes. Consequently r_{char} represents the percentage of total charging capacity and r_{disc} stands for the percentage of total discharge.

Table 16: Sensibility analysis of the Thermocline charging and discharging threshold temperature in the CR thermocline CSP solar energy yield compared with the two-tank molten salt. In **bold** the nominal design criteria used in the comparative analysis.

$T_{Threshold,char}$	°C	**465**	405	345
r_{char}	%	62%	40%	17%
$T_{Threshold,disc}$	r_{disc}			
°C	%			
520	17%	-14%	-19%	-28%
500	25%	**-13%**	-16%	-24%
460	40%	-10%	-13%	-18%

From the table, it can be stated the significant dependence of the solar energy yield and, consequently, the electricity that can be generated by the CSP system, with the operational threshold temperatures.

As the charging threshold temperature increases, we allow the thermocline to move further to the bottom part of the storage increasing the energy stored. Consequently, the solar output increases, and so does the electricity, and vice versa, when solar output decreases so does the electricity produced.

Table 17: Sensibility analysis of the Thermocline charging and discharging threshold temperature in the CR thermocline CSP electricity compared with the two-tank molten salt. In **bold** the nominal design criteria used in the comparative analysis.

$T_{Threshold,char}$	°C	**465**	405	345
r_{char}	%	62%	40%	17%
$T_{Threshold,disc}$ °C	r_{disc} %			
520	17%	-15%	-19%	-28%
500	25%	**-13%**	-16%	-24%
460	40%	-10%	-13%	-18%

However, the increase in the charging threshold temperature, $T_{Threshold,char}$, could affect the design criteria of the CSP plant and its CAPEX, (i.e. selecting a higher temperature withstanding pumps or increasing the temperature levels for the expansion system). Therefore, this energy performance analysis should be completed in further studies with the economic part, verifying the optimal charging threshold temperature.

On the other hand, as the discharging threshold temperature is lowered, $T_{Threshold,disc}$, i.e., the thermocline is allowed to move higher up, increasing the deliverable energy capacity. As mentioned earlier, this has a limit because the power block does not allow operation at temperatures well below the nominal temperature; in other words, the performance penalty is significant.

As a nominal design point for the present comparative analysis between the two-tank molten salt and the thermocline storage technologies, a charging threshold temperature of 465 °C and a discharging threshold temperature of 500 °C have been selected.

Table 18: Sensibility analysis of the Thermocline charging and discharging threshold temperature in the PTC thermocline CSP electricity compared with the two-tank molten salt. In **bold** the nominal design criteria used in the comparative analysis.

$T_{Threshold,char}$	°C	375	**365**	355	315
r_{char}	%	89%	79%	68%	26%
$T_{Threshold,disc}$ °C	r_{disc} %				
365	21%	-2%	-8%	n.a.	n.a.
360	26%	-1%	**-3%**	-10%	-28%
355	32%	0%	-2%	-3%	-29%

The table reveals the same conclusions as in the CR case: the solar energy yield and, consequently, the electricity that can be generated by the CSP system are significantly dependent on the temperature operational thresholds, and the storage capacity, solar energy yield, and electricity, increase when the charging threshold temperature is increased, or the discharging threshold temperature is lowered.

As a nominal design point for the present comparative analysis between the two-tank molten salt and the thermocline storage technologies, a charging threshold temperature of 365 °C and a discharging threshold temperature of 360 °C have been selected.

From the comparative analysis between PTC and CR, we can draw some additional conclusions. For the PTC case, a charging ratio, r_{char}, of 79 % was used, resulting in electricity production 3 % lower compared to the two-tank system. In contrast, for the CR case, which is limited by the maximum return temperature, the load ratio was restricted to 62 %, resulting in a 13 % decrease in electricity production compared to the conventional two-tank system. However, when examining the PTC case with a similar load ratio in Tab 18, i.e. case with 355 °C charging ratio, r_{char}, of 68 %, we observe a similar reduction in electricity production of around 10 %. This suggests that the thermocline behaviour in both systems is quite similar and depends on these charging discharging ratios, regardless of the system type.

6   Conclusions

The project's findings indicate that the novel Newcline's storage concept, developed under the umbrella of CSP-ERANET, achieves most of the intended technical objectives but not the completeness of the anticipated economic savings. The key findings of the project are listed below.

- The energy performance of the CSP plant, either CR or PTC, are significantly influenced on temperature threshold limits imposed on charging and discharging, which affects the *operational* storage capacity of the thermocline tank. The *nominal* storage capacity is the maximum capacity that can be achieved given a specific amount of salt and filler material (if any), specific heat capacities and the maximum and minimum temperatures of operation. The *operational* storage capacity is not a physical limitation, but a consequence of a control strategy that depends on temperature thresholds. Higher operational storage capacity allows for more thermal energy to be stored and, thus, more thermal energy to be converted into electricity. However, moving the temperature thresholds for the control too far, leads to situations in which the power block cannot be operated or in which some CSP components should be redesigned. Thus, a compromise needs to be found.

- Sensitivity analysis showed that, depending on the control strategy, the thermocline storage system could generate between 70 to 100 % of the electricity compared to a conventional storage two-tank system using the same nominal storage capacity. For the control strategy applied in this study on the reference cases, the thermocline CR plant generates 87 % of the electricity compared to a conventional two-tank system, while for PTC systems, it generates 97 % compared to the conventional storage.

- To obtain the same production of dispatchable electricity a thermocline storage should be designed to store more (from 5 % to 25 %) energy in nominal conditions compared to two-tank systems due to the lower energetic efficiency for not having a perfectly stratified thermocline storage and depending on the charging and discharging temperature thresholds

- In terms of the capacity factor [8] of the CSP plant, this minor dispatchable electricity represents a capacity factor reduction from 71 % for the two-tank molten salt's CR CSP to 62 % for the thermocline's CR CSP plant, and a reduction from 45 % to 43 % for the PT CSP plant.

- The economic assessment of thermocline tank costs involves some uncertainty. In-depth Finite Element Modelling (FEM) have been carried out for the correct structural dimensioning of the tank, which is designed to withstand the higher thermal stresses associated with the sharp temperature thermocline. However, high uncertainties remain about the final manufacturing cost of the structured filler material as well as the cost of assembling it. For this reason, the economic values presented (CAPEX, OPEX and LCOE) are within an uncertainty range which is larger for thermocline systems compared to conventional two-tank systems.

- The relative weight of salt costs in the total investment of the plant depends mainly on the difference between the maximum and minimum operating temperatures. Systems with lower temperature difference, such as PTC (95 K), require more molten salt mass compared to CR systems with a higher temperature difference (265 K) for the same nominal storage capacity. Thus, the proportion of salt costs in the total investment is much higher for PTC systems compared to CR systems. Although this is a disadvantage for PTC two-tank conventional storage systems, it becomes an advantage for thermocline storage. As a consequence, the advantage of salt reduction of the thermocline concept is higher for CSP plans with low temperature difference such as the PTC ones.

- The anticipated storage investment cost savings from reducing the number of tanks to half are not achieved despite of the reduction of the solar salt amount by more than 50 %. The main reason is the increased complexity of the tank's structural design required to handle higher weights as well as thermal and mechanical stresses. The thermocline storage has a 30 % higher weight compared to a single tank

---

[8]The capacity factor of a Concentrated Solar Power (CSP) plant is a measure of the plant's actual energy output over a specific period compared to the maximum possible energy output if the plant was operated at full capacity continuously during that period

due to the structured filler and the molten salts. The thermocline storage for PTC is constructively slightly simpler than that of the CR, due to a lower mechanical stresses associated to less temperature difference between hot and cold salts.

- Storage savings represent a smaller saving compared to the overall plant investment. The 5 % to 10 % anticipated savings in plant CAPEX from using the thermocline storage are estimated to be in the range of 3 % to −10 % for CR and in a range of 7 % to −9 % for PTC systems. Negative percentage means an increase in CAPEX, which means that depending on the cost assumptions, the *Newcline* CSP plants could also be more expensive than the two-tank conventional ones. Thus, thermocline systems for PTC systems have an opportunity to reduce CAPEX, but the implementation of thermocline in CR systems seems to have not such a potential.

- Thermocline systems are consistently more cost-effective in terms of operational expenses (OPEX) due to the lower number of tanks reducing maintenance costs.

- PTC CSP plants based on thermocline can have a 6 % lower LCOE compared to conventional two-tank PTC systems. However, depending on the cost uncertainties of thermocline storage in the PTC system, the LCOE can be up to 10 % higher than that of two-tank molten salt system. Thus, results are not yet conclusive to support or disregard this technology for PTC systems for CSP plants.

- With the cost assumptions taken in the NewCline project, the thermocline storage implemented in CR systems does not offer an economic advantage over its two-tank storage counterpart due to lower electricity production (87 %), which could be optimised by changing the threshold temperatures, and higher relative CAPEX compared to the PTC CSP plant.

Although the cost saving objectives have not been achieved to its completeness, the conclusions are promising for thermocline technology for the PTC CSP plants. To advance this technology further, it is imperative that future projects analyse its limitations and challenges to identify better solutions for achieving greater efficiency and economic competitiveness. Accordingly, several points for development in future studies are outlined:

- Optimise the design of the structured filler to reduce its production and implementation costs. The current design requires the production and deployment of 800,000 bricks for a thermocline tank with dimensions of 44 meters in diameter and 10 meters in height.

- Optimise the top and bottom buffer zones in order to reduce the amount of molten salt. The current design of these buffer zones contains 35 % of the total tank salt.

- Optimise the storage construction, including the potential redesign of conventional two-tank systems, by considering the failure analysis for molten salt thermal storage tanks in CSP plants conducted by NREL, e.g. Osorio et al. (2024)

- Conduct the economical analysis of charging-discharging thresholds complementing the energetic results presented in section 5.6. It will also be necessary to analyse the LCOE for cases in which the thermocline is sized such that the CSP system can deliver the same amount of electricity.

- Derive thermocline cost functions as a function of volume and maximum and minimum temperature difference. This will be very important to asses in which cases this technology has the highest cost reduction potentials including other applications such as process heat.

Overall, the novel thermocline storage system developed within the *Newcline* project shows promising outcomes, especially for systems where the cost of molten salt constitutes a significant portion of the total investment (lower difference between the maximum and minimum operational temperatures) as Parabolic Trough Collector CSP plants and for smaller volumes as analysed here. This extends the potential applications beyond CSP plants to include high-temperature storage in industrial processes, which is crucial for integrating solar concentrating technologies in industries requiring high temperatures. There are several industrial processes that could benefit from such a storage for example:

- Food Processing: Baking (150 °C to 250 °C) or high-temperature short-time (HTST) pasteurization (up to 150 °C), and drying (up to 240 °C).

- Chemical Industry: Polymerization (150 °C to 300 °C), distillation (150 °C to 350 °C).

- Pharmaceutical Industry: Sterilization (120 °C to 250 °C) and drying.

- Textile Industry: Dyeing and finishing (150 °C to 220 °C) and fabric drying (150 °C to 250 °C).

- Pulp and Paper Industry: paper drying (100 °C to 250 °C).

- Automotive Industry: Paint curing (150 °C to 250 °C) and rubber vulcanization (150 °C to 200 °C).

References

Angelini, G., Lucchini, A., and Manzolini, G. (2014). Comparison of Thermocline Molten Salt Storage Performances to Commercial Two-tank Configuration. *Energy Procedia*, 49:694–704.

Biencinto, M., Bayón, R., Rojas, E., and González, L. (2014). Simulation and assessment of operation strategies for solar thermal power plants with a thermocline storage tank. *Solar Energy*, 103:456–472.

Boubou, B., Kalawole Muritala, I., Makinta, B., Tizane, D., Guy Christian, T., Jacques, N., Téré, D., Antoine, B., and Rabani, A. (2021). Review on Thermocline Storage Effectiveness for Concentrating Solar Power Plant. *Energy and Power Engineering*, 13(10):343–364.

Bruch, A., Fourmigué, J., and Couturier, R. (2014). Experimental and numerical investigation of a pilot-scale thermal oil packed bed thermal storage system for CSP power plant. *Solar Energy*, 105:116–125.

Flueckiger, S. M., Yang, Z., and Garimella, S. V. (2012). Thermomechanical Simulation of the Solar One Thermocline Storage Tank. *Journal of Solar Energy Engineering*, 134(4):041014.

Galione, P. A., Pérez-Segarra, C. D., Rodríguez, I., Torras, S., and Rigola, J. (2015). Multi-layered solid-PCM thermocline thermal storage for CSP. Numerical evaluation of its application in a 50MWe plant. *Solar Energy*, 119:134–150.

Herrmann, U. and Kearney, D. W. (2002). Survey of Thermal Energy Storage for Parabolic Trough Power Plants. *Journal of Solar Energy Engineering*, 124(2):145–152.

Hoffmann, J.-F., Fasquelle, T., Goetz, V., and Py, X. (2016). A thermocline thermal energy storage system with filler materials for concentrated solar power plants: Experimental data and numerical model sensitivity to different experimental tank scales. *Applied Thermal Engineering*, 100:753–761.

IRENA (2012). Renewable Energy Technologies: Cost Analysis Series - Concentrating Solar Power. Technical report, IRENA.

Klasing, F., Hirsch, T., Odenthal, C., and Bauer, T. (2020). Techno-Economic Optimization of Molten Salt Concentrating Solar Power Parabolic Trough Plants With Packed-Bed Thermocline Tanks. *Journal of Solar Energy Engineering*, 142(051006).

Klein et al. (2010). Trnsys 17: A transient system simulation program, solar energy laboratory. Technical report, University of Wisconsin, Madison, USA, http://sel.me.wisc.edu/trnsys.

Kolb, G. J. (2011). Evaluation of Annual Performance of 2-Tank and Thermocline Thermal Storage Systems for Trough Plants. *Journal of Solar Energy Engineering*, 133(3).

Kolb, G. J. and Hassani, V. (2006). Performance Analysis of Thermocline Energy Storage Proposed for the 1 MW Saguaro Solar Trough Plant. In *Solar Energy*, pages 1–5, Denver, Colorado, USA. ASMEDC.

Kolb, G. J., Ho, C. K., Mancini, T. R., and Gary, J. A. (2011). Power Tower Technology Roadmap and Cost Reduction Plan. Technical report, Sandia National Laboratories.

Mira-Hernández, C., Flueckiger, S. M., and Garimella, S. V. (2014). Numerical Simulation of Single- and Dual-media Thermocline Tanks for Energy Storage in Concentrating Solar Power Plants. *Energy Procedia*, 49:916–926.

Odenthal, C., Breidenbach, N., and Bauer, T. (2017). Modelling and operation strategies of DLR's large scale thermocline test facility (TESIS). *AIP Conference Proceedings*, 1850(1):080019. Publisher: American Institute of Physics.

Odenthal, C., Klasing, F., and Bauer, T. (2019). A three-equation thermocline thermal energy storage model for bidisperse packed beds. *Solar Energy*, 191:410–419.

Odenthal, C., Tombrink, J., Klasing, F., and Bauer, T. (2023). Comparative study of models for packed bed molten salt storage systems. *Applied Thermal Engineering*, 226:120245.

Osorio, J., Mehos, M., Imponenti, L., Kelly, B., Price, H., Torres-Madronero, J., Rivera-Alvarez, A., Nieto-Londono, C., Ni, C., Yu, Z., Hamilton, W., and Martinek, J. (2024). Failure Analysis for Molten Salt Thermal Energy Storage Tanks for In-Service CSP Plants. Technical Report NREL/TP–5700-89036, 2331241, MainId:89815.

Pacheco, J., Showalter, S., Kolb, W., and Laboratories, S. N. (2001). Development of a Molten-Salt Thermocline Thermal Storage System for Parabolic Trough Plants. *Proceedings of Solar Forum 2001*.

Pacheco, J. E., Showalter, S. K., and Kolb, W. J. (2002). Development of a Molten-Salt Thermocline Thermal Storage System for Parabolic Trough Plants. *Journal of Solar Energy Engineering*, 124(2):153–159.

Patnode, A. M. (2006). Simulation and Performance Evaluation of Parabolic Trough Solar Power Plants. Master's thesis, University of Wisconsin-Madison.

Xie, B., Baudin, N., Soto, J., Fan, Y., and Luo, L. (2022). Wall impact on efficiency of packed-bed thermocline thermal energy storage system. *Energy*, 247:123503.